Markov type models for large-valued interbank payment systems

Xiaonan Che

A Thesis submitted for the degree of Doctor of Philosophy

Department of Statistics

The London School of Economics and Political Science

September, 2011

Declaration

I certify that the thesis I have presented for examination for the PhD degree of the London School of Economics and Political Science is solely my own work other than where I have clearly indicated that it is the work of others (in which case the extent of any work carried out jointly by me and any other person is clearly identified in it).

Xiaonan Che

Date

Abstract

Due to the reform of payment systems from netting settlement systems to Real Time Gross Settlement systems (RTGS) around the world in recent years, there is a dramatic increase in the interest in modeling the large-valued interbank payment system. Recently some queueing facilities have been introduced in the response to the liquidity management within the RTGS systems. Since stochastic process models have been wildly applied in social networks, and some aspects of which have similar statistical properties with the payment system, therefore, based on the existing empirical research, a Markov type model for RTGS payment system with queueing and collateral borrowing facilities was developed. We analysed the effect on the performance of the payment system of the parameters, such as the probabilities of payment delay, the initial cash position of participating banks and the probabilities of cross bank payments. Two models were proposed; one is the simplest model where payments were assumed to be equally distributed among participating banks, the other one is a so-called "cluster" model, that there exists a concentration of payments flow between a few banks according to the evidence from empirical studies. We have found that the performance of the system depends on these parameters. A modest amount of total initial liquidity required by banks would achieve a desired performance, that minimising the number of unsettled payments by the end of a business day and negligible average lifetime of the debts.

Because of the change of large-valued interbank payment systems, the concern has shift from credit risk to liquidity risk, and the payment systems around world started considering or already implemented different liquidity saving mechanisms to reduce the high demand of liquidity and maintain the low risk of default in the mean time. We proposed a specified queueing facility to the "cluster" model with modification with the consideration of the feature of the UK RTGS payment system, CHAPS. Some of the

payments would be submitted into a external queue by certain rules, and will be settled according an algorithm of bilateral or multilateral offsetting. While participating banks's post liquidity will be reserved for "important" payments only. The experiment of using simulated data showed that the liquidity saving mechanism was not equally beneficial to every bank, the banks who dominated most of the payment flow even suffered from higher level of debts at the end of a business day comparing with a pure RTGS system without any queueing facility. The stability of the structure of the central queue was verified.

There was evidence that banks in the UK payment system would set up limits for other members to prevent unexpected credit exposure, and with these limits, banks also achieved a moderate liquidity saving in CHAPS. Both central bank and participating banks are interested in the probability that the limits are excess. The problem can be reduced to the calculation of boundary crossing probability from a Brownian motion with stochastic boundaries. Boundary crossing problems are very popular in many fields of Statistics. With powerful tools, such as martingales and infinitesimal generator of Brownian motion, we presented an alternative method and derived a set of theorems of boundary crossing probabilities for a Brownian motion with different kinds of stochastic boundaries, especially compound Poisson process boundaries. Both the numerical results and simulation experiments are studies. A variation of the method would be discussed when apply it to other stochastic boundaries, for instances, Gamma process, Inverse Gaussian process and Telegraph process. Finally, we provided a brief survey of approximations of Lévy processes. The boundary crossing probabilities theorems derived earlier could be extended to a fair general situation with Lévy process boundaries, by using an appropriate approximation.

Acknowledgements

It is a pleasure to extend my heartfelt gratitude to the following persons who made this thesis possible. First of all, I would like to take the opportunity to thank my supervisor, Dr. Angelos Dassios, for his encouragement, guidance and supervision throughout my studies at London School of Economics and enable me to develop an understanding of the subject. I am grateful all the feedback and comments I received from other staffs at the Department of Statistics, and the University, for generous financial support.

I am indebted to many of my friends around the world to support me during the completion of the thesis.

Lately, I would like to express my gratitude to my beloved family in China; for their understanding and endless support through the duration of my time in the UK.

Contents

List of Figures

List of Tables

Chapter 1

Introduction to large-valued interbank payment systems

Payments and securities settlement systems are essential complements of any stable financial markets. In recent years, the interest in analysing the large-valued interbank payment systems has been growing rapidly. Some aspects of these systems have been investigated in-depth in several papers, for instance, the statistical properties of the UK and US current payment systems [9], [59] and [64]; the development of global interbank payment systems [8] and [23], the details will be discussed in the oncoming chapters.

The explosive growth in the volume of transactions in the national and international financial markets resulted in a corresponding increase in interbank payments flows. Two basic settlement models are applied in interbank (wholesale) payment systems: Deferred Net Settlement (DNS); and Real Time Gross Settlement (RTGS). In the Net settlement payment systems, payment orders are achieved at the end of a period, usually is a business day, on a net basis, and regardless the time they occurred. However, it may give change to build up credit exposures among participants

during the interval prior to settlement. On the other hand, under an RTGS payment system, each payment is immediately settled on a transaction-by-transaction basis throughout a business day, but with a higher liquidity demand.

The wholesale payment systems have been reformed during the past decades around the world [8]. The main reason for such reform is a liquidity management in large-valued payment systems. A large number of countries have introduced the Real Time Gross Settlement payment system instead of the Deferred Net Settlement payment system. In some RTGS payment systems, central bank grants daylight overdrafts to the participating banks in order to guarantee all the outgoing payments, so that maintaining the liquidity and the processing efficiency of net settlement systems. However, if central bank funds, which are so-called good funds, or acceptable collateral are not available, then payment orders could be rejected or delayed until funds become available to cover them. As a result, some RTGS payment systems have, or are thinking about to implement queueing facilities. In an RTGS system with queueing facilities, payment orders, for which no cover funding are available, are put into a queue to be processed when sufficient funds have been delivered to cover the incoming payments [23].

1.1 Reform of payment system

The basic settlement models are applied in interbank payment systems: *Deferred Net Settlement* (DNS); and *Real Time Gross Settlement* (RTGS). In the net settlement payment systems, payments are accumulated over time and achieved at the end of a period, usually is a business day, on a bilateral or multilateral net basis, and regardless the time they occurred. With which banks need to post liquidity only equal to their net obligations. However, the accumulation of huge number of

unsettled payments can generate considerable credit exposures among members of the payment system. Moreover, the largest risk in a netting settlement system is the risk that the failure to fulfil its obligations by one participant will lead to a system crash, which is known as the systemic risk. By now, it is well recognized by the global financial markets, that any interruption in wholesale payment system leads to ultimate gridlock that could have serious consequences on the real economy. The concerns from different users of financial market drove the reform of the large-valued interbank payment systems around the world. Real Time Gross Settlement payment systems have replaced the netting systems around the world in the recent decades [8]. An RTGS payment system is defined as a gross settlement system in which both processing and final settlement of funds transfer orders can take place on a continuous, transaction-by-transaction basis throughout a business day (i.e. in real time). As banks could make payment orders at any time during a business day, comparing with the net settlement payments system, the RTGS payment system takes the advantage, for which transfers are settled individually, and the system effects final settlement continuously but not periodically [23]. Hence, it prevents the sizeable credit exposures between banks, and the credit risk to receiving banks is at least reduced or even eliminated. This, however, comes at a higher demand for liquidity.

The two basic risks of a wholesale payment system are credit risk and liquidity risk[1] to the participants in a wholesale payment system. The Deferred Net Setting system can exacerbate interbank credit risk: if banks credit their customers' accounts during the day and before the final settlement has occurred, such risk will appear as soon as a bank defaults on its net obligation when in due course. An easy way to mitigate credit risk is to increase the frequency of netting in a DNS system, which

[1]other types of risk including operational and legal risks.

in the mean while increases the demand of liquidity unfavorably. Therefore, there is a trade-off between credit exposures and liquidity demands.

Liquidity risk is the risk that a counterparty will not settle a due payment for full value on time but at some unspecified time afterwards. The delay could adversely affect the expected liquidity level of the payee, and it may force the payee to cover its cash flow shortage by funding from other sources. Since the payee does not anticipate the delay, the funds used to cover the shortage is short-noticed, which may lead to a financial loss due to higher financing costs (higher interest rate for short notice borrowing) or to damage to its reputation. In more extreme cases, the payee may be unable to cover the cash flow shortage at any price, in which case it therefore may not be able to meet its obligations to others. Within a large-valued transaction payment system, the time gap between the execution of the transaction and its final completion is a main source of the liquidity risk. With the time gap, it becomes possible that the settlement of individual transactions will not take place as expected. A participating bank will not be certain what funds it will receive through the payment system until settlement of transactions is completed. Thus, the bank will not be sure whether its liquidity is adequate. If a bank overestimates the value of payments it will receive, it would lead to a shortage of cash, and if the shortage occurs around the end of a business day, the bank could have significant difficulty in raising the liquidity it needed from an alternative source.

In wholesale payment systems, central banks are particularly concerned with systemic risk, which is the failure of one participant to meet its obligation when due may cause other participants to fail to meet theirs. Such a failure could raise the financial difficulties and vacillate the stability of the payment system. As a result, central banks have a particular interest in limiting the systemic risk in large-valued transactions payment system, this is because that the aggregate exposures

tend to increase with the aggregate value of transactions, and the potential risk in large-valued transactions system are significantly higher than those in other systems [14].

In RTGS payment systems, settlements occur on the books of central bank. Central bank controls the systemic liquidity and credit risk by providing daylight overdrafts to participating banks. Central bank grants daylight overdrafts to participating banks by guaranteeing all outgoing payments, therefore preserving the liquidity and the processing efficiency of the net settlement system. Participating banks can make payments throughout the business day and square their positions or erase their overdrafts only at the end of the day. However, in the absence of collateral for such daylight drafts, the central bank assumes credit risk till the overdrafts are eliminated. Collateral requirements minimise credit risk, but they also may significantly reduce the liquidity of the system meanwhile. If central bank funds (so-called good funds) or acceptable collateral are not available, payments could be rejected or at least delayed till cover is available [14]. In response to such inefficiencies associated with the liquidity management, some RTGS payments have or are going to add queueing facilities. Payment messages, for which no covering fund is available, enter a queue to be processed when sufficient funds have been delivered to cover the incoming payments [14]. The most important advantage of RTGS payment systems with queueing facilities is that they allow for the introduction a searching mechanism which cancels offsetting payments in queues, thus reducing the amount of liquidity required by the system.

1.2 Real Time Gross Settlement payment systems

An RTGS payment system is used by participants to process large-valued payments, such as payment for the settlement of interbank purchases, sales of government funds; the purchase, sale and financing of securities transactions; the disbursement or repayment of loans and the settlement of real estate transactions [59].

For the RTGS payment system with queueing facilities, when the collaterised borrowing is no longer available, there are two possible ways to treat the payment orders; one way is for the system to reject the orders and return them to the sending bank, the rejected orders then will be put into the system again at a later time and pending payments within their internal systems. This is called the internal queue. An alternative is a centrally located queue or system queue. The system may temporarily keep the payment orders in its central database instead of rejecting them, in which case, the pending payments will be released for settlement when covering funds become available on the basis of predefined rules, which are agreed between the system and the participants. Rather than distinguishing the queues according to locations, queues can also differ according to the underling management, in other words, how a queue is controlled. The management may be carried out by the central bank (centralised management) or by individual banks (decentralised management). The combinations of possible locations and managements lead to various forms of queues. Most RTGS systems including the system considered in the thesis introduced the centralised queuing facilities.

According to Bank of International Settlements, most centrally located queue arrangements have adopted a form of the First In First Out (FIFO) rule [14]. Where the FIFO rule is applied, payment orders are held in the order in which they are dispatched by the sending bank; the payment at the top of the queue is released

and settled first when covering funds are available, and the payment behind it will be considered for settlement only when it fully settled. Besides, there are many other methods of queue processing and the outcome of the process will be distinct depending on the method. For instance, "bypass FIFO"[2] rule is a variation of the FIFO rule, under which the system tries to process the first transfer in the queue, but if that cannot be executed due to lack of funds it then tries to settle the next transfer instead. The order of the payments will affect the performance of queueing. Under the simplest condition, payments are ordered according to the time they occur. However, the flexibility of the queueing facilities could be improved by using the priorities of the payments. Payments are placed in the queue on the basis of the assigned priorities and are released for settlement on a FIFO basis within each priority level. In other words, no payments of a particular priority will be settled until all those of a higher priority level have been settled.

Besides prioritisation, queue management could also help the banks to control the number and value of the queue facilities. In general, there are two approaches to queue management, which are reordering and optimisation routines [14]. In the case of the reordering facility, it allows the central bank or the participating bank to change either the original order or the priority level of the payments in the queue. The optimisation routine typically attempts to settle payments simultaneously rather than in sequence. When a "cycle" of payments among participating banks occurs, optimisation routine may be able to provide a more effective solution, as some offsetting payments could be canceled out.

With centrally located queues, participating banks are provided with a range of information not only on outgoing transfers in their own queues but also on any incoming transfers being sent to them that are held in other banks' outgoing queues

[2]Belgium RTGS system with central queue, ELLIPS, applies "bypass FIFO".

by the central bank. The transparency of queued incoming orders could effect the risk and efficiency of the queue process. One view is that transparency could induce the payee to act upon queued incoming payments (i.e. unsettled payments), hence potentially generating risks in RTGS systems. The other view emphasises the possible advantages of transparency in reducing liquidity risk rather than increasing it. Since, when other things are equal, better information on expected payment flows may imply a smaller probability of a liquidity shortage. Moreover, greater transparency might enable banks to sequence incoming and outgoing payments in a more efficient way, thereby additionally improving their liquidity management. However, the automatic release of the information might involve greater risks, hence some RTGS system provide the information only on request.

When considering various approaches to queuing, one potentially important question is whether the central bank or the individual banks manage the queues. From the reducing the liquidity demand's point of view, the more the central bank can intervene in the queues by using queueing management, the more efficient the queue should in principle be. This is because the central bank can observe the information about the queued payments of all participating banks, thus adjust the queue configuration systematically, for example, canceling out any offsetting payments or "cycles" of payments, therefore, minimising the liquidity request and preventing credit exposures.

1.3 Structure of the thesis

In Chapter 2, we first propose a simple discrete time Markov model for a large-valued interbank payment system using a dynamic Monte Carlo simulation to investigate the statistical properties of the payment system with borrowing and queueing facil-

ities. More precisely, we investigate the performance of the proposed model under different combinations of characteristic parameters, such as

n the number of participating banks

p the probability for a participating banks to have one unit of cash at the beginning of an experiment

q the probability that a payment order is submitted to external queue

Under the framework of the simple homogeneous model, with the consideration of existing studies of modeling social networks, and empirical research about two major real time large-valued interbank payment systems in the world, Fedwire® Funds Service of the US and CHAPS of the UK, a modified "cluster" model is developed, in which members of a payment system are not identical. With the more parameters (N, number of groups in a system; P_{ij}, probability of inter-group payments and so on) are introduced to the "cluster" model, a more detailed results from the Monte Carlo simulation would be presented in this chapter.

Given the rapid reform of wholesale payment systems around the world, the risk of lacking liquidity has attacked great attention from different users of a payment system, especially central banks. In Chapter 3, we implement a specified liquidity saving mechanism to a model that captures the most significant features of the UK Real Time Gross Settlement payment system, CHAPS. The mechanism allows bilateral or multi-lateral offsetting. The experiment of using simulated data shows that the liquidity saving mechanism is not equally beneficial to every bank, the banks who dominate most of the payment flow even suffer from higher level of debts at the end of a business day comparing with a pure Real Time Gross Settlement payment system without any queueing facility. The stability of the structure of the

central queue is verified. Given the constant argument of whether historical data or artificial data should be used when carrying out a simulation study, we compare our model against the one where actual data has been used and hence emphasize the characteristics of our models.

There is evidence that banks in the UK payment system would set up limits for other members to prevent unexpected credit exposure, and with these limits, banks also would achieve a moderate liquidity saving in CHAPS [9], [10]. Both central bank and participating banks are interested in the probability that the limits are excess. The problem can be reduced to the calculation of a popular question in many fields of Statistics, the boundary crossing probability for a Brownian motion with stochastic boundaries. Chapter 4 is on the topic of boundary crossing probabilities. It is organized in the following ways; an in-depth survey about boundary crossing probabilities was provided at the beginning of the chapter; Anderson was the first to obtain the explicit representation for the distribution of the first-passage time of a Brownian motion through linear boundaries [2]. Recently, a simper formulae and briefer derivations are obtained by Hall [30]. In the rest of the existing literatures, some of the special cases of P_u and P_l are studied very well, most of which are worked on piecewise-linear boundaries. The existing results are generally divided into two types according to two kinds of boundaries. One is one-sided piecewise-linear boundary, the unconditional probability that a standard Brownian motion up-crosses a piecewise linear boundary in a finite time interval $[0, T]$ is obtained by Wang and Pötzelberger [61], However, the calculations involves evaluation of a multiple integral, which cannot always be expressed by an explicit formula and hence must be solved numerically. In additional to this, Abundo [1], by applying the time inversion property of Brownian motion, particularly derived a elementarily simple and explicit formula for the conditional boundary crossing probability of X_t

and piecewise-linear boundary, $u(t)$, consisting of two lines given that $X_s = \eta$ over a limit $[0, T]$. The other case is the two-sided boundaries, Abundo [1] also solved the conditional crossing probability for X_t with two symmetric linear boundaries. Novikov [43] derived a more general approximated solution by using piecewise-linear boundaries.

Overall, the explicit form of the probabilities only obtained for a few special non-linear boundaries, for example, squared root boundaries [61]. The boundary crossing probability for any other general boundaries only solved numerically. However, in practices, most of the time, general non-linear boundary is far more realistic, we are interested in deriving the exact boundary crossing probabilities for general boundary, in particular, stochastic boundary. We take linear boundaries as examples to present an alternative method, with powerful tools, such as martingales and infinitesimal generator of Brownian motion, to target the boundary crossing probability problem. Our approach allows to derive a simple formula for symmetric/asymmetric linear boundaries. Thereafter, a set of theorems of boundary crossing probabilities for a Brownian motion with stochastic boundaries is derived, which is aim at the concern from members of payment systems about bilateral/multi-lateral limits.

In Chapter 5, we discuss how the method proposed in Chapter 4 could be applicable to different types of non-decreasing Lévy boundaries, for instance, Gamma process and Inverse Gaussian process. Nevertheless, Chapter 5 provides a brief survey of approximations of Lévy processes. The boundary crossing probabilities theorems could be extended to a fair general situation with Lévy process boundaries, by using an appropriate approximation; finite variation case by Poisson approximation and infinite variation case by the combination of Poisson approximation and the small jumps are represented by their mean. Finally, we provide the conclusions in Chapter 6.

Chapter 2

Markov type model of Real Time Gross Settlement payment system

In this chapter, we going to propose a simple discrete time Markov model for a large-valued interbank payment system, which allows us to investigate the statistical properties of the system with borrowing and queueing facilities. More precisely, we are going to investigate the performance of the proposed model under different parameter settings. Furthermore, in the context of the simple homogeneous model, with the consideration of existing empirical research, we develop a more piratical model, namely "cluster" model. Firstly, we present some modeling approaches in the areas which share similar characteristics as large-valued interbank payment systems, for example, social networks.

2.1 Some modeling approaches in the area of social networks

Some aspects of the dynamics of social networks have similar statistical properties as the RTGS payment systems. Recently, more and more statisticians and sociologists work cooperatively, and use stochastic processes to model social networks. In this chapter, we are going to discuss some of the work in the area of social networks, and compare the proposed models to ones concerted with interbank payment systems.

2.1.1 Stochastic processes

First of all, a social network has been viewed as a general stochastic process in the existing literatures. We take the work by Wasserman as an example, in which the inter-personal relationships among a group of people was modeled as a stochastic process [62]. In this process, individuals are nodes while the appearance of link between two nodes represents the existence of relationship. Let $X(t)$ be a binary matrix-valued stochastic process with elements $X_{ij}(t)$, where

$$X_{ij}(t) = \begin{cases} 1 & \text{if individual } i \text{ chooses individual } j \text{ at time } t \\ 0 & \text{otherwise} \end{cases}$$

Consider a group with g members, hence $\mathbf{X}(t)$, a $(g \times g)$ binary matrix, is of the form

$$\begin{bmatrix} 0 & 1 & \cdots & \cdots & 1 \\ 1 & 0 & 1 & \cdots & 1 \\ \vdots & \cdots & \cdots & \ddots & \vdots \\ 1 & \cdots & \cdots & 1 & 0 \end{bmatrix}$$

Another property of this stochastic process is that the state space is finite, thought it is quite large, $2^{g(g-1)}$.

Consider a specific link between individuals i and j at time t, $X_{ij}(t)$, in a social network. At a time point t, there are two possible statues of the link, which is either "on", indicating there exists a relationship between individual i and j, or "off" indicating no relationship. Moreover, under the Markov assumption, the random variable $X_{ij}(t)$ remains in its 0 or 1 state for an exponentially distributed length of time.

The dynamics of a social network is viewed as a stochastic process, during a short time period $(t, t+h)$, an individual evaluates its current position in the group and makes decision on whether to change or not with different preferences. In the small time interval, a relationship can change in two ways;

i If there is no link from individual i to j at time t, then such a link may be present at $t+h$.

ii On the other hand, a link from i to j at time t may not be present at time $t+h$.

Wasserman has modeled the above processes of evaluation and decision as followed,

i A state, $X_{ij}(t)$, in $\mathbf{X}(t)$ receives binary inputs from n other links, say z_1,z_2,. . .,z_n and they are the elements of $\mathbf{X}(t)$. They are the set of relationships in the network that influence individual i's choice of j.

ii $X_{ij}(t)$ examines the length of time τ since it last underwent change.

iii $X_{ij}(t)$'s decision to change or not is determined by a binary output function f_{ij}.

iv During the time interval $(t, t+h)$, only one link is allowed to change in the model.

As other general stochastic process model, the stochastic processes for social networks have two assumptions. The first is that $\mathbf{X}(t)$ is a standard Markov chain with finite state space S and probability transition matrix P with elements $P_{xy}(t,h)$, which is defined as

$$P_{xy}(t,h) = \mathbb{P}\{\mathbf{X}(t+h) = y | \mathbf{X}(t) = x\} \tag{2.1}$$

The second assumption is that, for a small interval of time $(t, t+h)$, the changes in the relationships between individuals in the group are independent. In other words, for $h \to 0$,

$$P_{xy}(t,h) = \prod_{i,j} \mathbb{P}\{X_{ij}(t+h) = y_{ij} | \mathbf{X}(t) = x\} + o(h) \tag{2.2}$$

Hence, the elements $P_{xy}(t,h)$, given by equation (2.1), of the probability transition matrix can be defined further as,

$$\mathbb{P}\{X_{ij}(t+h) = 1 | \mathbf{X}(t) = x, X_{ij}(t) = 0\} = h\lambda_{0ij}(x,t) + o(h)$$
$$\mathbb{P}\{X_{ij}(t+h) = 0 | \mathbf{X}(t) = x, X_{ij}(t) = 1\} = h\lambda_{1ij}(x,t) + o(h)$$

where λ_{0ij} and λ_{1ij} are the infinitesimal transition rates for the continuous time Markov chain $\mathbf{X}(t)$, which are depended on the current state of the process $X_{ij}(t)$ and time t.

Based on the foundation of the stochastic process studies by Wasserman [62], variate models were developed for social networks. For each particular model, a

simpler stochastic process could be introduced. All of the further stochastic process models for social network satisfied the Markov assumption and the conditional change independence assumption, (2.2), of the general stochastic process. Some of the examples including reciprocity model, popularity model [62] and stochastic blockmodels [31], [60].

Further in Wasserman's paper [62], he considers two stochastic process models for social network, they correspond to the Markov assumption and the conditional change independence assumption of the general stochastic process respectively [62]. One is called the reciprocity model. In this model, the tendency over time for a choice of individual j by individual i (a link from i to j, $i \to j$) depends on whether or not there exists a link from j to i only. Hence, the dyads for the pair of nodes (i, j), as $D_{ij}(t) = (X_{ij}(t), X_{ji}(t))$, are independent. Thereby, $D_{ij}(t)$ is a stochastic process, more precisely, a Markov chain with state space D containing the following four states:

- the mutual state $D_{ij}(t) = (1, 1)$,
- two asymmetric states $D_{ij}(t) = (1, 0)$ and $D_{ij}(t) = (0, 1)$,
- the null state $D_{ij}(t) = (0, 0)$.

The new four-state space stochastic process will be easier to analyse than the standard stochastic process mentioned earlier in this section.

The other stochastic model is called popularity model, which is an attempt to postulate how the status of an individual within a group influences the choices made in reaction of it. In the model of popularity, the transition rate for a change in the relationship from node i to j depends on how popular node j is, which is measured by the indegree[1] of j, which is defined as, in a directed graph, for a node, the

[1]The measurement of the "social status" of the group members.

number of head endpoints adjacent to a node[2]. As with the reciprocity model, the computation of the original stochastic process is very difficult. Hence, instead of the original stochastic model, Wasserman defined the jth column processes of the digraph process $X(t)$ as $X_{\cdot j}(t) = (X_{1j}(t), X_{2j}(t), \cdots, X_{gj}(t))^T$, which is a zero-one valued vector of length g, and each individual process is a continuous time Markov chain. The entire process then can be represented as g independent column processes consisting of the columns of $X(t)$. Derived from the column processes, the indegree process is defined as $I_j(t) = \sum_i X_{ij}(t)$, the number of ones in the jth column process at time t. Since under the assumption made earlier, an indegree can only increase by one, decrease by one or remain the same at each time update, $I_j(t)$ is, therefore, a continuous time birth-and-death process, a special case of general Markov chain.

Nevertheless, in many social networks, individuals can be partitioned into subgroups, $B_1, \cdots, B_b$, based on one or some of the factors such as race, sex, geographic location and party affiliation. The stochastic process $X(t)$ will be composed of b^2 blocks. The general stochastic model by Wasserman ignores such a nodal information completely, therefore, is unable to explain any block structure. Holland *et al.* had proposed a simple block-model according to the general stochastic process model by assuming that the X_{ij}'s are mutually independent and any X_{ij} and X_{kl} are identically distributed with a common probability p_{rs} if $i, k \in B_r$ and $j, l \in B_s$, for some $r, s = 1, \cdots, b$ [31]. The second assumption means that the pattern of links in the data is a direct consequence of the density of links within and across "internally homogeneous" blocks. Essentially, any pair of nodes a and b in the same block is required to have an equivalent structure, i.e., node a relates to every other nodes of the category in exactly the same way as node b does [60].

To the extent of large-valued interbank payment systems, the dynamics of pay-

[2] `http://en.wikipedia.org/wiki/Directed_graph`

ment flows among participating banks in the system is described as a finite state, discrete-time Markov process. In the environment of payment system, $X_{ij}(t)$ as defined for social networks is the weight of the payment from bank i to j at time t, and it could equal to any nonnegative integer. Under our assumptions, neither of the reciprocity model nor the popularity model is applicable, but the blockmodel has provided us with a rudiment for our model. The model will be studied in Section 2.3 and 2.4 explicitly.

2.1.2 Random graph models

As with the stochastic process model, the dynamics of a general social network can be represented as graph of nodes and edges (i.e. links). The range of possible networks and their probability of occurrence under the model are represented by a probability distribution on the set of all possible graphs with the fixed number of nodes. By assuming that each link in the network is regarded as a random variable, a random graph model can be posited for a social network. In a network, for each pair of nodes i and j, which are distinct members of a set of fixed number nodes, N, say, there is a random variable $Y_{ij}(t)$ such that

$$Y_{ij}(t) = \begin{cases} 1 & \text{if there is a network tie from node } i \text{ to } j \\ 0 & \text{if there is no tie} \end{cases}$$

Moreover, let $\mathbf{Y}$ be the matrix of all variable Y_{ij}'s, then we can construe a graph with node set N and the edge set specified by these pairs (i, j) for which $Y_{ij} = 1$. $\mathbf{Y}$ might be directed random graph if Y_{ij} is distinguished from Y_{ji} or non-directed for $Y_{ij} = Y_{ji}$ by definition [12]. Under different assumptions of the random graph model, specific models are derived by different authors [42], [51] and [52].

The dependence of edges is the key criteria that classifying a random graph model. When all the edges are independent, the model is called the Bernoulli random graph [52]. In this model, all possible distinct links are independent of another, and they may occur with a fixed probability. The only possible configurations is the set of all single edges Y_{ij}. On the other hand, rather than the simple edges independence, when the dyads (has the same definition in the stochastic case, $D_{ij}(t) = (X_{ij}(t), X_{ji}(t))$) are assumed to be independent, the model is called the dyadic model [52]. With the dyadic independence assumption, there are two types of configurations, they are single edges and reciprocated edges. The dyadic independence is somewhat a more complicated assumption for directed graphs than the simple edges independence, however, it is still not very realistic [52].

A more realistic assumption, Markov dependence, was introduced by Frank and Strauss [26]. It says that a possible link from node i to j is assumed to be contingent on any other possible link involving node i or j, even if the status of all other links in the network are known. In this case, the two links are said to be conditionally dependent given the values of all other links. For instance, two network links are conditionally dependent when they share a common node. Comparing with the two dependence assumptions above, Markov dependence is more realistic in many circumstances.

As most social networks, an RTGS payment system could be viewed as a random graph model as well. The participating banks and directions of payment order represent the nodes and edges in a random graph respectively. Since the direction of each payment order is important, the dynamics could be viewed as a directed random graph.

2.2 Empirical research on interbank payment systems

The complexity of interbank payment system attracts statisticians to consider its statistical properties. Both transaction data from the Fedwire® Funds Service (Fedwire) and UK large-valued interbank payment system CHAPS were analyzed to create a interbank payment network.

Soramäki and Becher proposed the payment flows in both systems as a directed network and established a link from the sender of payment to the receiver of payment on the basis of payments sent [59], [9]. Despite the fact that there are far fewer banks in the United Kingdom than in the United States[3], the structures of both interbank payments are very similar in certain respects: when only considering the settlement banks in CHAPS, the payment flows in both systems were found to form a well-connected network, which means every bank is connected to every other bank by some set of payment flows. Nevertheless, the properties of the well-connected network change little from day to day.

The empirical studies [59], [9] show that:

- A giant strongly connected component (GSCC) has the largest percentage of the total banks in both Fedwire and CHAPS, and 90% of the value transferred occurs within the giant component for Fedwire[4], whilst four banks account for around 80% of CHAPS payments in terms of both value and volume. The analysis provides insights on the structure of liquidity flows in the payment system, any disruption in the system could cause serious consequences, especially in the giant strongly connected component.

[3]over 7500 participants in the Fedwire Funds Service, while CHAPS consists 15 settlement banks only in 2008

[4]the size of the component was varied over the sample period

- The interbank payment system has the small world phenomenon, which is common for many complex networks. Small world means that any node can be reached from any others in only a few steps. The significance is that the shorter the distances between banks in the network, the easier liquidity can be recirculated among the banks, on the other hand, a payment system where liquidity flows fast is also likely to be disrupted easily. Thus, the liquidity management is the most important reason for our analysis.

- In terms of a degree distribution, most banks have only a few links and a small number of banks have thousands of links originate from it. Both the payment systems have a power-law distribution, then the networks to describe the payment flows are referred to as scale-free networks. Hence, rather than assuming that the participants in the payment system are identical, we consider a more realistic assumption for our proposed model, which is the participating banks in the payment system are not homogeneous.

- It has been shown that the interbank payment system is disassortatice, which means nodes in a network with a given degree are more unlikely to have links with nodes of similar degree. The result has provided us the evidence to assume that, in general, in an RTGS payment system, the decision of the direction of a transaction is independent from time to time.

Other respects of the topology properties of interbank payment systems were investigated, some examples are the likelihood that two nodes which are the neighbors of the same node, share a link is another common correlation measure between nodes; clustering coefficient, link weights and node strength.

2.3 A simple discrete time Markov model

Several existing papers studied the theoretical behavior in RTGS systems, for example, the reaction of banks in an RTGS system in which they face costs of delay and borrowing was examined and it shows that the equilibria of a system suffered from excessive delay of payments [3]; a game-theoretic environment is specified and some equilibria of the system involving heavily delay [7]. The main focus of this section is to analysis the performance of RTGS systems with various queueing and collaterised borrowing facilities, in particular, how different queueing and/or collaterised borrowing facilities affect the excessive delay at equilibria.

2.3.1 The model

A simple model is proposed to an RTGS system, where all the participating banks are homogeneous, they experience identical queueing and collateral costs, and the payment flows are equally distributed among the participants. In other words, there is no substantial concentration of payment orders between any partition of the system.

In the simplest model, the dynamics of queues is described by a discrete time Markov process. A state of the process at a given time represents the payment orders put in the queue by each participating bank, the list of debts. Particularly, if the list of debts is empty, the amount of cash accumulated as a surplus from payments by other banks. For simplicity, we assume that the value of every payment order is one monetary unit.

At each time update, the state of the Markov process changes according to a random procedure. This includes two parts, one is the arrival of new payment

orders[5], at each time, only one occurs and is evenly distributed among all banks. The other is the decision by the receiving bank either to queue the payment or to settle it by borrowing from the central bank. For payments that are submitted into the queue, they would be ordered in the time of their appearance. The decisions are completely independent from time to time, with probability q for queueing and $1-q$ for borrowing. The initial state is also a key factor, where every participating bank is provided with one unit of cash independently with other banks at the beginning of a business day with probability p. A particular feature of this model is that, at each time update, the system carries a search for "cycles" of debt links or "chains" that ending at a bank with positive cash position. If such a cycle or chain appears, the corresponding debts are canceled and the states of the participating banks are renewed.

2.3.2 Simulation and results

At each step of the Markov process, a commercial bank (in short a bank), say i, receives a payment order from a customer to transfer a monetary unit to another participating bank, say j. The payment orders are evenly distributed among all participants. Formally, we consider a completely random graph where nodes represent banks $i = 1, \cdots, N$; the central bank observes the system from outside. The central bank acts as a regulator to whom all the information about the past and present states of the graph is available. We assume that every bank has an account with central bank which is characterised by three parameters: the cash position, debts (the outgoing payments put in a queue) and exposure to other participating banks (the incoming payments that are put in other queues). This means that every node

[5]requires bank i to make a payment to bank j, bank i is the receiving bank of the payment order

is characterised by

- a certain amount of non-negative reserves;
- negative, positive or zero debt (positive debts occurring only when the cash reserve is zero).

The system evolves in a discrete time with each time slot being numbered. The arrival of an order of transfer from bank i to j results in appearance of a directed link $i \to j$. Then, first of all, one checks if there already exists a link $j \to i$; if yes, the "oldest" existing link $j \to i$ is deleted, together with the newly arrived link $i \to j$. Thereby, the debt of j to i is diminished by one.

Now suppose that upon the arrival of link $i \to j$, there is no link such that $j \to i$. Then, if bank i in a positive cash position, the new link in instantly discounted, the cash reserve of node i decreases by one and the cash reserve of node j increases by one. Otherwise, i.e. if bank i in zero/negative cash position, the outgoing payment can be paid using collaterised credit, in which case node j again receives a unit of cash, or put in the central queue till sufficient funds become available from incoming payments. These two possibilities are chosen at random, with probabilities $1-q$ and q, respectively. In the later case (queueing), the positive debt of node i increases by one, and so does the exposure of node j.

After receiving the unit of cash, bank j uses it to pay its earliest debt, which results in disappearance of corresponding directed link $j \to k$ and transformation of the unit of cash to bank k. Then bank k acts accordingly and so on, until a cycle is established (when we return to bank i), or we encounter a bank, say l, with no debt. In the later case, the cash position of bank l increases by one while the indebtness of all other banks involved decreases by one. This completes the single Monte Carlo simulation step.

As was said before, in a "real" RTGS payment system, the central bank can regulate the behavior of the entire system by using available regulatory instruments. Such instruments include cost of collaterised borrowing, cost of queueing and start-of-the-day cash positions. In our model, it is reflected in variability of probabilities q and p measuring banks' incentives and possibilities to follow one strategy or another. The search for and cancelation of offsetting payments are functions and responsibility of central bank who supervises the system.

Queues of outgoing payments for each bank are transparent to the central bank. This allows central bank to implement a search mechanism in order to enhance the liquidity of the payment system. The search mechanism identifies offsetting payments in queues and automatically cancels them out.

The numerical experiments with $N = 20$ indicate that there are two regimes. Under the sub-critical regime, where p and q are both strictly between 0 and 1, the debts survive at the end of a business day and the distribution of the average lifetime of a single debt has thin tail and converges to zero. This might be because that the central bank wants complete the payment orders as early as possible in order to reduce the risk of overnight debts. In this regime, when p is fixed, as q increases, the average number of uncleared debts is increasing and the probability to complete the debts at the end of a day is decreasing.

On the other hand, the result for $p = 1$ is drastically different. The parameter q becomes irrelevant, all the banks in the system own one unit initial cash, the payment system is in a critical regime, where the payment system has ultimate clearance of all payment orders and zero lifetime of debts.

However, under the consideration, it is not clear whether the proposed Markov process is positive, null recurrent or transient for differen values of N and q. It maybe the unit cash initial position leads the process to a "positive recurrent part"

of its state space. In any case, a dramatic phenomenon presents, an appropriate amount of total initial liquidity equally distributed among all the banks can achieve a desired goal, i.e. complete clearance of debts by the end of a business day. Also, the system is robust comparing to random perturbations.

2.4 The modified model - cluster model

2.4.1 The model

The analyses based on empirical data in section 2.2 suggest that the simplest Markov process maybe not realistic in some circumstances. Although the nodes in the system may not be correlated, there is a concentration of links among a few number of banks [9] and [59]. In other words, the payment flows are not evenly distributed among the banks. Thus, using the multi-class queues model could give us an improved result.

In the modified model, all the participating banks with the same queueing probability q and one unit initial cash probability p as in the simplest Markov process model. The difference is that there are two types of the decisions on where a payment order goes. It could either be asked to transfer to a bank in the same group, or there is no preference about the direction. Nevertheless, the choices are independent from time to time.

Now assuming that the payments are more likely to be transferred between the banks in the same category than these across different categories, which means that there is a concentration of payments within the banks in the same category. This could happen in the real world due to higher cost or longer time for transactions across different commercial banks. Let P_{ij} denote the probability that a payment is transferred from bank in category i to a bank belonging to category j, then P_{ii}

is the probability that a payment moves between the banks in a single category i. We consider a simple case when P_{ij}'s are identical for all j and $P_{ij} = P_{ji}$, in other words once a payment is going to a bank in other groups, the probabilities of choosing which group are the same. Moreover, P_{ii}'s are all equal for all i. We assume that the numbers of banks in each category are equal, so if we suggest that there are n groups among the N banks, then, in each group, there are $\frac{N}{n}$ banks and $i, j = 1, \cdots, n$.

The dynamics of payment flows is viewed as a finite-state space, discrete time Markov process, and the process is determined by the four parameters:

- the number of participating banks N;
- number of bank categories n;
- the probability of queueing q;
- the probability for a bank owns one unit initial cash p.

The transition probabilities are P_{ii}'s and P_{ij}'s, they have to satisfy the constrains:

$$\frac{N}{n}P_{ii} + (N - \frac{N}{n})P_{ij} = 1 \tag{2.3}$$

$$P_{ii} > P_{ij} \tag{2.4}$$

which implies that,

$$P_{ij} = \frac{(1 - \frac{N}{n}P_{ii})n}{(n-1)N} \tag{2.5}$$

$$0 \leq P_{ij} < \frac{1}{N}$$

$$\frac{1}{N} < P_{ii} \leq \frac{n}{N}$$

There are two special cases we look at:

1. If $P_{ii} = P_{ij} = \frac{1}{N}$ the Markov model returns to the simplest case, where the participating banks are homogeneous, and the payment orders are equally distributed among them. The statistic properties of this simplest model has been discussed in the pervious section.

2. When P_{ii} reaches its extreme value, $P_{ii} = \frac{n}{N}, P_{ij} = 0$, in which case, for a payment order, it goes to banks in the same category only. This is the case where all the counterparties hold an account in every group of banks.

Now we can define the transition matrix for the Markov process with N nodes and n clusters as a block matrix of the form,

$$\begin{bmatrix} A_{11} & A_{12} & \cdots & \cdots & A_{1n} \\ A_{21} & A_{22} & A_{23} & \cdots & A_{1n} \\ \vdots & \vdots & \ddots & \vdots & \vdots \\ A_{n1} & \cdots & \cdots & \cdots & A_{nn} \end{bmatrix}$$

where A_{ij}'s are submatrics and for $i, j = 1, \cdots, n$ and $i \neq j$,

$$A_{ii} = \begin{bmatrix} 0 & P_{ii} & \cdots & P_{ii} \\ P_{ii} & 0 & \cdots & P_{ii} \\ \vdots & \vdots & \ddots & \vdots \\ P_{ii} & \cdots & P_{ii} & 0 \end{bmatrix}, \quad A_{ij} = \begin{bmatrix} P_{ij} & \cdots & P_{ij} \\ \vdots & \ddots & \vdots \\ P_{ij} & \cdots & P_{ij} \end{bmatrix}$$

Also, $A_{ij} = A_{ji}$, since $P_{ij} = P_{ji}$.

2.4.2 Simulation and results

The aim of this experiment is to find out what the average life of a debt is and how the debts distributed by the end of a business day for each participant, so that the central bank could adjust the level of initial liquidity, probability of queueing and the cost of collaterised borrowing to control the number of debts, consequently reduce the risk of unsettled payments.

We consider a random graph of N nodes where the nodes represent banks and each node is classified by three factors: the cash position (could be positive, negative or zero); number of debts (outgoing payments) and exposure to other participating banks (incoming payments). Upon an arrival of a payment order, the process that completes a single step of the Monte Carlo simulation is identical as under the simplest model in section 2.3.

We use the procedure described as in the simple homogeneous model and a Monte Carlo method (see more details in Appendix A.1) to simulate a Real Time Gross Settlement payment system consisting of 40 banks. All of the parameters have been assigned different values across their range; we notice that the results of the experiments are similar for parameters over a small interval. Hence, we reported two sets of numerical experiments with the choices of parameters listed as Table 2.1 only as illustrations. For each combination of the parameters (n, P_{ii}, p and q), the experiment starts from a random node and observed for 480 iterations. A thousand trials are carried out and the result is averaged.

The results from every separate procedure is illustrated by two histograms:

Left-hand plots of Figures 2.2 - 2.19, Figures 2.21 - 2.56 The average number of end-of-the-day debts per node, where the horizontal axis is the number of nodes and the vertical axis represents the number of debts at the end of a

parameters	values		
N	40		
n	5	8	
P_{ii}	$\frac{n}{N}$	$\frac{n/2}{N}$	$\frac{1}{N-1}$
P_{ij}	equation (2.5)		
p	0.3	0.7	1
q	0.2	0.5	0.9

Table 2.1: Values of parameters

business day at a particular node after 480 iterations.

Right-hand plots of Figures 2.2 - 2.19, Figures 2.21 - 2.56 The averaged lifetime of a single debts after 480 Monte Carlo iterations. In this graph, the number of iteration is along the horizontal axis, while how many debts on average were "alive" after a certain number of iterations is given by the vertical axis.

We get two types of results for different values of P_{ii}, when $P_{ii} = \frac{n}{N}$ or $P_{ii} \neq \frac{n}{N}$.

Critical case $P_{ii} = \frac{n}{N}$

We start the simulation with 40 banks. By dividing the banks into different numbers of groups, the snap-shot plots of the debt distribution at the end of a business day in the system are similar, even with different values of p and q. For instance, Figure 2.1 indicates the debt distribution at the end of an experiment in a system where $p = 0.1$, the probability of queueing is 0.6 and there are 8 groups among the 40 banks, i.e. $P_{ii} = \frac{1}{5}$. Each box in the two-dimensional picture represents the position of an end-of-the-day debt after 480 iterations. Taking the (n, m)th box as an example, the colour represents both the direction and volume of the debt(s) between bank n and bank m[6]. It notices that given the transition matrix of the Markov

[6]positive means bank m owes bank n,*vice versa*

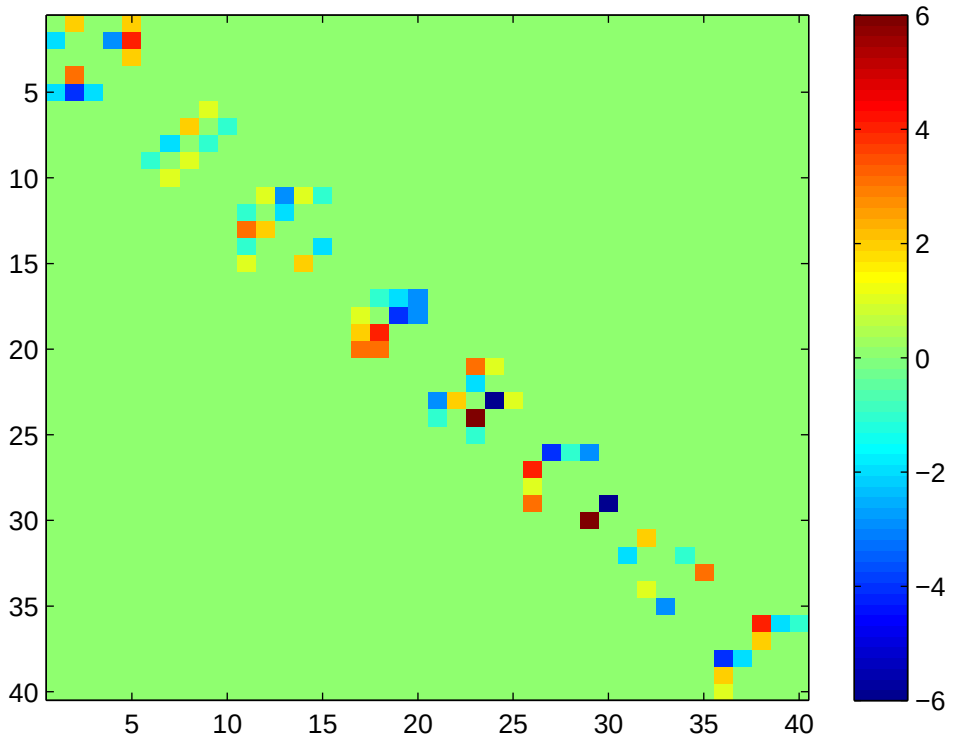

Figure 2.1: Distribution of end-of-the-day debts when $p = 0.1, q = 0.6, n = 8, N = 40, P_{ii} = \frac{1}{5}$

process is diagonal symmetric, the snap-shot plot is symmetric about the diagonal but with opposite sign. Furthermore, characteristically, the debts are located along the diagonal, as a linear function. A reason behind the linear relationship is that $P_{ij} = 0$, payments are impossible to go to banks in other categories, all the payments are thus concentrated around a single group. However, Figure 2.1 just shows a typical behavior of the simulation when $P_{ii} = \frac{n}{N}$, and the linear pattern is sustained when replacing these parameters (p, q, N, n) with any other values, hence, from which we could see that there are always unsettled debts at the end of a business day.

Figure 2.2-Figure 2.10 illustrate the results from the critical case (i.e. $p_{ii} = \frac{n}{N}$)

when $n = 8$, and Figure 2.11-Figure 2.19 illustrate the results when $n = 5$. When the number of categories is unchanged, remaining the value of p resulting an increase of the average number of end-of-the-day debts as the probability of queueing becoming larger. It was also observed that the distribution of average lifetime of a single debt has a massive concentration about short lifetime. Furthermore, as the value of q goes up, the tail of the average lifetime distribution becomes thinner and the distribution moves closer to zero with the average number of "alive" debts increases at early stage of the simulation.

In addition, it is observed that the average number of end-of-the-day debts slightly increased from member to member of the system, and one particular member suffers from an outstandingly high debts. The experiment does not provide the statues of every individual bank during the procedure, it therefore was unable to identify the "unlucky" member with the largest debts. Nevertheless, a possible interpretation of such phenomena could be that a small bank with relatively little business with the rest of the system aggregated a great amount of out-going payments with far more less incoming payments, the initial one unit of cash was be used to pay the first order at the beginning of the business day.

Other cases $P_{ii} \neq \frac{n}{N}$

With allowing payments transiting in between different groups of banks, while remaining the priority for same-group-payments, the pattern of the snap-shot plot of the end-of-the-day debt distribution in a system is random as shown in Figure 2.20, rather than the clear linear relationship as seen in the extreme case, Figure 2.1. However, there are more colored boxes near the diagonal, as P_{ii} is always greater than P_{ij}. The plot is still symmetric about the diagonal and it also suggests that there are always residual debts at the end of a business day.

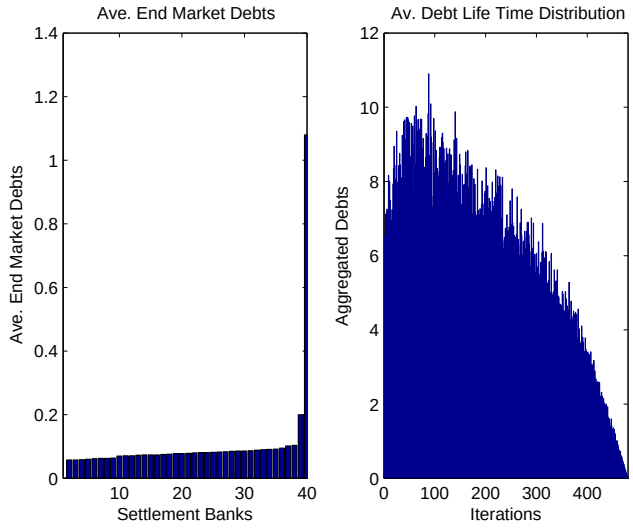

Figure 2.2: $n = 8$, $P_{ii} = 0.2$, $p = 0.3$, $q = 0.2$

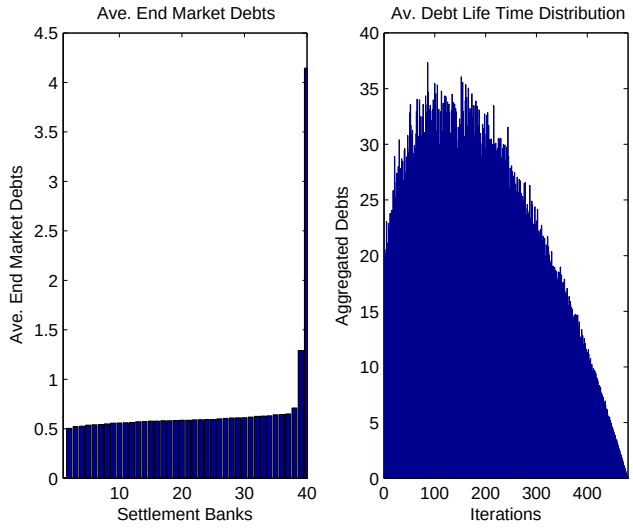

Figure 2.3: $n = 8$, $P_{ii} = 0.2$, $p = 0.3$, $q = 0.5$

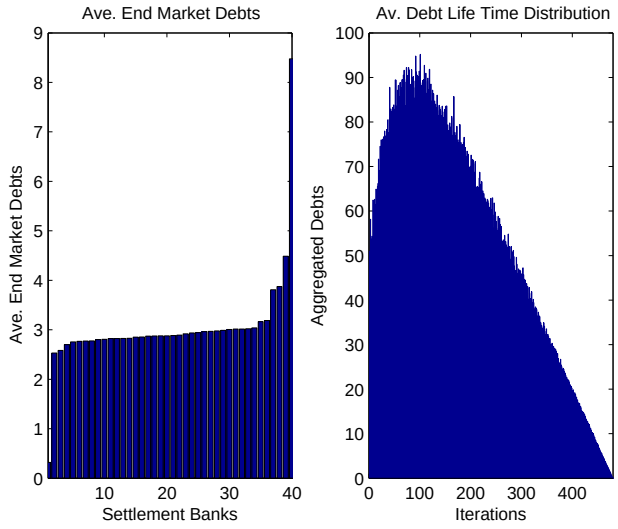

Figure 2.4: $n = 8$, $P_{ii} = 0.2$, $p = 0.3$, $q = 0.9$

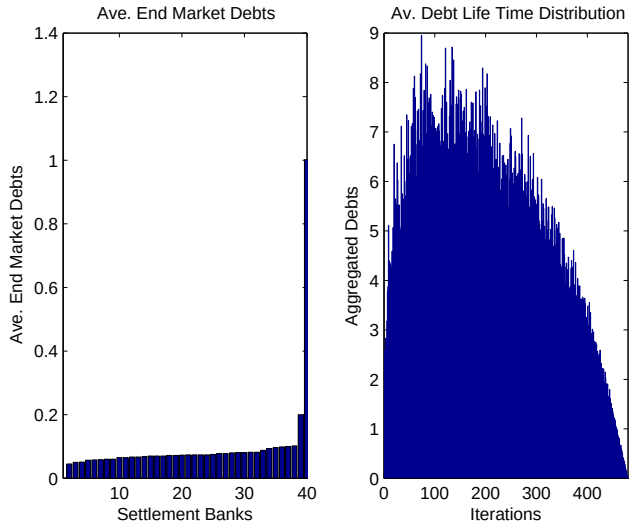

Figure 2.5: $n = 8$, $P_{ii} = 0.2$, $p = 0.7$, $q = 0.2$

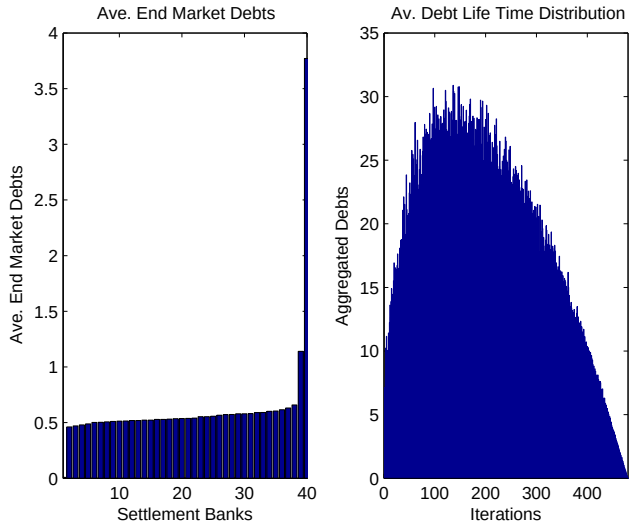

Figure 2.6: $n = 8$, $P_{ii} = 0.2$, $p = 0.7$, $q = 0.5$

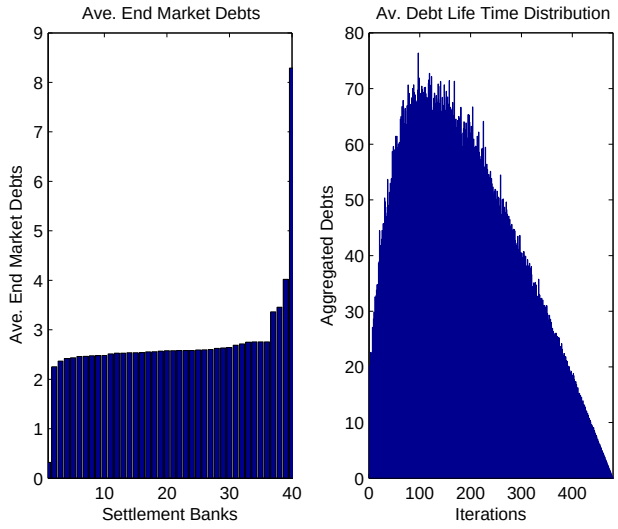

Figure 2.7: $n = 8$, $P_{ii} = 0.2$, $p = 0.7$, $q = 0.9$

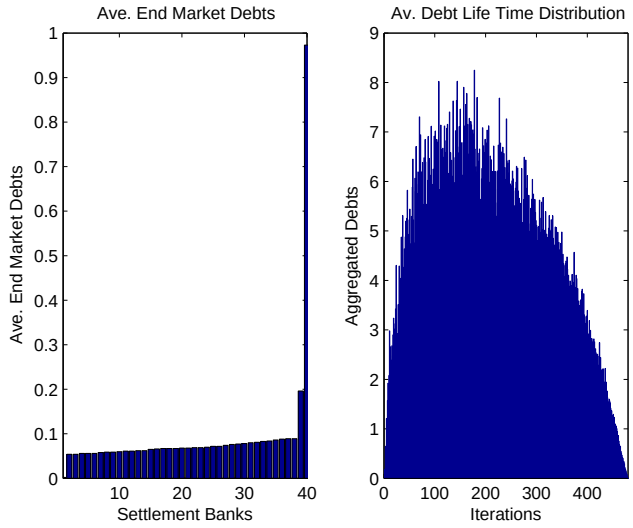

Figure 2.8: $n = 8$, $P_{ii} = 0.2$, $p = 1.0$, $q = 0.2$

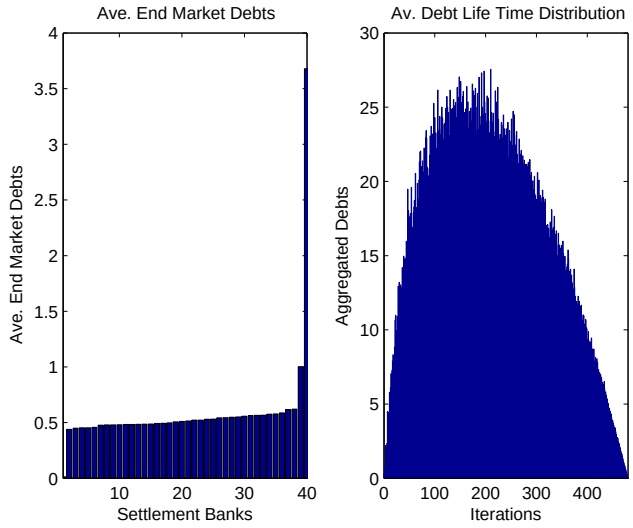

Figure 2.9: $n = 8$, $P_{ii} = 0.2$, $p = 1.0$, $q = 0.2$

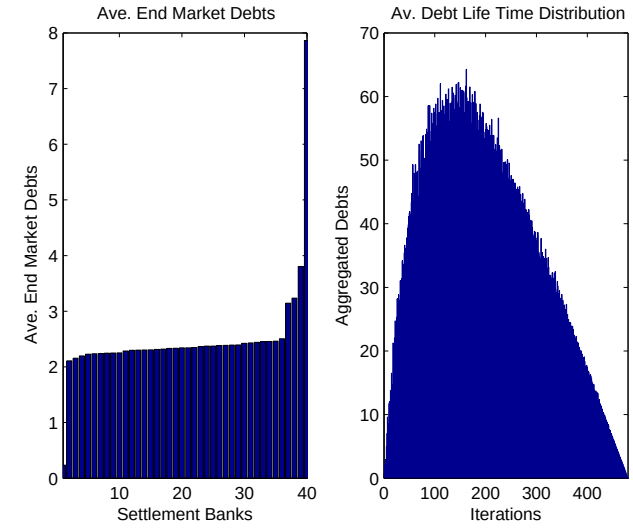

Figure 2.10: $n = 8$, $P_{ii} = 0.2$, $p = 1.0$, $q = 0.9$

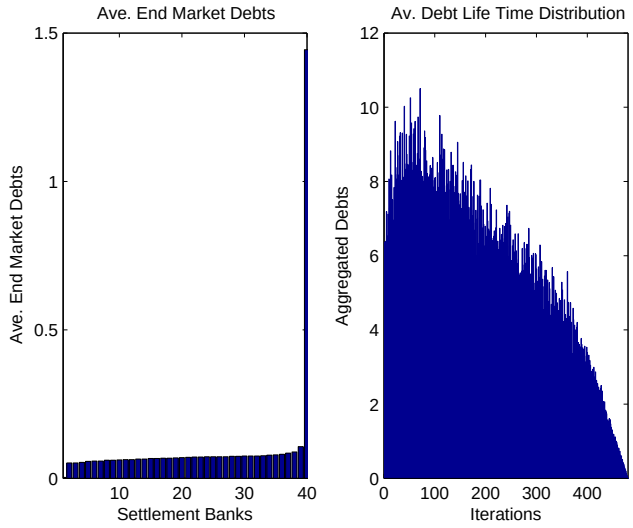

Figure 2.11: $n = 5$, $P_{ii} = \frac{1}{8}$, $p = 0.3$,$q = 0.2$

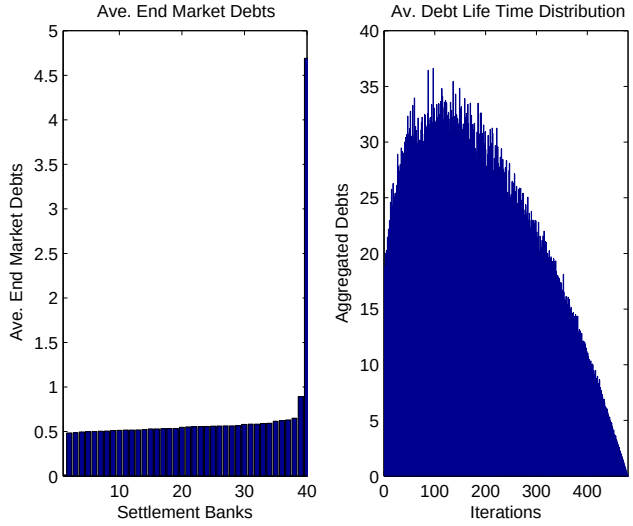

Figure 2.12: $n = 5$, $P_{ii} = \frac{1}{8}$, $p = 0.3$, $q = 0.5$

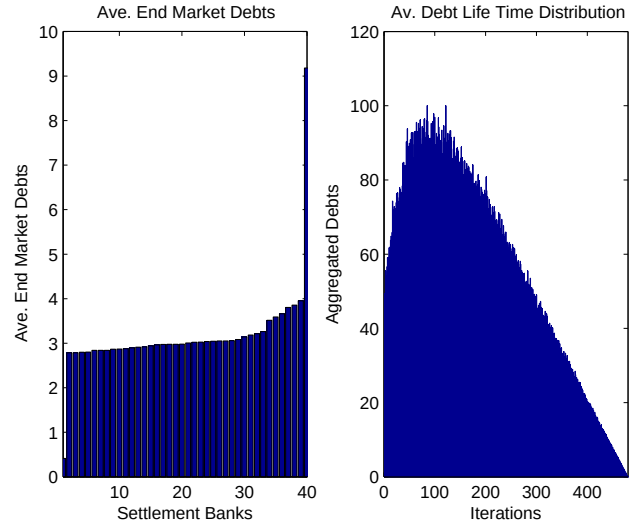

Figure 2.13: $n = 5$, $P_{ii} = \frac{1}{8}$, $p = 0.3$, $q = 0.9$

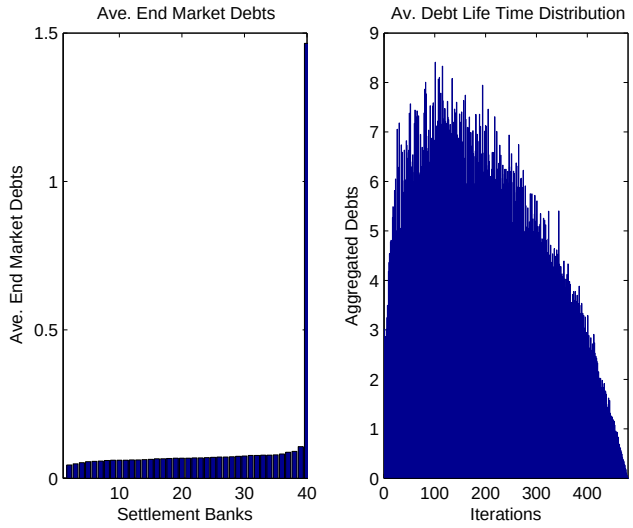

Figure 2.14: $n = 5$, $P_{ii} = \frac{1}{8}$, $p = 0.7$,$q = 0.2$

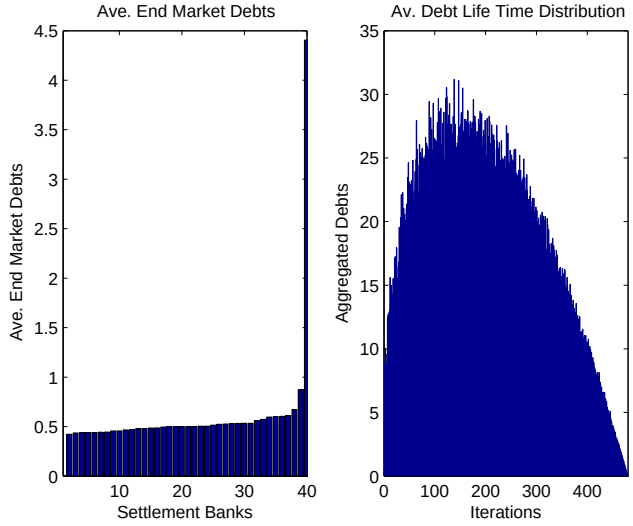

Figure 2.15: $n = 5$, $P_{ii} = \frac{1}{8}$, $p = 0.7$, $q = 0.5$

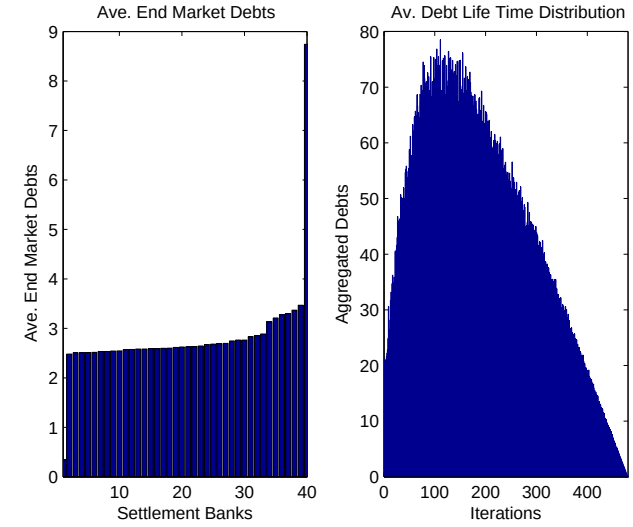

Figure 2.16: $n = 5$, $P_{ii} = \frac{1}{8}$, $p = 0.7$, $q = 0.9$

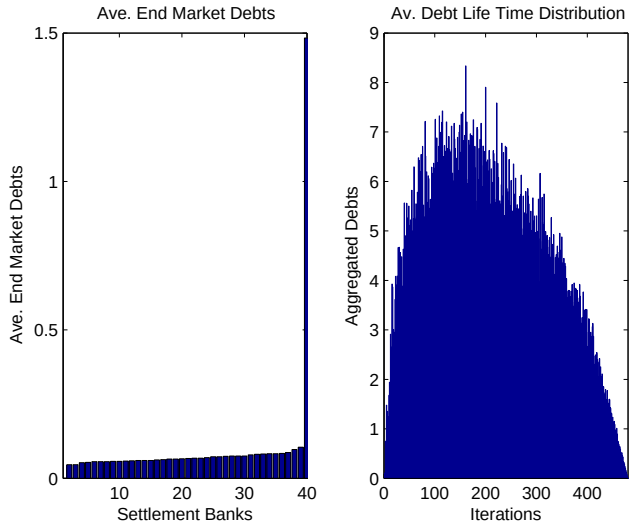

Figure 2.17: $n = 5$, $P_{ii} = \frac{1}{8}$, $p = 1.0$,$q = 0.2$

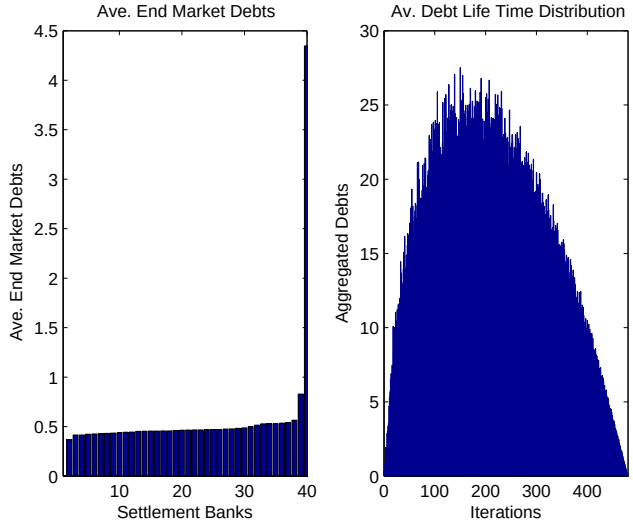

Figure 2.18: $n = 5$, $P_{ii} = \frac{1}{8}$, $p = 1.0$, $q = 0.5$

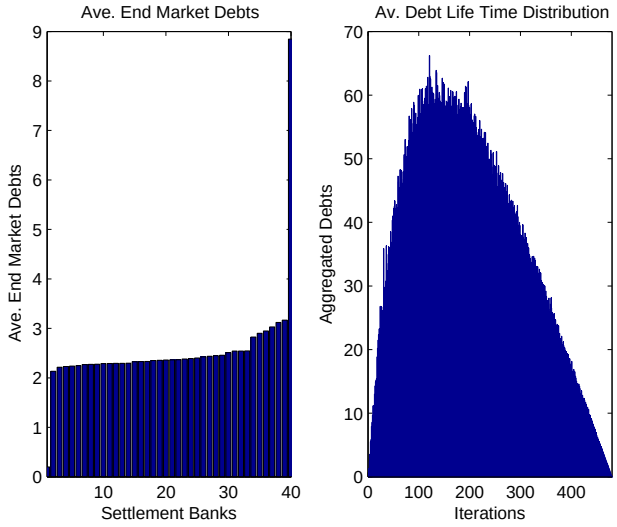

Figure 2.19: $n = 5$, $P_{ii} = \frac{1}{8}$, $p = 1.0$, $q = 0.9$

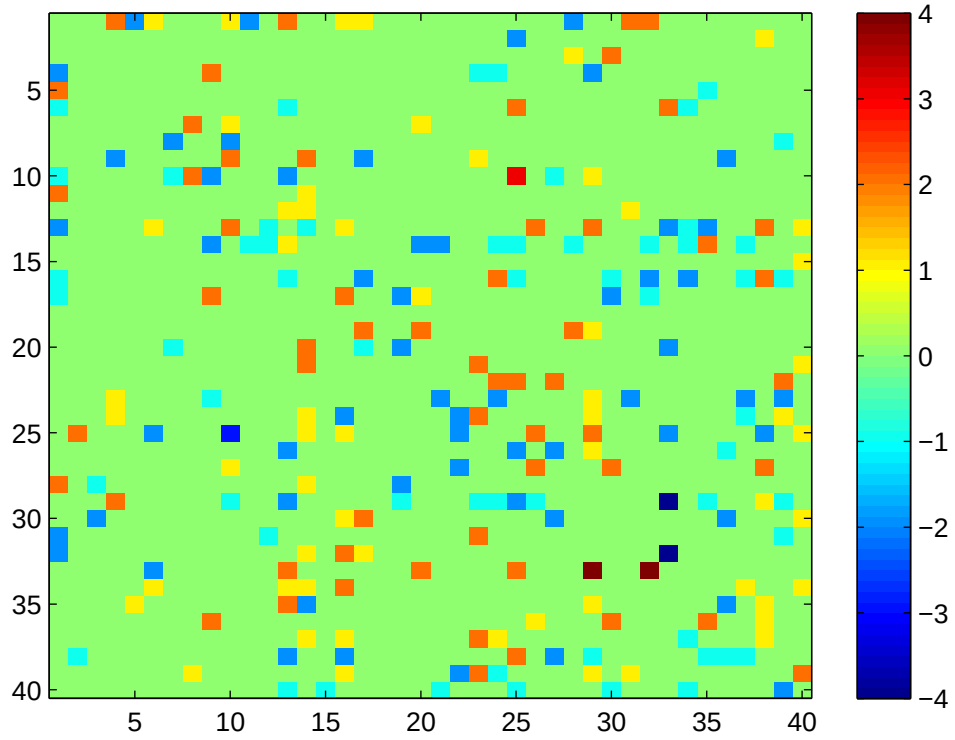

Figure 2.20: A distribution of end-of-the-day debts when $P_{ii} \neq \frac{n}{N}$

The results from the numerical experiments are analogical in the critical value case, and the histograms in the case where $n = 8$ are shown in Figure 2.21 - Figure 2.38, and Figure 2.39 - Figure 2.56 illustrate the results when there are 5 different groups of banks. In general, the end-of-the-day debts are positively related to the possibility of gaining one unit of cash at the very beginning under the same queueing strategy[7]. On the other hand, when the initial cash was distributed according to the parameter q, participating banks could send payments to central queue as less as possible to reduce the risk of unexpected amount of debts at the close of a business day. At all events, there is a dramatic boost for one anonymous member as seen in the extreme case.

[7]sending the same proportion of incoming payments to central queue

The distribution of average lifetime of all the debts in the entire system has changed from the case no inter-group banks are permitted. For a participating bank with constant possibility of getting one unit of cash, the more payments it submit to central queue, thinner the tail of the average lifetime distribution is, where the peak of the distribution moved away from zero, which means payments submit at the early stage of a day will be more likely to be settled, and late payments will be difficult to find available source[8] to be made. It was suggested that there is an incentive for participating banks to submit payments to central queue early to have the opportunity to have it settled.

The right-hand side histograms are right-skewed, hence, we fitted a Gamma distribution to the average lifetime distribution of a single debt where the parameters, shape parameter k and scale parameter θ, are estimated by the method of moments[9]. Table 2.2 lists the estimated Gamma distribution when there were 5 subgroups among the 40 banks, and Table 2.3 lists the result of the estimation in the case where 40 banks are divided to 8 subgroups. The fitted Gamma distributions are consisted with the pervious conclusions, once all the participating banks are allocated with $100p\%$ unit of cash, the Gamma distributions become less right-skewed when more and more payments have to rely on the central queueing facility. As the difference between the shape parameter k and scale parameter θ is minished along with increasing q when p is unchanged.

[8] cash or offsetting payments

[9] The reason of using method of moments estimation instead of other methods is the fact of the data collected from the simulations, it was unable to restore the original random variables from it

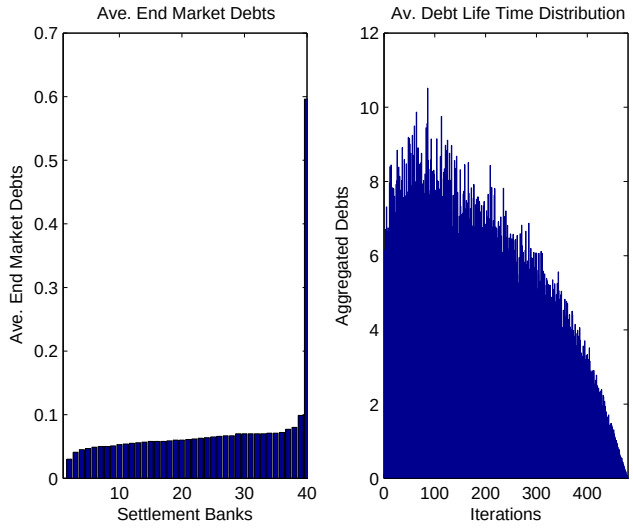

Figure 2.21: $n = 8$, $P_{ii} = 0.1$, $p = 0.3$, $q = 0.2$

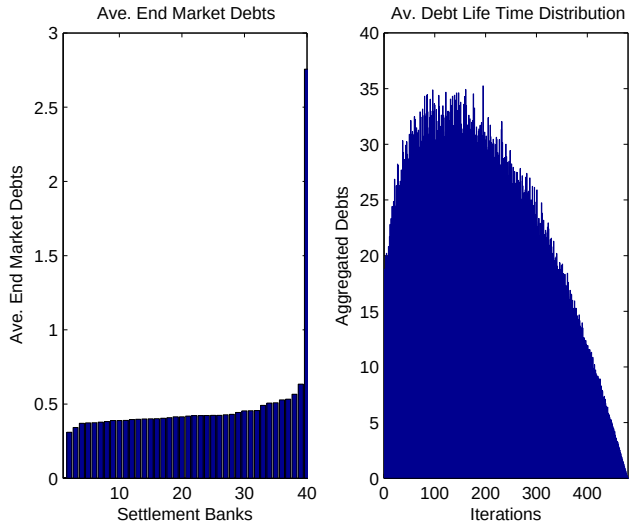

Figure 2.22: $n = 8$, $P_{ii} = 0.1$, $p = 0.3$, $q = 0.5$

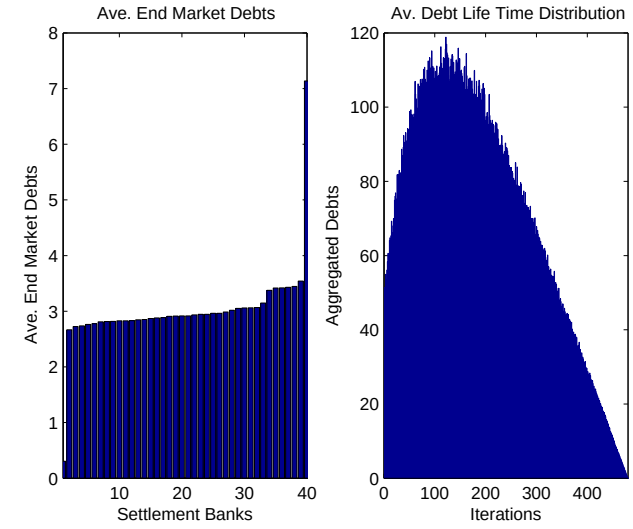

Figure 2.23: $n = 8$, $P_{ii} = 0.1$, $p = 0.3$, $q = 0.9$

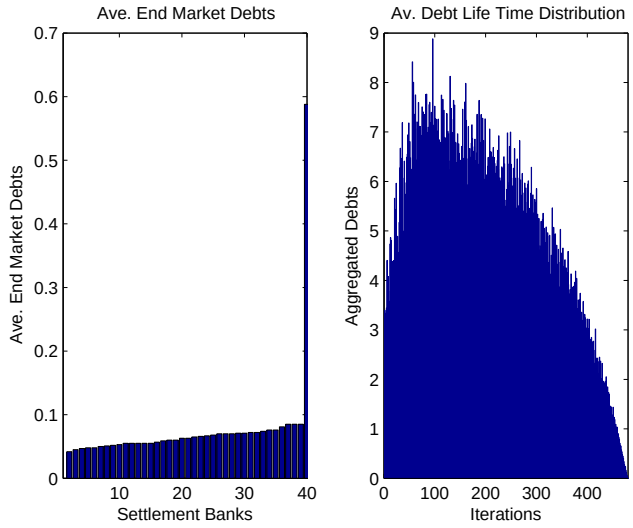

Figure 2.24: $n = 8$, $P_{ii} = 0.1$, $p = 0.7$, $q = 0.2$

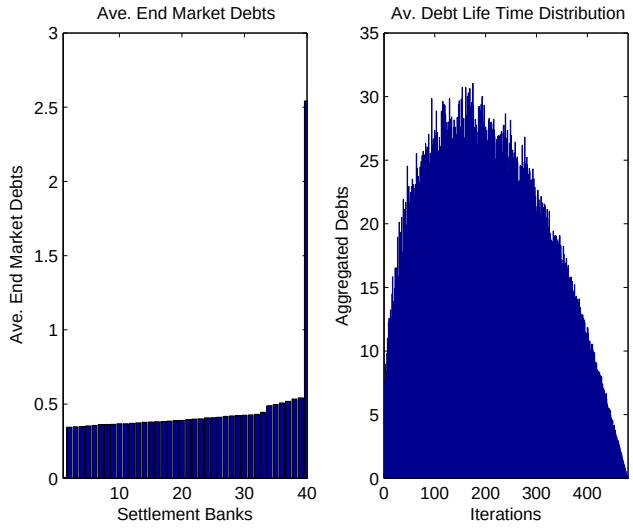

Figure 2.25: $n = 8$, $P_{ii} = 0.1$, $p = 0.7$, $q = 0.5$

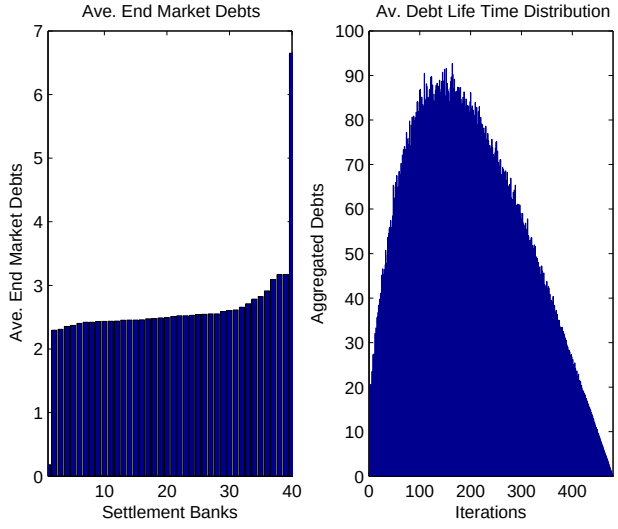

Figure 2.26: $n = 8$, $P_{ii} = 0.1$, $p = 0.7$, $q = 0.9$

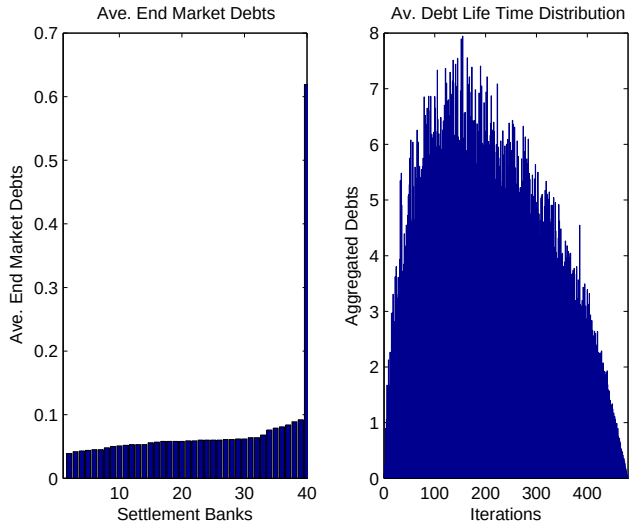

Figure 2.27: $n = 8$, $P_{ii} = 0.1$, $p = 1.0$, $q = 0.2$

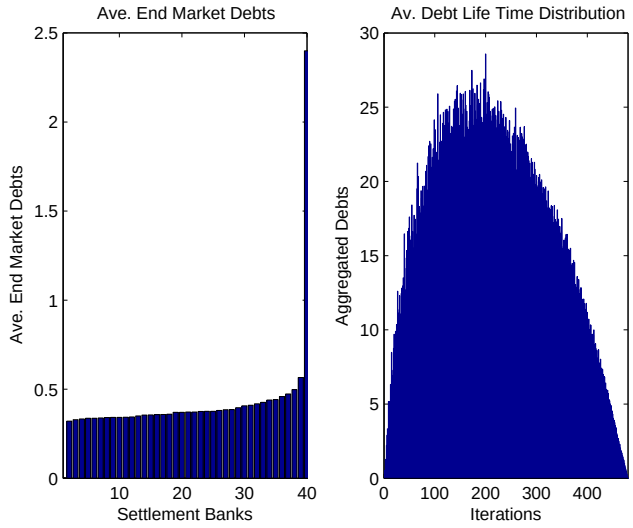

Figure 2.28: $n = 8$, $P_{ii} = 0.1$, $p = 1.0$, $q = 0.5$

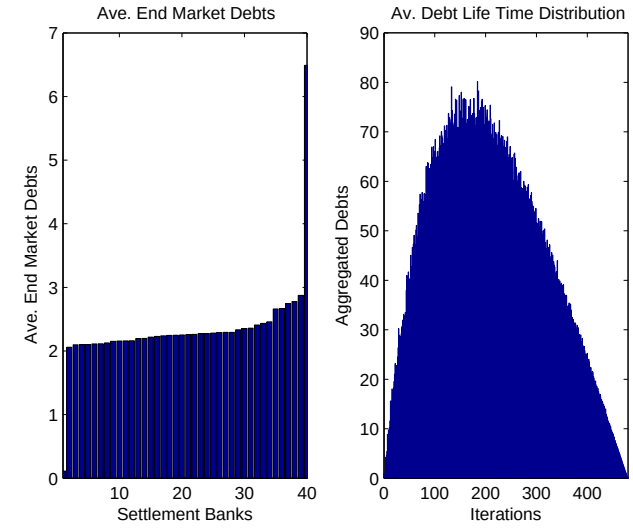

Figure 2.29: $n = 8$, $P_{ii} = 0.1$, $p = 1.0$, $q = 0.9$

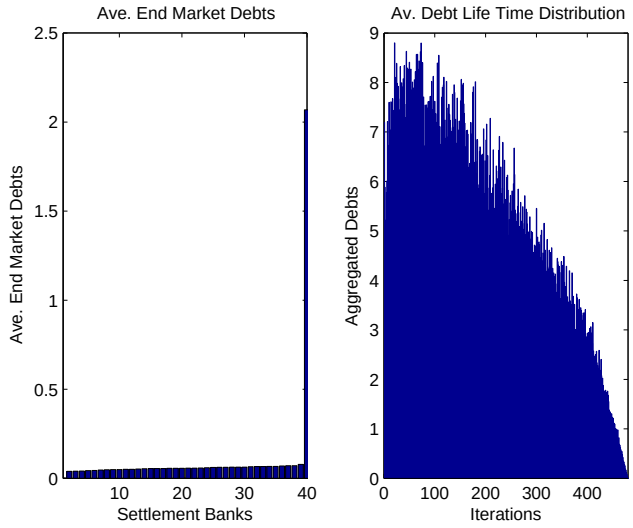

Figure 2.30: $n = 8$, $P_{ii} = \frac{1}{39}$, $p = 0.3$, $q = 0.2$

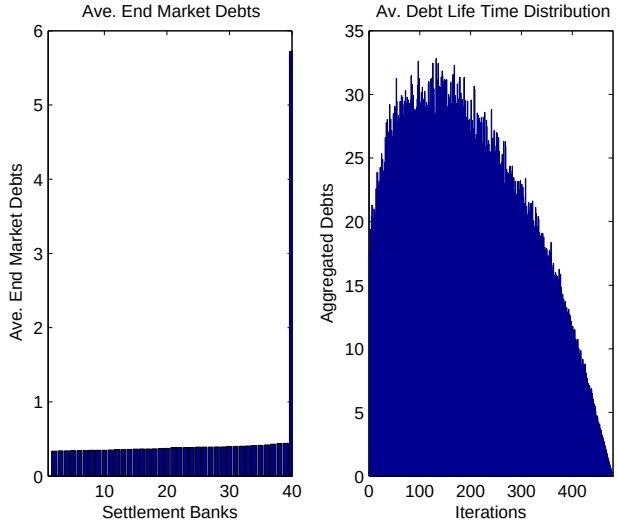

Figure 2.31: $n = 8$, $P_{ii} = \frac{1}{39}$, $p = 0.3$,$q = 0.5$

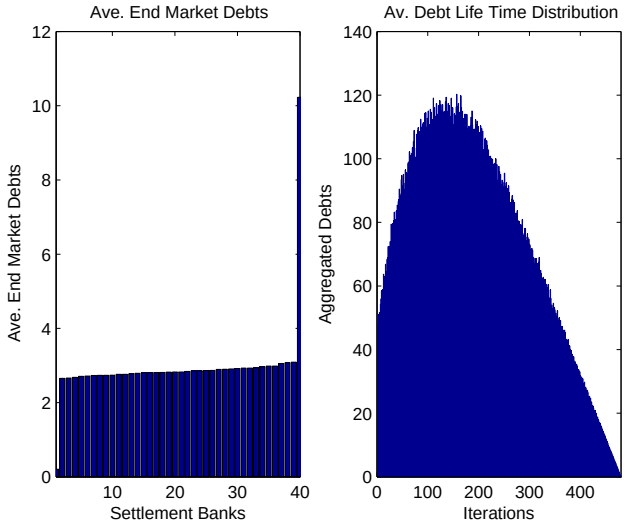

Figure 2.32: $n = 8$, $P_{ii} = \frac{1}{39}$, $p = 0.3$,$q = 0.9$

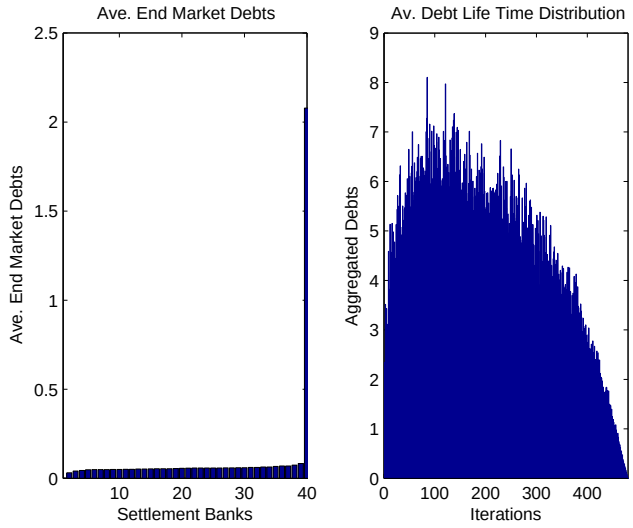

Figure 2.33: $n = 8$, $P_{ii} = \frac{1}{39}$, $p = 0.7$, $q = 0.2$

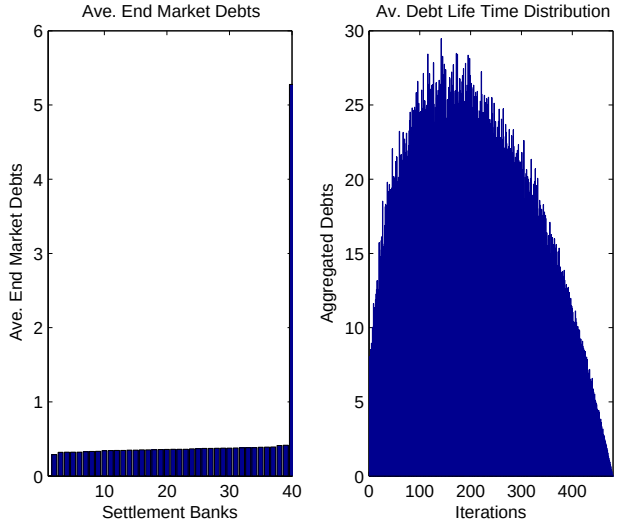

Figure 2.34: $n = 8$, $P_{ii} = \frac{1}{39}$, $p = 0.7$, $q = 0.5$

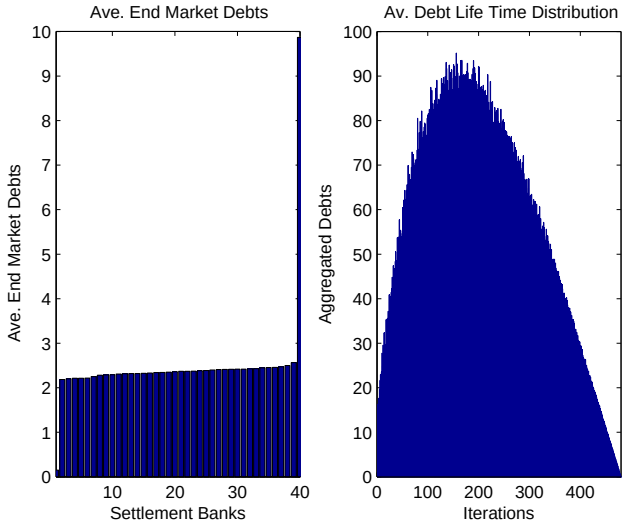

Figure 2.35: $n = 8$, $P_{ii} = \frac{1}{39}$, $p = 0.7$, $q = 0.9$

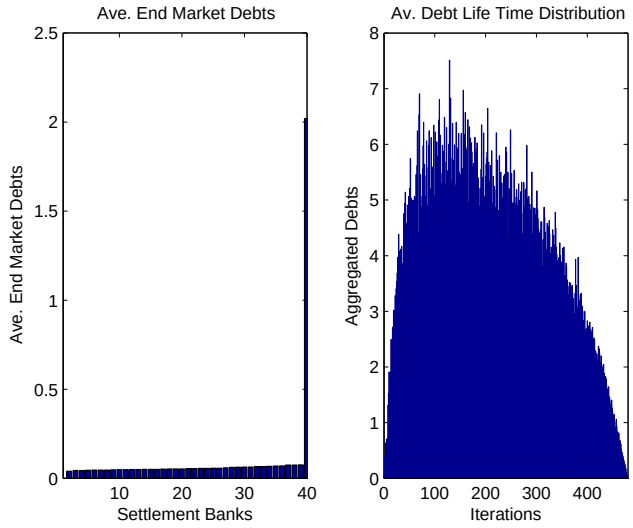

Figure 2.36: $n = 8$, $P_{ii} = \frac{1}{39}$, $p = 1.0$, $q = 0.2$

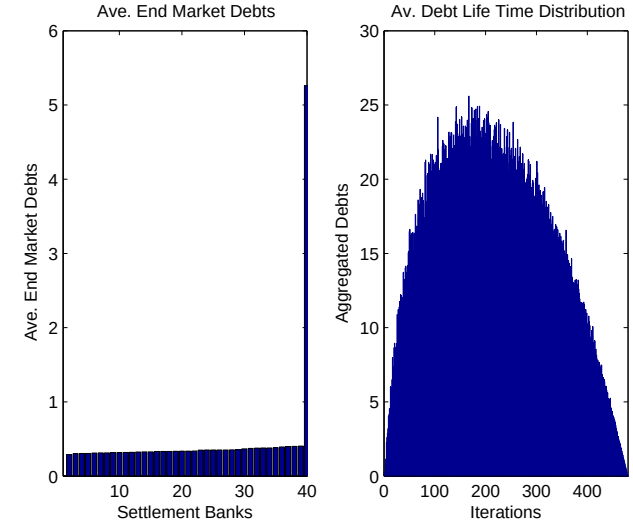

Figure 2.37: $n = 8$, $P_{ii} = \frac{1}{39}$, $p = 1.0$, $q = 0.5$

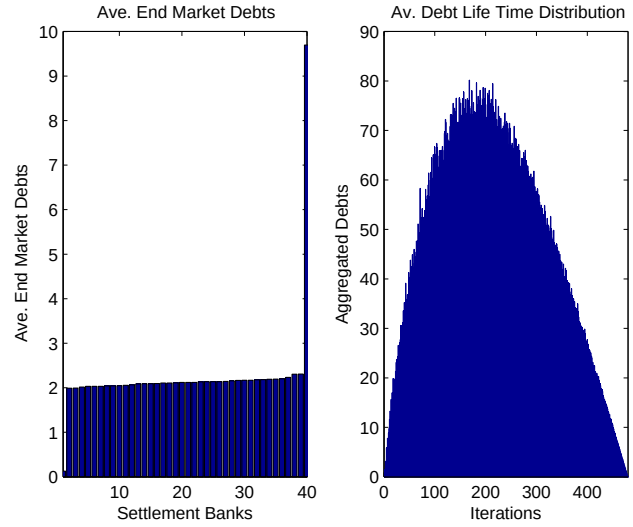

Figure 2.38: $n = 8$, $P_{ii} = \frac{1}{39}$, $p = 1.0$, $q = 0.9$

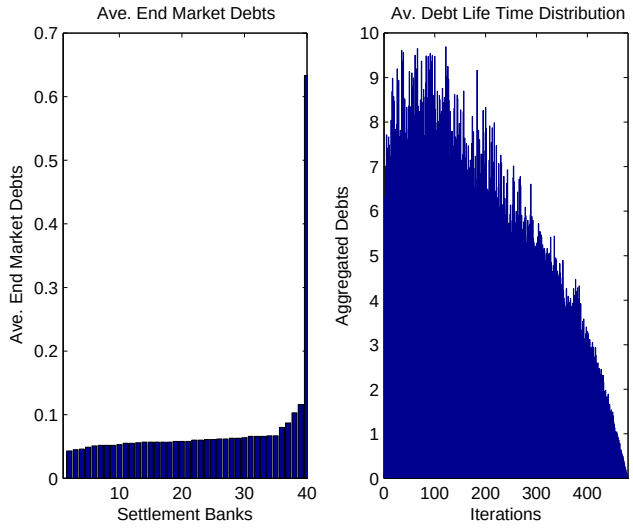

Figure 2.39: $n = 5$, $P_{ii} = \frac{1}{16}$, $p = 0.3$, $q = 0.2$

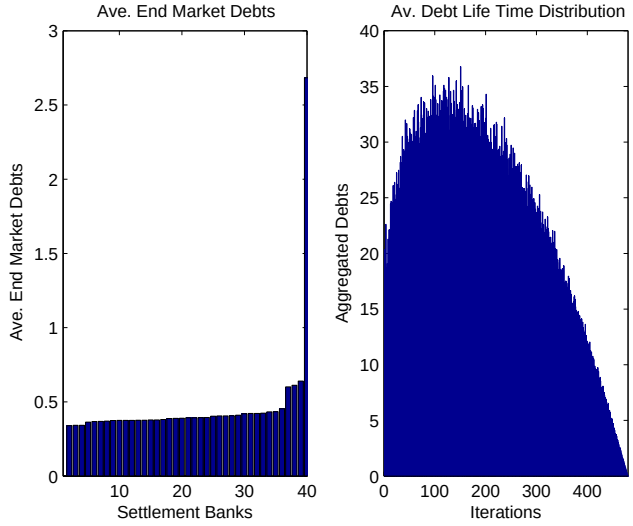

Figure 2.40: $n = 5$, $P_{ii} = \frac{1}{16}$, $p = 0.3$, $q = 0.5$

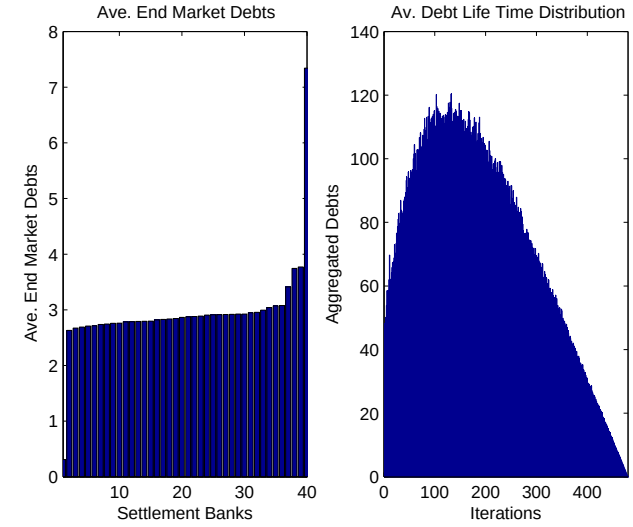

Figure 2.41: $n = 5$, $P_{ii} = \frac{1}{16}$, $p = 0.3$, $q = 0.9$

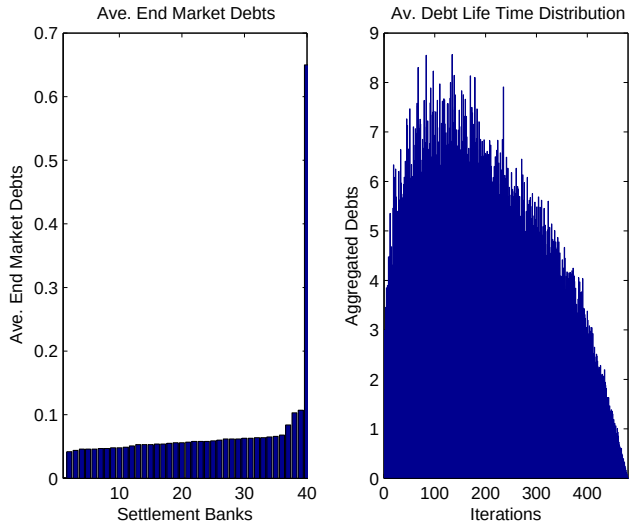

Figure 2.42: $n = 5$, $P_{ii} = \frac{1}{16}$, $p = 0.7$, $q = 0.2$

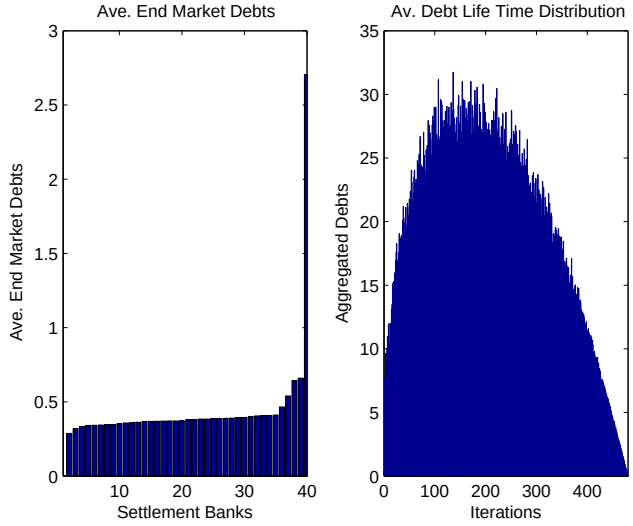

Figure 2.43: $n = 5$, $P_{ii} = \frac{1}{16}$, $p = 0.7$, $q = 0.5$

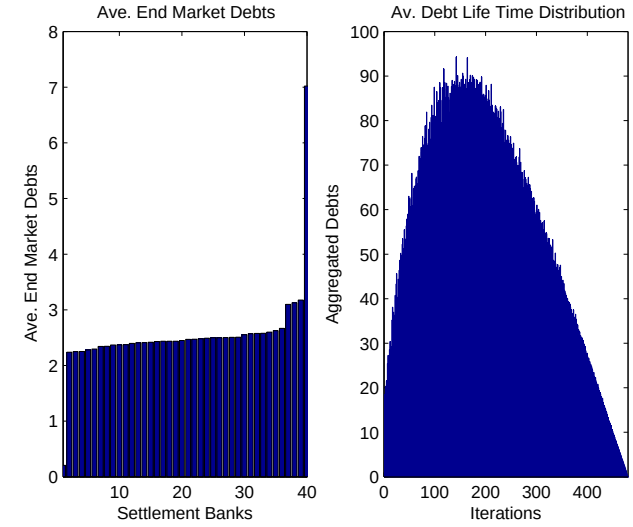

Figure 2.44: $n = 5$, $P_{ii} = \frac{1}{16}$, $p = 0.7$, $q = 0.9$

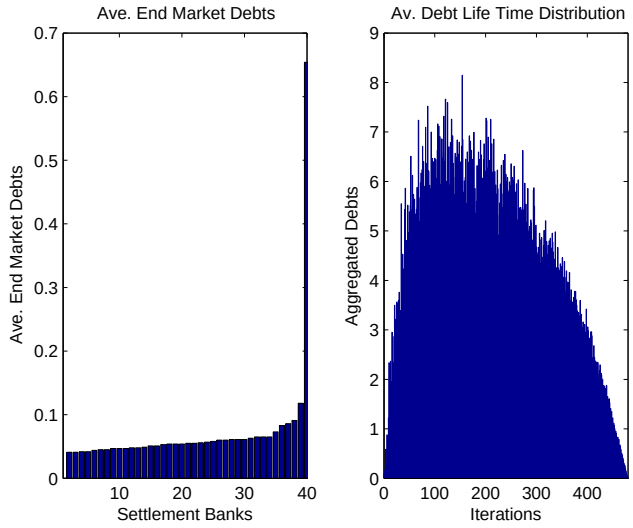

Figure 2.45: $n = 5$, $P_{ii} = \frac{1}{16}$, $p = 1.0$, $q = 0.2$

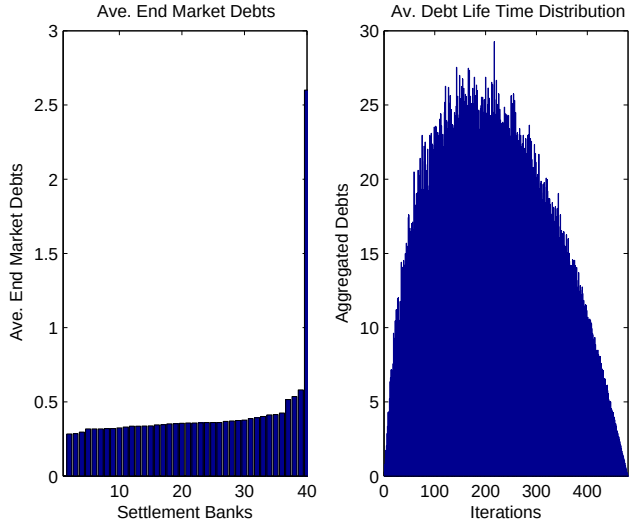

Figure 2.46: $n = 5$, $P_{ii} = \frac{1}{16}$, $p = 1.0$, $q = 0.5$

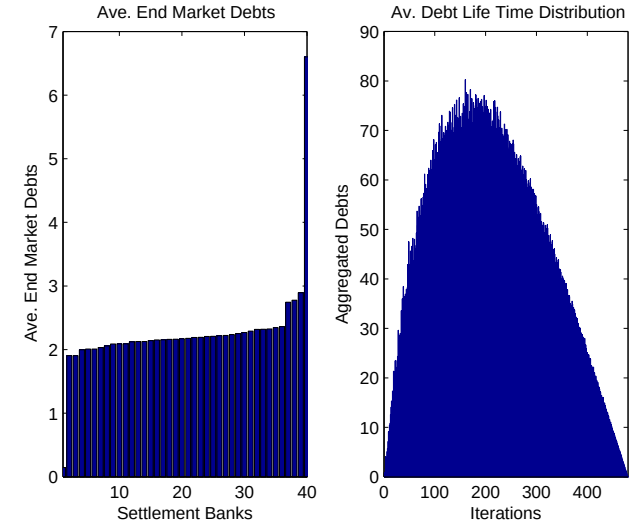

Figure 2.47: $n = 5$, $P_{ii} = \frac{1}{16}$, $p = 1.0$, $q = 0.9$

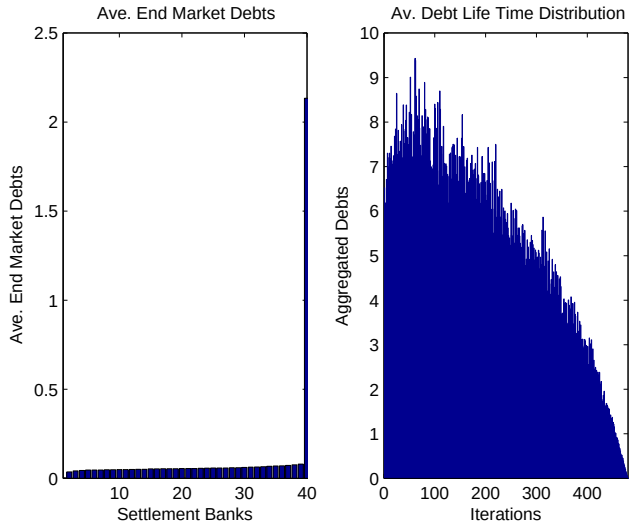

Figure 2.48: $n = 5$, $P_{ii} = \frac{1}{39}$, $p = 0.3$, $q = 0.2$

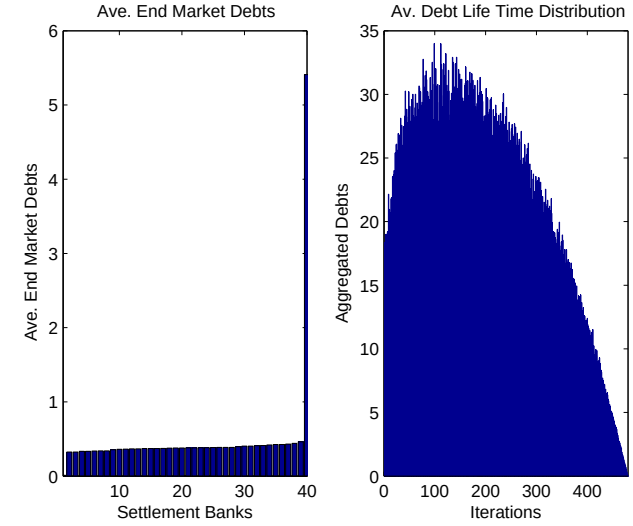

Figure 2.49: $n = 5$, $P_{ii} = \frac{1}{39}$, $p = 0.3$, $q = 0.5$

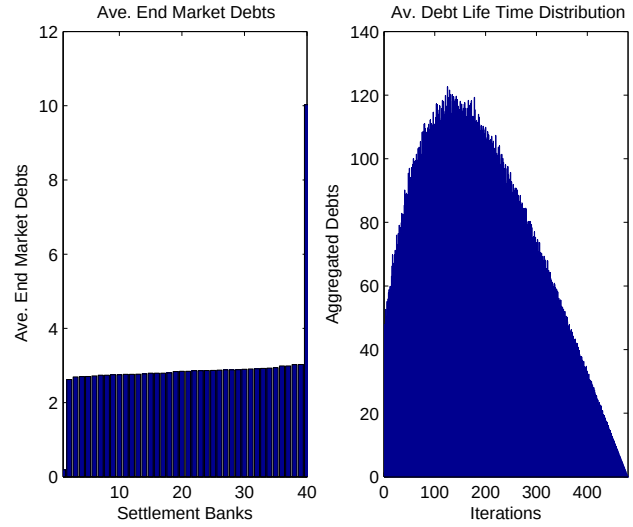

Figure 2.50: $n = 5$, $P_{ii} = \frac{1}{39}$, $p = 0.3$, $q = 0.9$

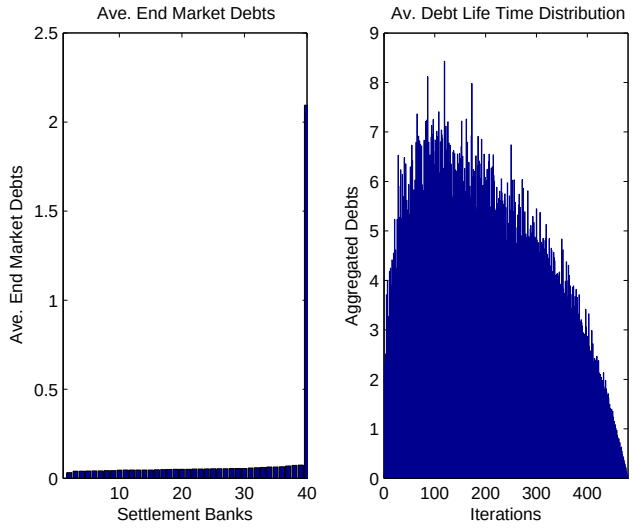

Figure 2.51: $n = 5$, $P_{ii} = \frac{1}{39}$, $p = 0.7$, $q = 0.2$

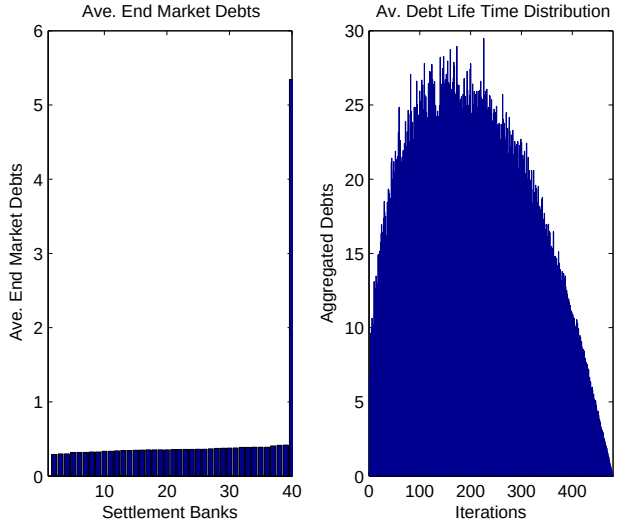

Figure 2.52: $n = 5$, $P_{ii} = \frac{1}{39}$, $p = 0.7$, $q = 0.5$

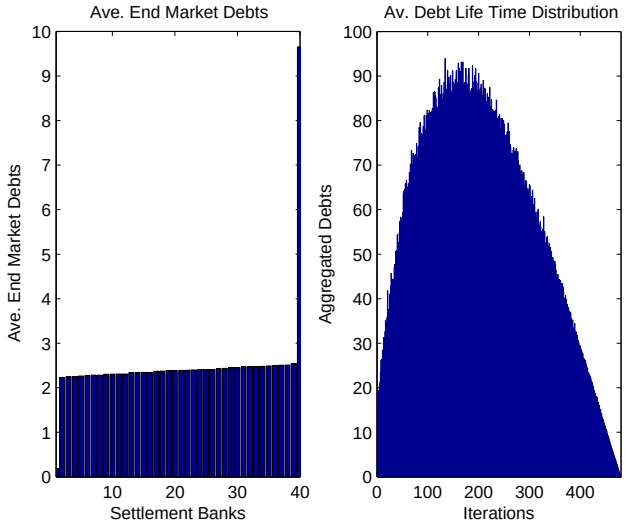

Figure 2.53: $n = 5$, $P_{ii} = \frac{1}{39}$, $p = 0.7$, $q = 0.9$

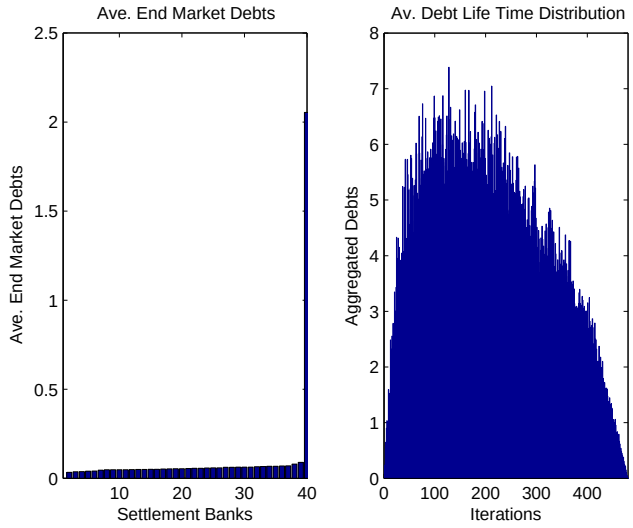

Figure 2.54: $n = 5$, $P_{ii} = \frac{1}{39}$, $p = 1.0$, $q = 0.2$

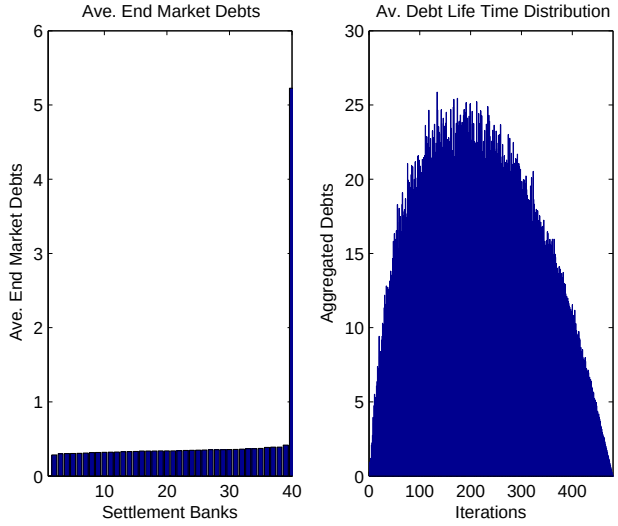

Figure 2.55: $n = 5$, $P_{ii} = \frac{1}{39}$, $p = 1.0$, $q = 0.5$

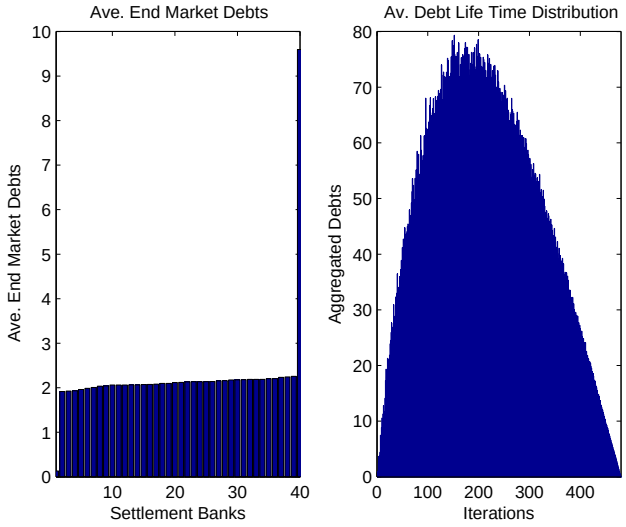

Figure 2.56: $n = 5$, $P_{ii} = \frac{1}{39}$, $p = 1.0$, $q = 0.9$

P_{ii}	p	q	$\hat{k}$	$\hat{\theta}$
	1	0.9	4.0297	52.5439
	1	0.5	3.7993	56.6558
	1	0.2	3.4175	61.7267
	0.7	0.9	3.4259	58.3498
$\frac{1}{16}$	0.7	0.5	3.3221	62.1027
	0.7	0.2	2.9681	67.5149
	0.3	0.9	2.9109	64.2137
	0.3	0.5	2.8906	67.2747
	0.3	0.2	2.4802	75.9005
	1	0.9	4.1339	51.8969
	1	0.5	3.8536	56.3957
	1	0.2	3.3846	62.5070
	0.7	0.9	3.5590	57.2439
$\frac{1}{39}$	0.7	0.5	3.3281	61.9059
	0.7	0.2	2.8119	70.8081
	0.3	0.9	3.0262	63.0463
	0.3	0.5	2.8852	67.8596
	0.3	0.2	2.4452	76.6149

Table 2.2: Estimated parameter for Gamma distribution when 40 banks dividing to 5 groups

2.5 Conclusions

In this chapter, we have proposed two discrete time Markov-type models to the Real Time Gross Settlement payment system with queueing facilities. Comparing with the simple homogeneous model, in the modified "cluster" model, the participating banks are not identical, they have been classified into different groups according to the corresponding business management, therefore, the payment flows are not distributed evenly in the system. The model takes the management of the central bank for each group into account.

It has been found that debts are settled at the end of the experiment after 480 iterations, the average number of debts per bank at the end of a business day depends on the parameters. The model has shown an significant linear relationship

P_{ii}	p	q	$\hat{k}$	$\hat{\theta}$
$\frac{1}{10}$	1	0.9	3.9171	53.4689
	1	0.5	3.8911	55.6918
	1	0.2	3.4052	62.1144
	0.7	0.9	3.3762	58.7325
	0.7	0.5	3.3683	61.4826
	0.7	0.2	2.9136	68.4730
	0.3	0.9	2.8502	64.9207
	0.3	0.5	2.8918	67.6019
	0.3	0.2	2.5429	74.3532
$\frac{1}{39}$	1	0.9	4.1150	52.1354
	1	0.5	3.8718	56.3658
	1	0.2	3.3084	63.8024
	0.7	0.9	3.5684	57.1059
	0.7	0.5	3.3408	61.9793
	0.7	0.2	2.8420	69.4956
	0.3	0.9	3.0195	63.1586
	0.3	0.5	2.8805	67.8822
	0.3	0.2	2.4075	77.0545

Table 2.3: Estimated parameters for Gamma distribution when 40 banks dividing to 8 groups

phenomenon for the position of end-of-the-day debts after the Monte Carlo iterations in the critical case corresponding to $P_{ii} = \frac{n}{N}$, moreover, the linear function is independent of the rest of the parameters (n, p and q). In the sub-critical cases ($P_{ii} \neq \frac{n}{N}$), the linear relationship does not appear. Note that the simulation results suggest that the proposed model is stable, since the distribution reaches an equilibrium (getting to zero) regardless the values of the parameters.

The characteristics feature of the "cluster" model could help not only the headquarters of each groups of banks but also the central bank to make decisive policies on queueing and borrowing in order to control the payment flows, therefore, manage the liquidity risk of a system. More comprehensive discussion on the strategy by participants and central bank is present in Chapter 3.

Chapter 3

Simulation approach to a payment system with Liquidity Saving Mechanisms

A specified liquidity saving mechanism is implement to a "cluster" model that captures the most significant features of the UK Real Time Gross Settlement payment system, CHAPS, as a remedy for the risk of lacking liquidity because of the reform.

3.1 Overview of Liquidity Saving Mechanisms

3.1.1 Liquidity risk in large-valued payment system

With Real Time Gross Settlement (RTGS) systems having replaced the netting settlement systems around the world[1], the attention and concern have shifted from credit risk to liquidity risk. This is because in an RTGS system, payments are settled on a real time individual basis. It prevents the considerable credit exposures between

[1]By the end of 2006, 93 of world's 174 central banks were using RTGS systems already [8].

banks, hence the credit risk to receiving banks is eliminated. In the mean time, banks are required to post a large amount of liquidity to meet all their obligations. As a result, the settlement banks' behavior may depend on the cost of liquidity[2]. A number of piece of existing literature [3], [7], [16] and [64] has emphasized the risk of high liquidity cost. The high liquidity cost will force banks to delay their payments, and wait for incoming payments to sufficiently cover them. In the extreme, the delay can lead to girdlock. According to Furfine and Stehm, gridlock is the situation where the failure of some transfer instructions to be executed prevents the execution of a substantial number of other instructions [28]. On the other hand, banks may find delay is costly. Some payments are urgent according to some definitions: failing to make these, banks will face some financial penalty or reputational damage. If the information about the bank's delay behavior is observable by other banks, others may wish to withhold payments to it. A remedy for this problem is to introduce a central managed queue, which would hold any payments either insufficient funds available or that do not need to settle immediately. Such a central queue is called Liquidity Saving Mechanism (LSM).

3.1.2 Introduction to Liquidity Saving Mechanisms

In contrast to the standard theory of inter temporal trade, there is no market for short-term (intraday) credit in interbank payment systems. Instead, under particular arrangements, banks can borrow from the central bank at a fixed price or delaying payments till sufficient funds are available towards the end of a business day. Improving the flow of payments is one of the important concern for the policy markers at central bank. The traditional approach, netting settlement systems, was seen by policy markers as too prone to cascades of defaults. On the other hand,

[2]banks may choose to delay settlement, awaiting the flow of incoming funds

while the risk of cascades of defaults was eliminated in RTGS system, banks require large amount of liquidity[3], consequently it increases the cost of making payments and potentially increases liquidity risk faced by banks. In broad terms, an archetypal LSM aims to combine the advantages of net settlement and RTGS system. In other words, the central queue is intended to combine the reduced credit risk in RTGS system and the significantly lower amount of liquidity required in Deferred Settlement Netting (DNS) payment system.

Liquidity Saving Mechanisms have been on the agenda of policy markers for about a decade, and now many large-valued interbank payment systems already have embedded different centeralised queue facilities as a complement to their RTGS systems[4]. There are two main types of hybrid systems which combining the advantages of DNS and RTGS systems. One is the Continuous Net Settlement (CNS)[5], which has been developed from DNS. The settlement risk is dramatically reduced in CNS systems, however, it is not completely eliminated. The other type is an RTGS system with a queuing facility. The receipt-reactive gross settlement (RRGS) system [21] proposed by Ercevik and Jackson is an example of this type hybrid system. In this RRGS system conditions the settlement of queued payments on the arrival of incoming payments exclusively, which ensures the liquidity post by a bank is used to make time-critical payments only. For such RTGS system with queuing facility, the liquidity risk is reduced, while settlement risk does not rise, but banks may face extra costs on settlement delays. As in RTGS system, under the condition that sufficient fund is available, LSMs still provide banks the options between

[3]For example, according to Bank of England payments database, CHAPS banks require on average three times more liquidity under RTGS than they would have needed under a DNS

[4]For instance, European Central Bank launched TARGET 2 on 19 November 2007 and In October 2008, the Bank of Japan implemented Phase 1 of the Next-Generation RTGS (RTGS-XG) project, and Phase 2 of the project is scheduled for November 2011.

[5]the CHIPS system in the US is the leading example of a CNS

sending a payment directly and delaying the payment. Otherwise, in conjunction with collateral borrowing facilities, banks are still able to make urgent payments and pool others together in the central queue. The payments held in the central queue are released according to some pre-specified algorithms. The most important functionality of LSMs is bilateral/multilateral off-setting algorithm, by which banks do not need the full funds to cover their queued payments: if the payment(s) is a link of a bilateral/multilateral cycle of payments, then banks need the net amounts only to settle the payments belonging to the cycle. Consequently, LSMs attempt to reduce the demand for intra-day liquidity in RTGS system. But banks still are able to make time-critical payments via RTGS system, for example, via liquidity reservation functionality. The ways of defining a time-critical payment depend on several factors. a) special-purpose payments, for instance, the payments to CLS[6] in CHAPS, b) some extreme large payments, c) urgent customer payments *etc* [41].

The LSM research in this chapter satisfies all these criteria. With central queue facility, it promises to reduce the liquidity by releasing payments via bilateral and multilateral algorithms upon the arrival of an individual payment on a continuous basis. Specifically, we are going to consider the implement of a LSM to the UK RTGS system, CHAPS (Clearing House Automated Payment System)[7], and simulating a simple system of payment flows that captures the most significant feature of CHAPS.

[6]CLS is the Continuous Linked Settlement system which provides payments settlement of FX transactions

[7]It is worth mentioning that although CHAPS does feature a central queue, it is not considered to be a hybrid system in most circumstance, banks prefer to queue payments in their internal schedulers rather than submitting them to the central queue. A gridlock has never occurred by far, due to the posting of ample amounts of liquidity by CHAPS banks at the beginning of each day.

3.2 Liquidity Saving Mechanisms

3.2.1 Assumption

CHAPS Sterling system, the UK RTGS system, is one the largest of its kind in the world. According to the empirical studies in Chapter 2, payments are not generally evenly distributed among members of a payment system. At the time the work was carried out, CHAPS comprised 14 members, About 80% of payments in CHAPS is dominated by four banks in terms of both value and volume over the period from July 2005 to June 2006. The number of settlement banks has increased from 14 to 18[8] since 2008. Based on the fact that the payment flows in CHAPS form a well-connected network and the properties change little from day to day [9], we are still going to consider a network that consists of 14 members. So in this simulation, 14 banks are split into two groups: one has the four largest banks and the other contains the rest. When a big bank plans to make a payment, the probability for the payee to be another big bank is 0.8, and to one of the small banks is 0.2. But when small banks think about to make payments, all banks are equally likely to be the recipient. In other words, from the groups of banks' point of view, the transition probability matrix[9] looks like

$$\begin{array}{cc} & \begin{array}{cc} big\ group & small\ group \end{array} \\ \begin{array}{c} big\ group \\ small\ group \end{array} & \begin{pmatrix} 0.8 & 0.2 \\ 0.5 & 0.5 \end{pmatrix} \end{array}$$

Within each group, these probabilities of receiving payments from different banks

[8] Abbey, ABN Amro Bank quit the system since 2008 and Danske Bank (Northen Bank) and J. P. Morgan are the new members, the rest of the system are: Bank of America Merrill Lynch, Bank of England, HBOS, Barclays Bank, Citibank, CLS, Clydesdale, The Co-operative Bank, Deutsche Bank, HSBC Bank, Lloyds TSB Bank, NatWest Bank, RBS, Santander UK, Standard Charterd Bank and UBS

[9] rows are sending banks, and columns describe the receiving banks

are equally distributed. In general, the transition matrix has the form of

$$\begin{bmatrix} A_{11} & A_{12} \\ A_{21} & A_{22} \end{bmatrix} \tag{3.1}$$

where

- A_{11} is a 4×4 matrix where diagonal entries are 0 and the rest is $0.267(= \frac{0.8}{3})$;
- A_{12} is a 4×10 matrix and all the entries equal to $0.02(= \frac{0.2}{10})$;
- A_{21} is a 10×4 matrix and all the entries equal to $0.077(= \frac{1}{13})$;
- A_{22} is a 10×10 matrix with zero diagonal entries and the rest is $0.077(= \frac{1}{13})$

In order to investigate the efficiency of the off-setting algorithms, all payments are assumed to have unit value. At the end of this chapter, we will discuss our result that used artificial data in the comparison with a pervious studies using historical data by Ercevik and Jackson [21].

3.2.2 Simulation

In the proposed model, the central bank observes the system from the outside. The central bank acts as a regulator to whom all the information about the past and present states of the network is available.

The system evolves in a discrete time with each time slot being numbered. Every payment is characterised by

- The time when the payment occurs;
- the payer and payee of the payment;

- the type of the payment (Time-critical payments are type I payments, while others are non-type-I payments).

At each step of the process, a bank, say m, receives a payment order to transfer a monetary unit to another bank, n. The arrival of an order of payment from bank m to n results in appearance of a directed link $m \to n$. Then, according to its type[10], it will be submitted into the appropriate stream.

RTGS If the payment needs to be made via RTGS payment system[11], then the payment is completed by using the liquidity held by bank m, and the new link $m \to n$ is instantly settled. It is rare for banks to suffer from lack of liquidity in UK RTGS system, no queues will not be considered here.

LSM If the payment is not urgent, the payment is submitted into the LSM. First of all, the programme performs the search of the shortest cycle[12] of payments which is established by the newly arrived payment. In other words, to check if there already exist bilateral off-setting payments first, and then trilateral payments and so on. If the programme is successful in identifying a cycle, payments which are parts of the bilateral/multilateral cycle are cleared without using any liquidity due to the unit value assumption. Delayed payments are settled by a First-In-First-Out rule. Otherwise, the payment is kept at the central queue at the moment and labeled by the submission time.

This completes a single Monte Carlo simulation step. A complete description of the simulation is included in Appendix B.1.

[10] determined by the simulation

[11] there are several different managements of incoming payments, but here the strategy used by all settlement banks is the same, under which they want to achieve that $X\%$ of payments by volume are made immediately using RTGS

[12] a cycle is the path where the start node and end node are the same

The experiment is to simulate a system that consists of 14 banks with 8400 payments[13], and the results are averaged over 200 repetitions[14].

Our aim is to investigate the potential benefits of implementing a central queueing facility to a system that believed as a proxy of CHAPS. An important parameter is the proportion of payments that are time-critical, denoted as q, i.e. $(1-q)100\%$ is the percentage of payments that is going to submitted to LSM. The numerical experiments are performed for $q = 0, 0.2, 0.4, 0.6, 0.8$ and 1 respectively.

3.2.3 Results

The results are represented by the following figures and table:

1. In Figure 3.2 - 3.6, each pair of plots represents the result when q equals a particular value. In the left subplot, the average volumes of ultimate delayed payments, i.e. the payments left in the LSM queue at the end of the experiment, are shown together with the average volumes of net payments in RTGS. In the right subplots, there are the maximum values have ever shown during the experiment. Figure 3.1 consists of the corresponding plots of a pure RTGS system without central queueing facility. We are going to use it as a baseline against which to compare liquidity saving when LSM is introduced.

2. The snapshots, Figure 3.7 - 3.11, are used to present the bilateral position of end-of-the-day delayed payments, where the coordinate and colour of every box indicate the direction and volume of the payments respectively.

3. Figures 3.12 and 3.13 illustrate the efficiencies of the entire system and individual banks when q equals different values.

[13] 10 hours from 6am to 4pm and each bank makes a payment every minute

[14] with 200 iterations, a steady-state solution could be obtained, since over 200 iterations, the output of the simulation from one iteration to the next changes negligibly

4. Table 3.1 lists the mean numbers and probabilities of cycles with particular lengths.

Volumes and positions of end-of-the-day delayed payments

In Figures 3.2 - 3.6, we observe that the benefit of introducing the central queueing facility is not evenly distributed for al members of the system. Generally speaking, the banks that dominated approximately 80% of the payments are less capable to save liquidity under the proposed LSM. The number of delayed payments in LSM is more for big banks than small banks, the difference keep growing when more and more payments are sent to central queue. For small banks, the average saving liquidity is not significant, however, as less payments need to be settlement immediately, the total liquidity requirement will be dropped slightly. A possible interpretation of why different size banks act differently with this particular LSM, particularly, why big banks suffer from extra liquidity requirement is that the payments which big banks were expected and would have been received from other members in a pure RTGS system have been sent to the central queue instead. In a pure RTGS system, with these payments, large banks would be able to finance some of them outgoing payments, and it is no longer the case in the hybrid system. Nevertheless, banks are still obligated to make the time-critical payments regardless the statues of the system. Hence, big banks have to use liquidity reservation functionality to settle those incoming payments. Small banks would not face a breakdown as serious as big banks has, because of the relatively small number of payments that small banks involved. By adding up the RTGS payments on top of LSM payments, the average amount of liquidity required so that banks are able to meed their targets set in advance[15] is given.

[15]zero unilateral balance

Figure 3.1 provides an idea of how much liquidity would be needed to reserve in a pure RTGS system on average and at maximum, with which we could identify some necessary change of liquidity reservation in a hybrid system with different queueing management. The figures illustrated that both average and maximum liquidity have increased in a manner that inversely correlated with q, in other words, the number of payments submitted into LSM stream.

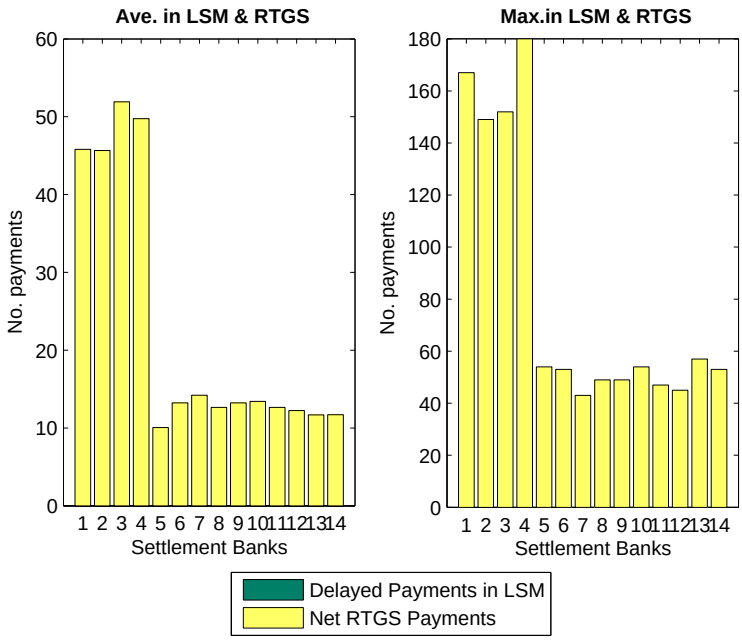

Figure 3.1: Average and maximum volumes of payments in pure RTGS

In addition to the requirement of liquidity, banks could thereby briefly make individual conclusions on how to manage their liquidity to achieve minimum ultimate delayed payments. According to Figures 3.2-3.5, the sufficient liquidity required does not need to be justified on a daily base, since both big and small banks expect similar amounts of permanent delayed payments in the course of the experiment, which implied the average amount is not influenced by bank's policy rapidly[16]. Otherwise,

[16]bank's target to make $X\%$ payments via RTGS

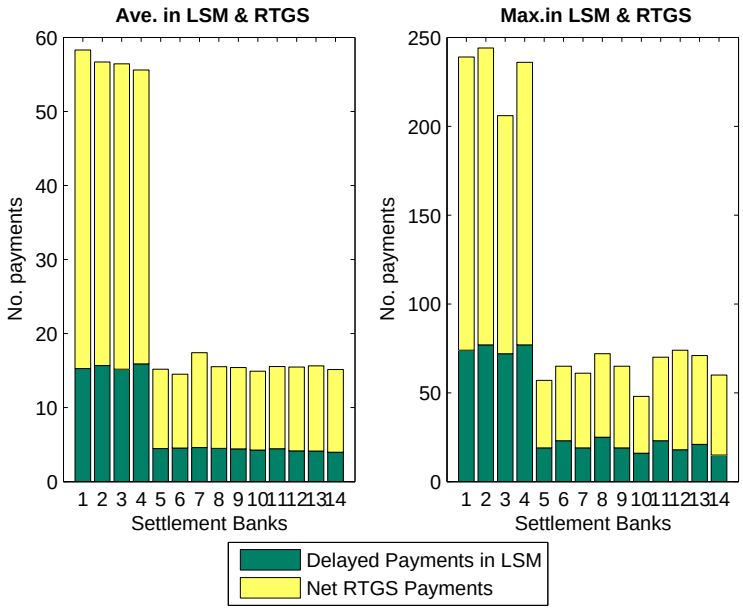

Figure 3.2: Average and maximum volumes of payments in RTGS and LSM $q = 0.2$

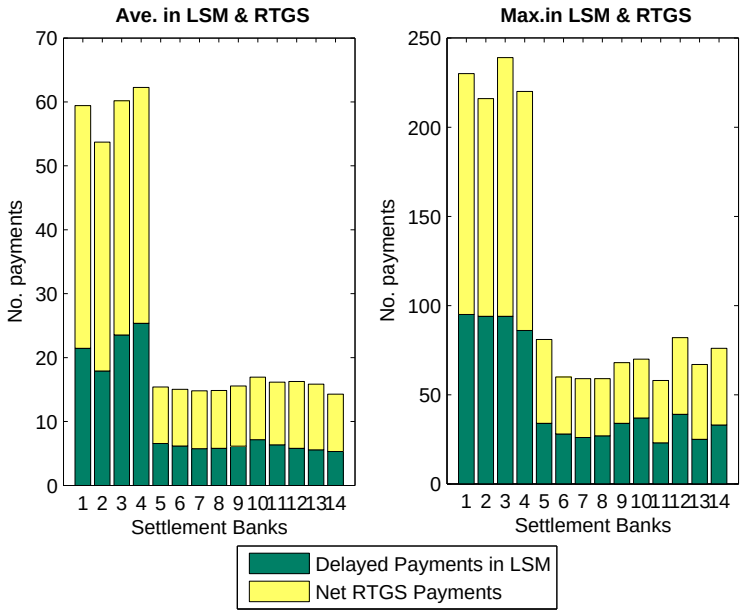

Figure 3.3: Average and maximum volumes of payments in RTGS and LSM $q = 0.4$

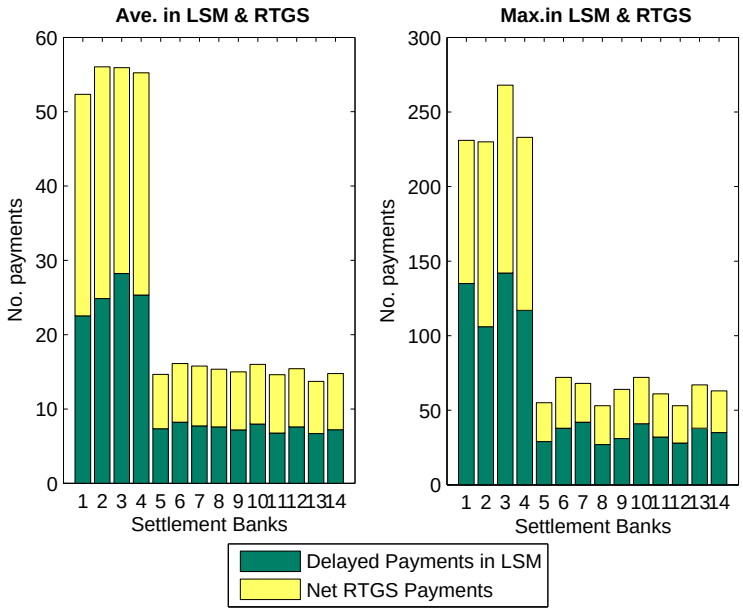

Figure 3.4: Average and maximum volumes of payments in RTGS and LSM $q = 0.6$

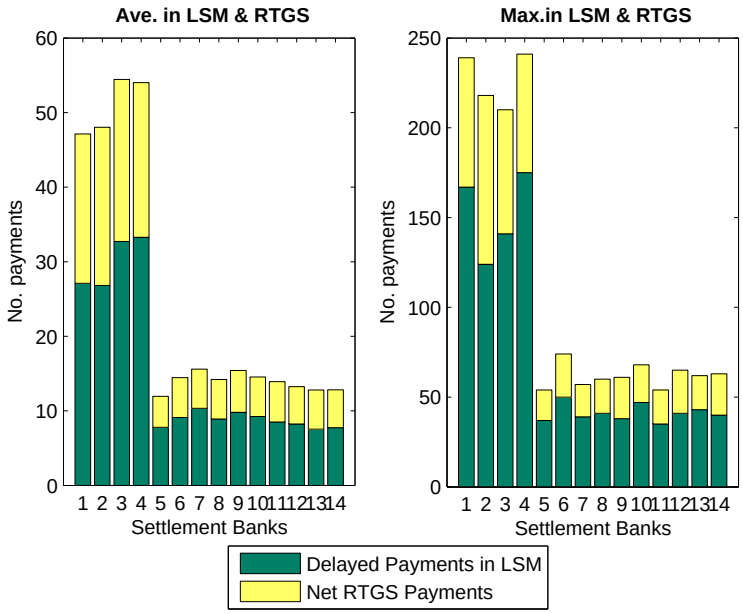

Figure 3.5: Average and maximum volumes of payments in RTGS and LSM $q = 0.8$

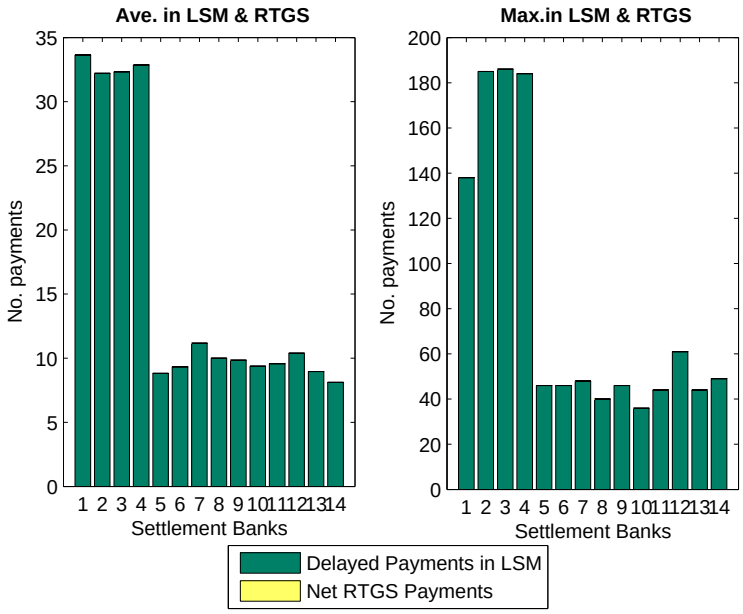

Figure 3.6: Average and maximum volumes of payments in pure LSM

bank could rely on others, as soon as some of the members use extra liquidity to make their end-of-the-day delayed payments, it could be able to use the incoming fund to cover its own queued payments. However, this is heavily dependent to the visibility of banks' behaviors: if a bank is unable to see the opportunity that some banks will use liquidity to clear their payments in the central queue, it would post extra liquidity itself to avoid any disappointment. Banks can also consider reserving liquidity according to the maximum valued obtained during the simulation, the right plots on Figures 3.2-3.6, to prevent any operational accidents.

Under the assumption that the transition probabilities (3.1) are not identical, payments are not equally distributed among banks: the snapshots, Figures 3.7-3.11, indicate where the end-of-the-day bilateral delayed payments are in each case. We notice that when banks are conservative about the central queueing facility, and only submit a small portion of their daily payments into LSM stream, most of the

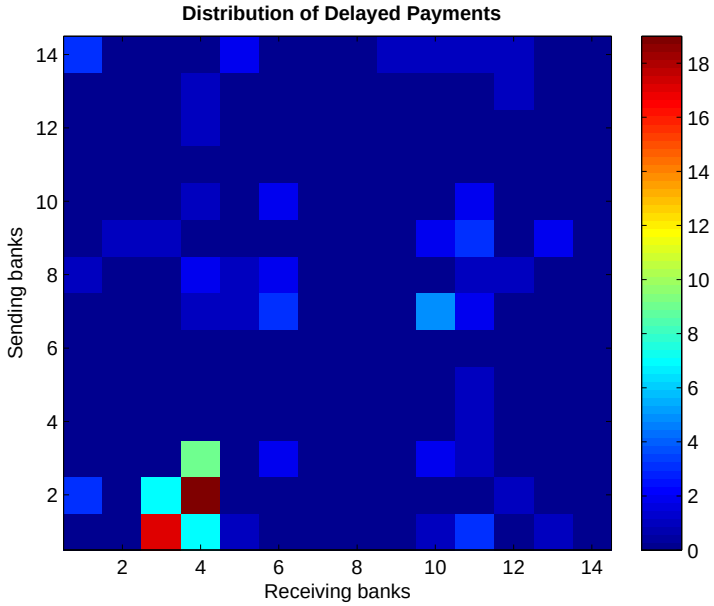

Figure 3.7: Distribution of end-of-the-day delayed payments $q = 0.2$

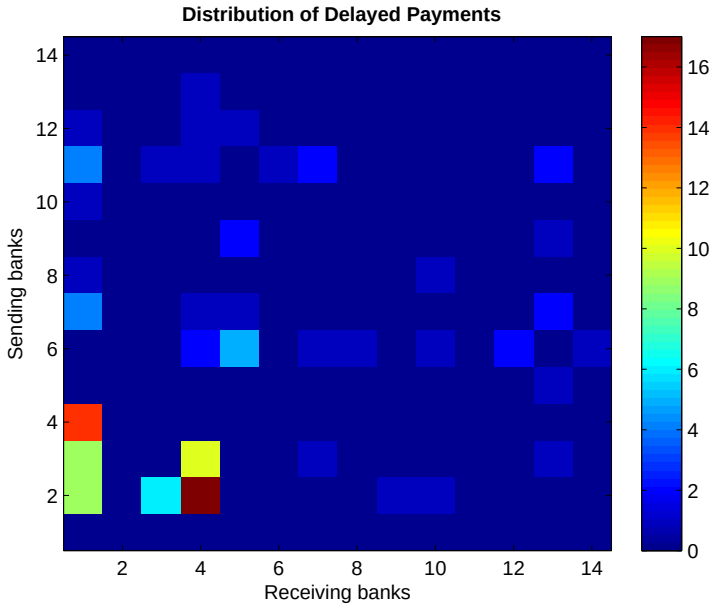

Figure 3.8: Distribution of end-of-the-day delayed payments $q = 0.4$

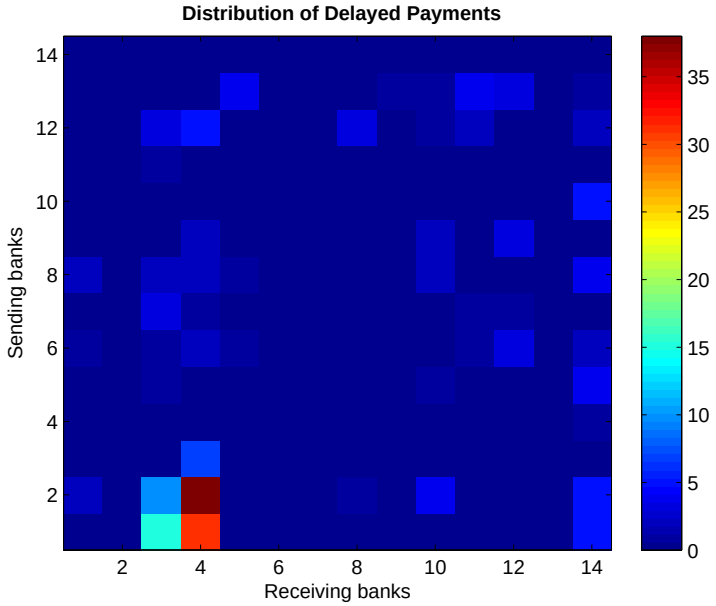

Figure 3.9: Distribution of end-of-the-day delayed payments $q = 0.6$

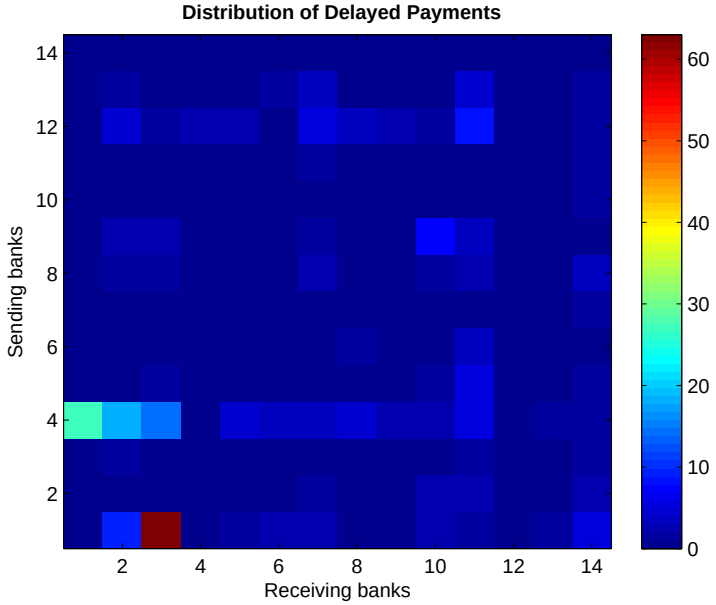

Figure 3.10: Distribution of end-of-the-day delayed payments $q = 0.8$

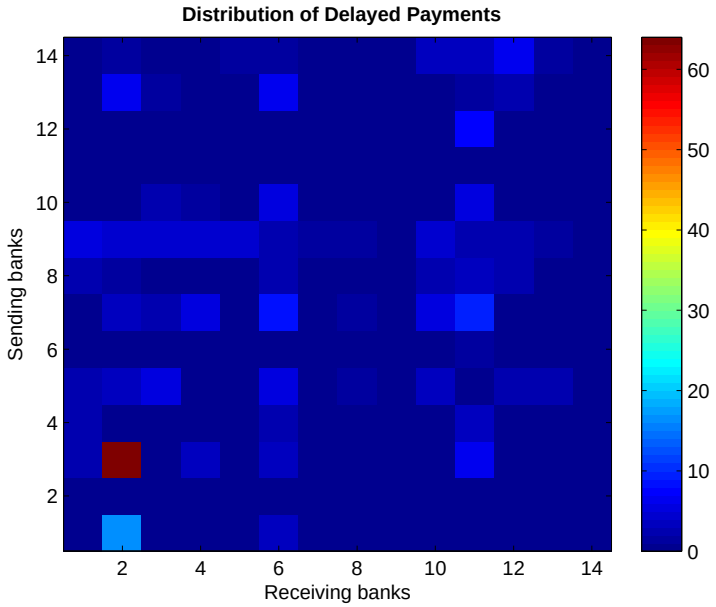

Figure 3.11: Distribution of end-of-the-day delayed payments $q = 1$

end-of-the-day delayed payments are distributed among these big banks, with more payments using LSM, the concentration of delayed payment is tend to be dissolved in the system. The figures suggest that it may be worth to consider an injection of liquidity by central bank periodically to some members of the system, with which could cut the number of delayed payment significantly.

Efficiencies of the LSM

We are also interested in investigating the efficiency of the LSM, let us define the efficiency, denoted by α, by

$$\alpha = \frac{\text{no. of payments solved with off-setting payments}}{\text{total no. of payments in LSM}} \times 100\% \qquad (3.2)$$

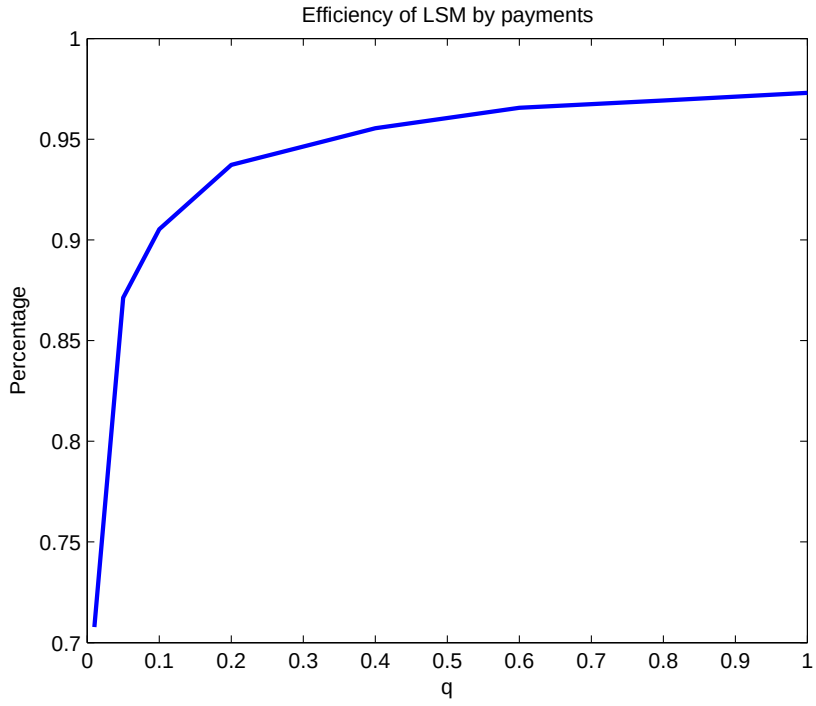

Figure 3.12: Efficiencies of LSM by payments

i.e., $\alpha = \frac{\bar{X}}{\bar{Y}} \times 100\%$, where $\bar{X}$ and $\bar{Y}$ are the average number of payments solved in LSM and total amount of payments in LSM respectively, so $\alpha = \frac{\bar{X}}{8400 \times q} \times 100\%$[17].

We can see from Figure 3.12, the proposed central queuing facility could save approximately 75% of liquidity that central bank needs to lent to members of payment system at least. Moreover, with more and more payments aggregating at the central queue, around 97% of queued payments could be settlement without extra liquidity requirement. In the equation of α (3.2), both the numerator and denominator increase but with different rates. The closer the rates of increase are, the flatter the plot in Figure 3.12 would look like, as it towards $q = 1$.

At the beginning of the experiment, payments arriving at the LSM helped to establish a complete network: banks found it highly likely to have payment(s) netting

[17] $(1 - q)100\%$ of CHAPS payments made via RTGS system

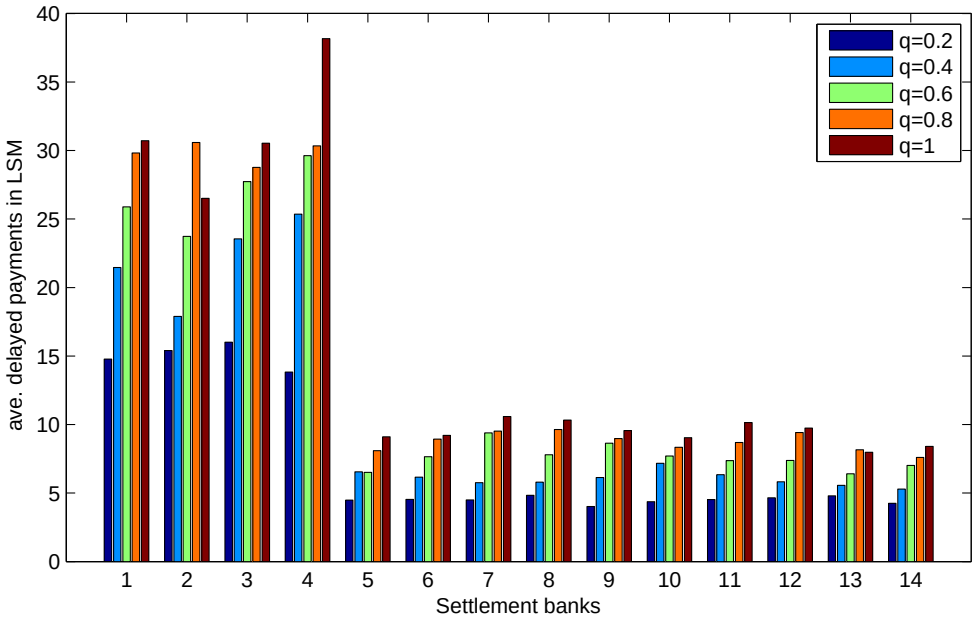

Figure 3.13: Average delayed payments under different management

to a newly arrived payment, so links occurred during this period have relatively short lifetime and could be disconnected very quickly. Thus, banks have an incentive to submit payments in central queue as early as possible to gain more change to offset. As more and more payments aggregated in LSM, the ten small banks operated as smoothly as earlier, while big banks suffered from gridlock more and more badly with possible reasons discuss in the previous section. Figure 3.13 is consistent with the finding we drew.

Stable proportions of cycles with particular lengths

Table 3.1 lists the average numbers of solved cycles with different lengthes and the probabilities to settle payments using the particular cycle. The massive majority of the queued payments could be solved by bilateral or trilateral payments ($\approx 98\%$). The numbers are positively related to q, but the proportions are more or

Table 3.1: Probabilities of cycles with different lengthes

q	Length 2		Length 3		Length 4		Length ≥ 5	
0.2	648.43	88.17%	73.02	9.93%	11.71	1.59%	2.31	0.31%
0.4	1350.30	89.32%	139.10	9.20%	19.20	1.27%	3.10	0.21%
0.6	2085.00	90.40%	193.70	8.40%	24.20	1.05%	3.50	0.15%
0.8	2819.60	91.00%	245.40	7.92%	29.40	0.95%	4.00	0.13%
1	3554.90	91.27%	301.80	7.75%	33.80	0.87%	4.50	0.12%
ave.		90.03%		8.64%		1.15%		0.18%

less unchanged. The stable distribution can be proved by applying a standard χ^2 goodness-of-fit test of a multinomial distribution. We have recognised the distribution is indeed multinomial. Let us set out the following terms:

- $p_i \geq 0$ for $i = 2, 3, 4, 5$ be the probabilities that cycle has length 2,3,4 and ≥ 5 respectively, $\sum_{i=2}^{5} p_i = 1$.
- n_i be the number of cycles with length 2,3,4 and ≥ 5 respectively.
- $n = \sum_{i=2}^{5} n_i$.

Hence, the parameters for the multinomial distribution are n and p_i's. The appropriate estimations for the probabilities are the Maximum Likelihood Estimators (MLSs), and they are $\hat{p}_i = \frac{n_i}{n}$ for $i = 2, 3, 4, 5$.

To test if the multinomial distribution is stable during the experiment, χ^2 goodness-of-fit tests are performed. In the comparisons between each set of p_i's and the average values, $\bar{p}_i$'s, Table 3.2 tabulates the values of the test statistic and p-values.

All the p-values indicated that there are no strong evidence against the null hypothesis of the underlying distribution in each is as same as the averaged distribution[18]. In other words, the multinomial distribution is stable across the ex-

[18]For the χ^2 goodness-of-fit test, when $q = 0.8$ and 1, the last two categories are combined, as the expected frequencies have to be at least 5.

Table 3.2: χ^2 goodness-of-fit test statistics

q	χ^2 test statistic	p-value
0.2	3.548	0.1697
0.4	0.882	0.6433
0.6	0.384	0.8253
0.8	3.715	0.2939
1	7.830	0.0497*

periment. It implies that with more payments aggregated at the internal queue, the total volume of settled payments goes up quickly, still, in terms of proportion, as shown in Figure 3.12, the percentage of total payments solved remains approximately constant, and the probabilities of finding a cycle with certain length are almost unchanged. The central bank to which all these information are available, may consider taking account of this steady distribution of cycles when estimate the cost of queue management.

3.3 Conclusions

In this chapter, we investigated the potential impact of offering a liquidity saving solution to the UK large-valued interbank payment system, CHAPS.

3.3.1 In a comparison of simulations using historical data

It has been continuously controversial about should simulations of all kinds use artificial or historical data. In particular, when analysing payment systems, data could be difficult to obtain for business and security reasons. The advantages and disadvantages of both of them have been listed in the book by Manning *et al.* [40]. The historical data is realistic, as it defined, however, when verifying some unusual events using actual data, one always assumes that banks would not later

their behavior under an alternative scenario [40]. Also, it is impossible to exactly "repeat the experiment" in search for statistical properties. These downside can be overcome by using generated data. Therefore, we think it is worth to check our results with others where actual data was used. Considering the similarity of the mechanisms between Ercevik and Jackson [21], RRGS, and ours, and the fact that they have used both real payment data and synthetic data, we are going to put their work in the comparison.

First of all, here is a short summary of the set up. Ercevik and Jackson applied the Bank of Finland payment and settlement simulator (BoF-PSS2[19]) to the historical dataset of December 2006. As similar as we did, they assumed the extreme case of the liquidity reservation functionality: high profile/time-critical payments would be made using post liquidity, while low-profile/non-time-critical payments would be settled by offsetting with other queued payments in the central queue, i.e., by the arrival of incoming payments. Moreover, incoming funds not only can be used to finance queued payments but also time-critical payments. Since the actual dataset has been used, some of the time-critical payments are identifiable, payments from and to CLS are examples. Not all time-critical payments are stated clearly in the dataset, they tried to proxy it in two different ways: (a) payments of a size greater than or equal to a certain value threshold, (b) a proportion of payments (as we defined the value of q).

They concluded that the benefit of RRGS depends on having a mass of payments whose settlement is made via the queue-release algorithm. From the entire system's point of view, both of liquidity saving and settlement delays increased in the numbers of payment queued. When less than half of the payments submitted to RRGS, there is neither liquidity savings nor payment delays. For individual banks, the mean

[19]details were described in Leinonen and Soramäki [37]

liquidity requirements increases slightly for the largest two banks; the next two medium size banks gained moderate mean liquidity saving; at last the rest ten[20] small banks are the most beneficial members from RRGS. RRGS can potentially disrupt the recycling of payments for banks who already use liquidity very efficiently in a pure RTGS system. To summaries, "the precise distribution of benefits is likely to be dependent on a range of factors relating to the structure of individual banks' payment flows under RTGS. In the case of CHAPS, we find that banks with fewer payments typically face a proportionally higher liquidity need to settle these payments under an RTGS design. It is these banks who would benefit most from the introduction of a RRGS design. By contrast, a subset of large banks who currently achieve high recycling ratios would see no savings and may even face a small increase in their liquidity needs" [21].

3.3.2 The significance of our simulations

Instead of using actual historical payment dataset, we generated a system that captures one of the most important structure feature of CHAPS dataset based on some existing studies. Nevertheless, as same as where an actual historical payment dataset was used, we found that liquidity saving is achieved by implementing this particular mechanism, however, the efficiencies are not equal for banks with different sizes. Big banks[21] have a low performance throughout the process due to shortage of incoming funds. For individual banks, the total amount of intra-day liquidity are similar from time to time, and the proportions between RTGS and LSM are needed to be defined by the value of q and bank's size. Banks are encouraged to make individual strategies to post collateral most efficiently, some of which is exclusively relying on

[20] 14 settlement banks of CHAPS excluding Bank of England and CLS
[21] banks dominate approx. 80% payments

the transparency of information: if a bank is not being aware of other members' plans, it will require collateral proactively to avoid any possibility of unsettled payments. From a central bank's point of view, the system-wide payments information is always available, central bank could guide banks on collateral borrowing, so as to reduce delayed payments significantly. When considering recruiting second-tier banks, central bank can use these experiences to train the banks and coach them through the liquidity management process.

Last but not least, the most significance of our work is that despite only the most simplest possible system was generated, the main results was consistent with where real historical data was used. In addition to which, the simulation also allows us to investigate the distribution of particular length cycles, it is particularly interested by central banks and policy makers. With a stable distribution of cycles, central bank can estimate the approximate number of particular cycles, therefore calculate the cost of queue management.

Chapter 4

Boundary crossing probabilities for Brownian motion

This chapter is particularly motivated by the innovative development in Banking system, especially, the large-valued interbank payment system as stated in Chapter 1 and 3. In this particular payment system, the participating banks are concerned the credit risk, and wish to prevent the considerable credit exposure between others[1]. Till the time any liquidity saving solution was enforced in the UK large-valued interbank payment system, CHAPS, it is observed that there is anecdotical evidence that participating banks would set up bilateral or multi-lateral limits between it and other members of the system to protect itself from unexpected credit exposures, and achieved a moderate liquidity saving in RTGS. The limits will be adjusted during the course of the business day under certain circumstances. Both the participating banks and central bank are interested in the efficiency of these limits, which leads to the calculation of boundary crossing probabilities for Brownian motion with stochastic

[1] Although RTGS system had replaced the Netting settlement system around the world, by the end of 2006, 93 of world's 174 central banks were using RTGS systems already [8], the possibility of unexpected exposures still exists

boundaries.

First of all, let us define the general boundary crossing problem. Let $\{X_t\}_{t\geq 0}$ be a standard Brownian motion and two continuous(or piecewise continuous) functions $u(t)$ and $l(t)$ be the upper boundary and lower boundary respectively. Define τ_1 as the upper first-passage time and τ_2 as the lower first-passage time with respect to the filtration $\{\mathcal{F}_t : t \geq 0\}$ as below,

$$\tau_1 = \inf_{t>0}\{X_t \geq u(t)\} \tag{4.1}$$

$$\tau_2 = \inf_{t>0}\{X_t \leq l(t)\} \tag{4.2}$$

Moreover, $\tau_1 = \infty$ if $X_t < u(t)$ and $\tau_2 = \infty$ if $X_t > l(t)$ for all $t > 0$.

We are interested in the boundary crossing probabilities such that,

$$P_u^{(2)} = \mathbb{P}(\tau_1 < \infty, \tau_1 < \tau_2)$$

$$P_l^{(2)} = \mathbb{P}(\tau_2 < \infty, \tau_2 < \tau_1)$$

Calculations of this kind of probabilities are very popular in many fields of statistics, they have played an important role in certain sequential statistical analysis [57], for instance, power-one tests [49], confidence sequences [47], repeated significance tests [58], sequential probability ratio test [2], non-parametric statistics [56] *etc.* Another application is the testing of structural change in regression models, for example, the asymptotic local power of cusum test [15] and the fluctuation test [35]. These boundary crossing probabilities also have attacked great amount of attention in finance. The problem of the pricing of so-called time-dependent barrier options can be reduced to the calculation of boundary crossing probabilities for a Brownian motion with deterministic function [27], [44] and [50]. Moveover, there are

applications in other areas such as biophysical models [46].

In Chapter 2, it has been shown that Markov type model is adequate to model the Real Time Gross Settlement system. Hence, in the content of interbank payment system, the problem of boundary crossing probabilities can be defined in the following ways. For a single bank, namely Bank A, let the standard Brownian motion X_t be the net balance in between Bank A and Bank i at time t. Meanwhile, $u_i(t)$ is the bilateral limit set up by Bank A for Bank i. Therefore, this problem can be reduced to the calculation of the boundary crossing probability for Brownian motion with time-determine boundaries. This approach can be adopted by both the policy makers at central bank and credit control departments of participating banks to lay down decisive actions.

In this chapter, above all, we are going to provide an alternative method to derive the boundary crossing probabilities for standard Brownian motion with symmetric and asymmetric linear boundaries. With powerful tools such as martingales and infinitesimal generator of Brownian motion, our approach allows to obtain a simple formula for the two-sided boundaries crossing probabilities. Nevertheless, the method will be modified to stochastic boundaries and both numerical examples and simulations will be studied.

4.1 Literature review

In this section we are going to give a detailed summary of the existing literatures.

Anderson was the first to obtain the explicit form of the distribution of the first-passage time of a Brownian motion through linear boundaries [2]. In his paper, firstly, the probability for a Brownian motion of touching one boundary before the other when the process can go without limit ($T = \infty$) is derived, (in our notations)

Theorem 4.1 (Anderson 1960)**.** *Let $\{X_t\}_{t\geq 0}$ be a standard Brownian motion, then for $b_1 > 0, b_2 > 0$ and $c_1 \geq -c_2$ (not $c_1 = c_2 = 0$), the the upper boundary crossing probability is*

$$P_u^{(2)} = \begin{cases} \sum_{r=1}^{\infty} \left(e^{-2A_r} - e^{-2B_r}\right) & c_1 \geq 0 \\ 1 - \sum_{r=1}^{\infty} \left(e^{-2C_r} - e^{-2D_r}\right) & c_1 \leq 0 \\ \frac{e^{2b_1c_2}-1}{e^{2(b_1+b_2)c_1}-1} & c_1 = -c_2 \neq 0 \end{cases} \tag{4.3}$$

where

$$\begin{aligned} A_r &= (b_1+b_2)(c_1+c_2)r^2 - [b_2(c_1+c_2) + c_2(b_1+b_2)]r + b_2c_2 \\ B_r &= (b_1+b_2)(c_1+c_2)r^2 + (b_2c_1 - b_1c_2)r \\ C_r &= (b_1+b_2)(c_1+c_2)r^2 - [b_1(c_1+c_2) + c_1(b_1+b_2)]r + b_1c_1 \\ D_r &= (b_1+b_2)(c_1+c_2)r^2 + (b_1c_2 - b_2c_1)r \end{aligned}$$

For the lower boundary $l(t) = -b_2 - c_2t$, the constants $b_1, b_2, c_1, c_2 > 0$ and $b_1 \neq b_2$, $c_1 \neq c_2$, the Corollary follows immediately,

Corollary 4.1 (Anderson 1960)**.** *The lower boundary crossing probability is,*

$$P_l^{(2)} = \begin{cases} \sum_{r=1}^{\infty} \left(e^{-2C_r} - e^{-2D_r}\right) & c_2 \geq 0 \\ 1 - \sum_{r=1}^{\infty} \left(e^{-2A_r} - e^{-2B_r}\right) & c_2 \leq 0 \\ \frac{e^{2b_2c_1}-1}{e^{2(b_1+b_2)c_2}-1} & c_1 = -c_2 \neq 0 \end{cases} \tag{4.4}$$

where A_r, B_r, C_r, D_r are given in Theorem 4.1.

When comparing equations (4.3) and (4.4), We notice that the subscripts of b and c are interchanged.

Secondly, Anderson also found the probability for $\{X_t\}_{t\geq 0}$ of touching one line

first conditional on the path going through a particular point.

Theorem 4.2 (Anderson 1960). *If $\{X_t\}_{t\geq 0}$ is a standard Brownian motion, and if T, b_1, b_2, c_1, c_2 are numbers such that $b_1, b_2 > 0, b_1 + c_1 T \geq -b_2 - c_2 T, T > 0$, the conditional upper boundary crossing probability given $X_T = \eta$ (not $b_1 + c_1 T = -b_2 - c_2 T = \eta$) is*

$$P_u^{(2)}(T|\eta) = \begin{cases} \sum_{r=1}^{\infty} \left(e^{-\frac{2}{T} A_r^T} - e^{-\frac{2}{T} B_r^T} \right) & b_1 + c_1 T \geq \eta \\ 1 - \sum_{r=1}^{\infty} \left(e^{-\frac{2}{T} C_r^T} - e^{-\frac{2}{T} D_r^T} \right) & b_1 + c_1 T \leq \eta \\ \frac{e^{\frac{2}{T} b_2 (b_1 + c_1 T - \eta)} - 1}{e^{\frac{2}{T} (b_1 + b_2)(b_1 + c_1 T - \eta)} - 1} & b_1 + c_1 T = -b_2 - c_2 T \neq \eta \end{cases} \tag{4.5}$$

where

$$\begin{aligned} A_r^T &= (b_1 + c_1 T - \eta)[(b_1 + b_2) r - b_2] r + (b_2 + c_2 T + \eta)[(b_1 + b_2) r - b_2](r - 1) \\ B_r^T &= (b_1 + c_1 T - \eta)[(b_1 + b_2) r + b_2] r + (b_2 + c_2 T + \eta)[(b_1 + b_2) r - b_1] r \\ C_r^T &= (b_1 + c_1 T - \eta)[(b_1 + b_2) r + b_1](r - 1) + (b_2 + c_2 T + \eta)[(b_1 + b_2) r + b_1] r \\ D_r^T &= (b_1 + c_1 T - \eta)[(b_1 + b_2) r - b_2] r + (b_2 + c_2 T + \eta)[(b_1 + b_2) r + b_1] r \end{aligned}$$

As similar as Corollary 4.1, the formula for $P_l^{(2)}(T|\eta)$ can be derived from equation (4.5) by replacing b_1, c_1 by b_2 and c_2.

Finally, in Anderson's paper, the explicit form of the unconditional probability of touching one line first over a limit $[0, T]$ is found.

Theorem 4.3 (Anderson 1960). *If $\{X_t\}_{t\geq 0}$ is a standard Brownian motion, and b_1, b_2, c_1, c_2, T are defined in Theorem 4.2, the unconditional upper boundary crossing*

probability is

$$\begin{aligned} P_u^{(2)}(T) &= 1-\Phi\left(\frac{b_1T+c_1}{\sqrt{T}}\right) \\ &\quad +\sum_{r=1}^{\infty}\left\{e^{-2A_r}\Phi\left(\frac{c_1T-2(r-1)b_2-(2r-1)b_1}{\sqrt{T}}\right)\right. \\ &\quad -e^{-2B_r}\Phi\left(\frac{c_1T-2rb_2-(2r-1)b_1}{\sqrt{T}}\right) \\ &\quad -e^{-2C_r}\left[1-\Phi\left(\frac{c_1T+2rb_2+(2r-1)b_1}{\sqrt{T}}\right)\right] \\ &\quad \left.+e^{-2D_r}\left[1-\Phi\left(\frac{c_1T+(2r+1)b_1+2rb_2}{\sqrt{T}}\right)\right]\right\} \end{aligned}$$

where A_r, B_r, C_r and D_r are given by the expressions in Theorem 4.1, and $\Phi(\cdot)$ is the cumulative distribution function of a standard Normal distribution.

Hall simplified one of the three conditional probabilities of crossing the upper linear boundary $u(t) = b_1 + c_1 t$ over an interval $[0, T]$, as in equation (4.5) [30],

Theorem 4.4 (Hall 1997)**.** *Let $\{X_t\}_{t\geq 0}$ be a standard Brownian motion, the probability of X_t crossing the upper linear boundary $u(t)$ before crossing the lower boundary given the condition that by a fixed time T, $X_T = \eta$, is followed,*

$$\begin{aligned} P_u^{(2)}(T|\eta) &= \sum_{j=1}^{\infty}\exp\left(2(jc-b_2)\left[b(2j-1)+\frac{\eta-\bar{c}t-(jc-b_2)}{T}\right]\right) \\ &\quad -\exp\left(2j\left[2b(jc-\bar{b})+\frac{(\eta-\bar{c}t-jc)c}{T}\right]\right) \end{aligned} \tag{4.6}$$

for $\eta < u(T)$, where

$$\bar{b}=\frac{b_1-b_2}{2} \quad \bar{c}=\frac{c_1-c_2}{2} \quad c=b_1+b_2 \quad b=-\frac{c_1+c_2}{2}$$

Meanwhile, it has been verified that equation (4.6) agrees with the first piece of

equation (4.5) by Anderson.

Corollary 4.2. *Assume $\eta > l(T)$, similarly, $P_l^{(2)}(T|\eta)$ is given by the formula of $P_u^{(2)}(T|\eta)$ with (b_1, c_1) replaced by (b_2, c_2).*

In the rest of the existing literatures, the results are generally divided into two types according to two kinds of boundaries. One is single boundary, most of the results dealt with linear or (approximated) piecewise linear boundary [1], [38], [54] and [61], the calculations of these probabilities involves evaluation of a multiple integral, which can not always be expressed by an explicit formula and hence must be solved numerically. The explicit form of the boundary crossing probabilities are only obtained for a few special non-linear boundaries, for example, squared root boundaries [61] and a particular class of functions [48].

Scheike has derived a set of results in the situation where the single boundary is of the form $u(t) = b + ct$ [54].

Theorem 4.5 (Scheike, 1992)**.** *Let $\{X_t\}_{t\geq 0}$ be a standard Brownian motion, and $\Phi(\cdot)$ denote the cumulative distribution function of a standard Normal distribution. When $u(t) = b + ct$, then,*

1. *The one-sided unconditional boundary crossing probability without time limit is,*

$$P_u^{(1)} = \begin{cases} e^{-2bc} & b, c > 0 \\ 1 & b \leq 0 \quad or \quad c \leq 0 \end{cases} \tag{4.7}$$

2. *The one-sided unconditional boundary crossing probability over $[0, T]$ is,*

$$P_u^{(1)}(T) = \begin{cases} 1 - \Phi\left(\frac{b}{\sqrt{T}} + c\sqrt{T}\right) + e^{-2bc}\Phi\left(c\sqrt{T} - \frac{b}{\sqrt{T}}\right) & b > 0, T < \infty \\ 1 & b \leq 0 \end{cases} \tag{4.8}$$

3. *The one-sided boundary crossing probability conditional on* $X_s = \eta$ *over* $[0, T]$ *is,*

$$P_u^{(1)}(T|\eta) = \begin{cases} e^{-\frac{2b(b+cT-\eta)}{T}} & b > 0, T < \infty, \eta < b + cT \\ 1 & b \leq 0 \end{cases} \tag{4.9}$$

In a more general case, consider that $u(t) \forall t$, is a piecewise continuous function, and it is a polygonal function on the interval $[0, T]$. Let $0 = t_0 < t_1 < \cdots < t_n = T$, assume that $u(t)$ is linear on each of the interval $[t_{j-1}, t_j]$, for $j = 1, 2, \cdots, n$ and $u(0) > 0$, then denote $u_j = u(t_j)$ and $u = (u_1, u_2, \cdots, u_n)$. Wang and Pötzelberger derived the unconditional probability that a standard Brownian motion up-crosses a piecewise linear boundary in a finite time interval $[0, T]$ [61].

Theorem 4.6 (Wang and Pötzelberger 1997)**.** *Let* $\{X_t\}_{t \geq 0}$ *be a standard Brownian motion, and define that*

$$P_u^{(1)}(T) = \mathbb{P}(X_t \geq u(t), t < T)$$

Then the probability of up-crossing the piecewise linear boundary $u(t)$*, over the period* $[0, T]$*, is given by*

$$P_u^{(1)}(T) = 1 - \int_{-\infty}^{u} \prod_{j=1}^{n} \left[1 - \exp\left(-\frac{2(u_{j-1} - x_{j-1})(u_j - x_j)}{t_j - t_{j-1}} \right) \right] f(x) dx$$

where $X_{t_j} = x_j$*,* $x = (x_1, \cdots, x_n)'$ *and*

$$f(x) = \prod_{j=1}^{n} \frac{1}{\sqrt{2\pi(t_j - t_{j-1})}} \exp\left[-\frac{(x_j - x_{j-1})^2}{2(t_j - t_{j-1})} \right]$$

To the extent of more general (nonlinear) boundaries, Theorem 4.6 can be used

to obtain approximated boundary crossing probabilities for these boundaries, which are uniformly limit to the piecewise linear function $u(t)$.

Theorem 4.7 (Wang and Pötzelberger 1997)**.** *For $\{X_t\}_{t\geq 0}$, a standard Brownian motion, if $u_n(t) \to u(t)$, as t tends to infinity, uniformly on $[0,T]$, then*

$$P_{u_n}^{(1)}(T) = 1 - \int_{-\infty}^{u} \prod_{j=1}^{n} \left(1 - \exp\left[-\frac{2(u_{j-1} - x_{j-1})(u_j - x_j)}{t_j - t_{j-1}}\right]\right) f(x)dx$$

where x and $f(x)$ are defined as in Theorem 4.6.

Moreover, Abundo, by applying the time inversion property of Brownian motion, particularly derived a elementarily simple and explicit formulae for the conditional boundary crossing probability of $\{X_t\}_{t\geq 0}$ and piecewise-linear boundary, $u(t)$, consisting of two lines given that $X_s = \eta$ over a limit $[0,T]$, i.e. $P_u^{(1)}(T|\eta) = \mathbb{P}(X_t \geq u(t), t < T | X_s = \eta)$, where

$$u(t) = \begin{cases} b_1 + c_1 t & 0 \leq t < N \\ b_1' + c_1' t & N \leq t \end{cases} \tag{4.10}$$

and $u(0) = b_1 > 0$ [1].

Theorem 4.8 (Abundo 2002)**.** *Let $\{X_t\}_{t\geq 0}$ be a standard Brownian motion, and given $N < T < \infty$, the probability that X_t up-crosses $u(t)$ in $[0,T]$ with the condition that the value of X_t at the instant $s > T$ is equal to η is*

$$\begin{aligned} P_u^{(1)}(T|\eta) &= 1 - \phi\left(\frac{b_1' s + (c_2' s - \eta)T}{\sqrt{sT(s-T)}}\right) \\ &\quad + \int_{-\infty}^{\frac{b_1' s + (c_2' s - \eta)T}{\sqrt{sT(s-T)}}} J\left(N, T, \frac{y\sqrt{sT(s-T)} + \eta T}{s}\right) \frac{e^{-\frac{y^2}{2}}}{\sqrt{2\pi}} dy \end{aligned}$$

where $J(N,T,\cdot)$ *is defined as*

$$\begin{aligned} J(N,T,x) &= 1-\Phi(hN_T)+\exp(-2b_1'b')\Phi((h-2b')N_T) \\ &\quad +\exp(-2b_1b)\Phi\left(\frac{hN_T^2-2b_1}{N_T}\right) \\ &\quad -\exp[-2b_1b-2(b_1'-2b_1)b']\Phi\left(\frac{(h-2b')N_T^2-2b_1}{N_T}\right) \end{aligned}$$

where

$$\begin{aligned} h &= \min\left(\frac{b_1+c_1N}{N}-\frac{x}{T},\frac{b_1'+c_1'N}{N}-\frac{x}{T}\right) \\ N_T &= \sqrt{\frac{TN}{T-N}} \\ b &= c_1+\frac{b_1-x}{T} \\ b' &= c_1'+\frac{b_1'-x}{T} \end{aligned}$$

The result will be different when $s<T$.

Theorem 4.9 (Abundo 2002)**.** *Let* $u(t)$ *be defined as in Theorem 4.8, and* $s<T$*. Then, if* $\eta<u(t)$*,*

$$\begin{aligned} P_u^{(1)}(T|\eta) &= P_{u'}^{(1)}(T-s)+\frac{e^{\frac{\eta^2}{2s}}}{\sqrt{2\pi s}}\left[1-P_{u'}^{(1)}(T-s)\right] \\ &\quad \times\left[\begin{cases} \frac{e^{-\frac{\eta^2}{2s}}}{\sqrt{2\pi s}}e^{-2b_1\frac{b_1+c_1s-\eta}{s}} & 0<u\le N \\ \frac{e^{-\frac{\eta^2}{2s}}}{\sqrt{2\pi s}}J(N,s,\eta) & N<u<T \end{cases}\right] \end{aligned}$$

where

$$u'(t)=\begin{cases} (b_1+c_1s-\eta)+c_1t & 0\le t<N-s \\ (b_1'+c_1's-\eta)+c_1't & N-s\le t\le T-s \end{cases}$$

and $P^{(1)}_{u'}(T-s)$ *can be derived from equation (4.8) in Theorem 4.5. If* $\eta \geq u(t)$*, the probability is 1.*

Robbins and Siegmund have made the use of the martingale $\int_0^\infty e^{-\frac{1}{2}ty^2+yx}dF(y)$ to evaluate the probability that $\{X_t\}_{t\geq}$ would ever cross a certain class of functions $g(t)$, including which are approximately $(2t\log\log t)^{\frac{1}{2}}$ as t goes to infinity [48].

Let F denote any measure on $(0,\infty)$, which is finite on bounded intervals, then define for x, t and $\varepsilon > 0$

$$\begin{aligned} f(x,t) &= \int_0^\infty e^{-\frac{1}{2}ty^2+yx}dF(y) \\ g(t,\varepsilon) &= \inf\{x : f(x,t) \geq \varepsilon\} \end{aligned} \tag{4.11}$$

$f(x,t)$ is a nonnegative continuous function on $D = \mathbb{R}\times(\tau,\infty)$, where $0 \leq \tau < \infty$. The infinitesimal generator of the space time Brownian motion is $\frac{\partial f}{\partial t} + \frac{1}{2}\frac{\partial^2 f}{\partial x^2} = 0$ on D, hence $f(X_t,t)$ is a positive martingale. Nevertheless, it is easy to see that $x = g(t,\varepsilon)$ is the unique solution of $f(x,t) = \varepsilon$, and $g(t,\varepsilon)$ in this class is increasing, infinitely differentiable and concave.

Theorem 4.10 (Robbins, Siegmund 1970)**.** *1. For any* b, h *and* ε*, if* $f(b,h) < \varepsilon$*, then for some* $t \geq 0$*,*

$$\mathbb{P}(X_t \geq g(t+h,\varepsilon) - b) = \frac{f(b,h)}{\varepsilon} \tag{4.12}$$

2. For any b, h, ε and $\tau < 0$, then for some $t \geq \varepsilon$,

$$\begin{aligned}
&\mathbb{P}(X_t \geq g(t+h,\varepsilon) - b, t \geq \varepsilon) \\
&= 1 - \Phi\left(\frac{g(\tau+h,\varepsilon) - b}{\sqrt{\tau}}\right) \\
&+ \frac{1}{\varepsilon}\int_0^\infty e^{-\frac{1}{2}hy^2+by}\Phi\left(\frac{g(\tau+h,\varepsilon) - b}{\sqrt{\tau}} - y\sqrt{\tau}\right) dF(y)
\end{aligned}$$

Robbins and Siegmund [48] also indicated that suppose $f(b,0) < \infty$ for all b, for any $h \geq 0$ and $\varepsilon \geq f(b,h)$, equation (4.12) implies that

$$P_g^{(1)}(b) = \mathbb{P}(X_t \geq g(t,\varepsilon)|X_h = b) = \begin{cases} \frac{f(b,h)}{\varepsilon} & b < g(h,\varepsilon) \\ 1 & b \geq g(h,\varepsilon) \end{cases} \tag{4.13}$$

Lerche [38] further showed that if $g(t,\varepsilon)$ is the solution of $f(\frac{x}{t}, \frac{1}{t}) = \varepsilon$, and $\int_0^\infty e^{-\frac{ay}{2}} dF(y) < \infty$ for all $a > 0$, then,

Theorem 4.11 (Lerche 1986)**.** *Equation (4.13) becomes*

$$P_g^{(1)}(b) = \frac{f\left(\frac{b}{h}, \frac{1}{h}\right)}{\varepsilon}$$

for $b < g(h,\varepsilon)$, otherwise the probability is 1.

Note that for $F = \delta_{2y}$, which is the Dirac measure at $2y$, $g(t,\varepsilon) = y + bt$ where $b = \frac{\log(\varepsilon)}{2y}$, so the class contains linear boundaries.

The other case is the two-sided boundaries, Abundo also derived the explicit expressions for the conditional probability for two symmetric linear boundaries [1], in which case $u(t) = -l(t) = b_1 + c_1 t$ for all t. There are two cases depends on the value of s.

Theorem 4.12 (Abundo 2002)**.** *Let $s > T$, define*

$$P_u^{(2)}(T|\eta) = P_l^{(2)}(T|\eta) = \mathbb{P}(|X_t| \geq u(t)|X_s = \eta)$$

then,

$$\begin{aligned} P_u^{(2)}(T|\eta) &= P_l^{(2)}(T|\eta) \\ &= 1 + \int_{\frac{-u(T)s-\eta T}{\sqrt{sT(s-T)}}}^{\frac{u(T)s-\eta T}{\sqrt{sT(s-T)}}} \left[H\left(\frac{y\sqrt{sT(s-T)} + \eta T}{s}, T \right) - 1 \right] \frac{e^{-y^2/2}}{\sqrt{2\pi}} dy \end{aligned}$$

where

$$\begin{aligned} H(z,\omega) &= 1 - \sum_{n=-\infty}^{\infty} (-1)^n \exp\left(-2b_1 n \left[\left(c_1 + \frac{b_1}{\omega} \right) n - \frac{z}{\omega} \right] \right) \qquad (4.14) \\ u(t) &= b_1 + c_1 t \end{aligned}$$

On the other hand, when $s < T$,

Theorem 4.13 (Abundo 2002)**.** *Let $s < T$, if $|\eta| < u(t)$, it holds,*

$$\begin{aligned} &P_u^{(2)}(T|\eta) = P_l^{(2)}(T|\eta) = \\ &1 - [1 - H(\eta, s)]\mathbb{P}\left(\bigcap_{[0,T-s]} -(u(s) + \eta + c_1 t) \leq X_t \leq u(s) - \eta + c_1 t \right) \end{aligned}$$

where $H(\eta, s)$ is given by the equation (4.14) in Theorem 4.12 and

$$\begin{aligned} &\mathbb{P}\left(\bigcap_{[0,T]} -(\alpha + \beta t) \leq B_t \leq a + bt \right) \\ &= \int_{-(\alpha+\beta T)}^{a+bT} \frac{e^{-\eta^2/2T}}{\sqrt{2\pi T}} G\left(\alpha, \beta + \frac{a+\eta}{T}, a, b + \frac{a-\eta}{T} \right) d\eta \end{aligned}$$

The function G is given by the theorem by Doob, 1949.

Last but not least, in addition to $u(t)$, consider another deterministic function, namely $l(t)$, which is continuous for all t and not necessary be symmetric to $u(t)$. $l(t)$ is the lower boundary for X_t. Define that

$$P_T(u, l, K) = \mathbb{P}(l(t) < X_t < u(t), t \leq T; X_T > K)$$

then $1 - P_T(l, u, K)$ will be the first-passage time probability of reaching one of the boundaries $u(t)$ and $l(t)$.

Novikov *et al.* derived a more general solution in terms of piecewise function [43]. Given that $\hat{u}(t)$ and $\hat{l}(t)$ are piecewise linear functions with the nodes $0 = t_0 < t_1 < \cdots < t_n = T$, which are considered as approximations of $u(t)$ and $l(t)$. Novikov *et al.* found an approximation of $P_T(l, u, K)$ by $P_T(\hat{l}, \hat{u}, K)$, hence, $1 - P_T(l, u, K)$.

Theorem 4.14 (Novikov, Frishling and Kordzakhia 1999)**.** *The first-passage time probability for a standard Brownian motion with two boundaries $u(t)$ and $l(t)$ is*

$$1 - P_T(\hat{l}, \hat{u}, K) = 1 - \mathbb{E}\left[\mathbb{1}_{\{X_t > K\}} \prod_{j=0}^{n-1} P(j, \hat{l}, \hat{u} | x_j, x_{j+1})\right]$$

where

$$P(j, \hat{l}, \hat{u} | x_j, x_{j+1}) = \mathbb{P}(\hat{l}(t) < X_t < \hat{u}(t), t_j \leq t \leq t_{j+1} | X_{t_j} = x_j, X_{t_{j+1}} = x_{j+1})$$

and $\mathbb{1}_{\{X_t > K\}}$ is an indicator function.

In summary, the existing results are generally divided into two types by two kinds of boundaries;

One-sided piecewise-linear boundary in our notations, $u(t)$ is a piecewise linear function and $l(t) = 0$, $\forall t > 0$. The expression of the unconditional probability is obtained as Theorem 4.6 [61], $P_u^{(1)}(T) = \mathbb{P}(X_t \geq u(t), t < T)$, where $u(t)$ is a polygonal function on the interval $[0, T]$, let $0 = t_0 < t_1 < \cdots < t_n = T$ and $u(t)$ be linear on each of the intervals $[t_{j-1}, t_j]$ for $j = 1, 2, \cdots, n$. However, in the calculations of $P_u^1(T)$, it involves evaluation of a multiple integral, which cannot always be expressed by an explicit formula and hence must be solved numerically. In addition to this, by applying the time inversion property of Brownian motion, Abundo particularly derived a elementarily simple and explicit formula for the conditional boundary crossing probability $P_u^{(1)}(T|\eta) = \mathbb{P}(X_t \geq u(t), t < T|X_s = \eta)$, where $u(t)$ is given by equation (4.10) and $u(0) = a_1 > 0$ by Theorem 4.8 [1].

Two-sided boundaries the conditional crossing probability with two symmetric linear boundaries, $P_u^{(2)}(T|\eta) = P_l^{(2)}(T|\eta) = \mathbb{P}(|X_t| \geq u(t), t < T|X_s = \eta)$, where $u(t) = -l(t) = a + bt$ for all t, is also studied by Abundo in Theorem 4.12 [1]. A more general solution in terms of piecewise function is derived by Novikov *et al.* Let $\hat{u}(t)$ and $\hat{l}(t)$ be the approximations for $u(t)$ and $l(t)$ respectively, that are piecewise-linear functions with the nodes $0 = t_0 < t_1 < \cdots < t_n = T$. Hence, the approximated boundary crossing probabilities $P_{\hat{u}}^{(2)}(T)$ and $P_{\hat{l}}^{(2)}(T)$ can be found accordingly.

Overall, the explicit form of the probabilities only obtained for a few special non-linear boundaries, for example, squared root boundaries [61]. The boundary crossing probability for any other general boundaries only solved numerically. However, in practices, most of the time, general non-linear boundary is far more realistic, we are interested in deriving the exact boundary crossing probabilities for general boundary,

in particular, stochastic boundary.

4.2 Linear boundaries

In this section, we are going to provide an alternative method to derive the boundary crossing probabilities for standard Brownian motion with symmetric and asymmetric linear boundaries. With powerful tools such as martingales and infinitesimal generator of Brownian motion, our approach allows to obtain a simple formula for the two-sided boundaries crossing probabilities.

4.2.1 Symmetric linear boundaries

Let $\{X_t\}_{t\geq 0}$ be a standard Brownian motion, where the generater $\mathcal{A}f(x)$ acting on the function $f(x,t)$ is in the form of,

$$\mathcal{A}f = \frac{1}{2}\frac{\partial^2 f(x,t)}{\partial x^2} + \frac{\partial f(x,t)}{\partial t} \tag{4.15}$$

And define τ as the first-passage time, such that $\tau = \inf_{t\geq 0}\{t : |X_t| \geq b + ct\}$, where b, c are all nonnegative, and $\tau = \infty$ if $|X_t| < b + ct$.

Theorem 4.15. *For a standard Brownian motion $\{X_t\}_{t\geq 0}$, the two-sided boundary crossing probability for a pair of symmetric linear boundaries, $u(t) = -l(t) = b + ct$, is*

$$\mathbb{P}(\tau < \infty) = 1 + 2\sum_{i=1}^{\infty}(-1)^i e^{-4bci(2i+1)} \tag{4.16}$$

Proof. The solution of the equation $\mathcal{A}f = 0$ that we are concerned about is in the form of

$f(t) = e^{-\beta t}(e^{\sqrt{2\beta}X_t} + e^{-\sqrt{2\beta}X_t})$. This is a martingale indeed, and with the indicator functions $\mathbb{1}_{\{\tau<t\}}$ and $\mathbb{1}_{\{\tau\geq t\}}$, we get, because of Dood's optional stopping theorem,

$$\begin{aligned}\mathbb{E}\left[e^{-\beta\tau}(e^{\sqrt{2\beta}X_\tau} + e^{-\sqrt{2\beta}X_\tau})\mathbb{1}_{\{\tau<t\}}\right] + \mathbb{E}\left[e^{-\beta t}(e^{\sqrt{2\beta}X_t} + e^{-\sqrt{2\beta}X_t})\mathbb{1}_{\{\tau\geq t\}}\right] \\ = \mathbb{E}[e^{\sqrt{2\beta}X_0} - e^{-\sqrt{2\beta}X_0}] \\ \mathbb{E}\left[e^{\sqrt{2\beta}b+(-\beta+\sqrt{2\beta}c)\tau}\mathbb{1}_{\{\tau<t\}}\right] + \mathbb{E}\left[e^{-\sqrt{2\beta}b+(-\beta-\sqrt{2\beta}c)\tau}\mathbb{1}_{\{\tau<t\}}\right] + \\ \mathbb{E}\left[e^{-\beta t}(e^{\sqrt{2\beta}X_t} + e^{-\sqrt{2\beta}X_t})\mathbb{1}_{\{\tau\geq t\}}\right] = \mathbb{E}\left[e^{\sqrt{2\beta}X_0} - e^{-\sqrt{2\beta}X_0}\right] \quad (4.17)\end{aligned}$$

The last term of the left hand side of equation (4.17) will be vanished when t tends to infinity, as

$$\begin{aligned}&\lim_{t\to\infty}\mathbb{E}\left[e^{-\beta t+\sqrt{2\beta}X_t}\mathbb{1}_{\{\tau\geq t\}} + e^{-\beta t-\sqrt{2\beta}X_t}\mathbb{1}_{\{\tau\geq t\}}\right] \\ =\ &\mathbb{E}\left[\lim_{t\to\infty}e^{-\beta t+\sqrt{2\beta}X_t}\mathbb{1}_{\{\tau\geq t\}} + \lim_{t\to\infty}e^{-\beta t-\sqrt{2\beta}X_t}\mathbb{1}_{\{\tau\geq t\}}\right] \\ =\ &\mathbb{E}\left[\exp\left(-\lim_{t\to\infty}t(\beta-\sqrt{2\beta}\frac{X_t}{t})\right)\mathbb{1}_{\{\tau=\infty\}} + \exp\left(-\lim_{t\to\infty}t(\beta+\sqrt{2\beta}\frac{X_t}{t})\right)\mathbb{1}_{\{\tau=\infty\}}\right] \\ =\ &0\end{aligned}$$

since $\beta > 0$ and by the Strong Law of Large Numbers for Brownian motion, $\lim_{t\to\infty}\frac{X_t}{t} = 0$. Moreover, by applying the Monotone convergence theorem, equation (4.17) becomes

$$e^{\sqrt{2\beta}b}\mathbb{E}\left[e^{(-\beta+\sqrt{2\beta}c)\tau}\mathbb{1}_{\{\tau<\infty\}}\right] + e^{-\sqrt{2\beta}b}\mathbb{E}\left[e^{(-\beta-\sqrt{2\beta}c)\tau}\mathbb{1}_{\{\tau<\infty\}}\right] = e^{\sqrt{2\beta}x_0} + e^{-\sqrt{2\beta}x_0}$$

where $X_0 = x_0$ is the starting point of the standard Brownian motion.

Let $\sqrt{2\beta} = \kappa_j$, then $\beta = \frac{\kappa_j^2}{2}$, where $j = 0, 1, 2, \ldots$, which yields the following set

of equations,

$$e^{\kappa_0 b}\mathbb{E}\left[e^{(-\frac{\kappa_0^2}{2}+\kappa_0 c)\tau}\mathbb{1}_{\{\tau<\infty\}}\right] + e^{-\kappa_0 b}\mathbb{E}\left[e^{(-\frac{\kappa_0^2}{2}-\kappa_0 c)\tau}\mathbb{1}_{\{\tau<\infty\}}\right]$$
$$= e^{\kappa_0 x_0} + e^{-\kappa_0 x_0}; \tag{4.18}$$

$$\cdots$$

$$e^{\kappa_j b}\mathbb{E}\left[e^{(-\frac{\kappa_j^2}{2}+\kappa_j c)\tau}\mathbb{1}_{\{\tau<\infty\}}\right] + e^{-\kappa_j b}\mathbb{E}\left[e^{(-\frac{\kappa_j^2}{2}-\kappa_j c)\tau}\mathbb{1}_{\{\tau<\infty\}}\right]$$
$$= e^{\kappa_j x_0} + e^{-\kappa_j x_0}; \tag{4.19}$$

$$e^{\kappa_{j+1} b}\mathbb{E}\left[e^{(-\frac{\kappa_{j+1}^2}{2}+\kappa_{j+1} c)\tau}\mathbb{1}_{\{\tau<\infty\}}\right] + e^{-\kappa_{j+1} b}\mathbb{E}\left[e^{(-\frac{\kappa_{j+1}^2}{2}-\kappa_{j+1} c)\tau}\mathbb{1}_{\{\tau<\infty\}}\right]$$
$$= e^{\kappa_{j+1} x_0} + e^{-\kappa_{j+1} x_0} \tag{4.20}$$

In equations (4.19) and (4.20), we choose κ_j such that $\frac{\kappa_{j+1}^2}{2} - \kappa_{j+1}c = \frac{\kappa_j^2}{2} + \kappa_j c$, so $\kappa_j = 2cj + \kappa_0$. Now multiplying equations (4.19) and (4.20) by $e^{\kappa_{j+1} b}$ and $e^{-\kappa_j b}$ respectively, we get

$$e^{\kappa_{j+1} b}e^{\kappa_j b}\mathbb{E}\left[e^{(-\frac{\kappa_j^2}{2}+\kappa_j c)\tau}\mathbb{1}_{\{\tau<\infty\}}\right] + e^{\kappa_{j+1} b}e^{-\kappa_j b}\mathbb{E}\left[e^{(-\frac{\kappa_j^2}{2}-\kappa_j c)\tau}\mathbb{1}_{\{\tau<\infty\}}\right]$$
$$= e^{\kappa_{j+1} b}\left(e^{\kappa_j x_0} + e^{-\kappa_j x_0}\right)$$
$$e^{-\kappa_j b}e^{\kappa_{j+1} b}\mathbb{E}\left[e^{(-\frac{\kappa_{j+1}^2}{2}+\kappa_{j+1} c)\tau}\mathbb{1}_{\{\tau<\infty\}}\right] + e^{-\kappa_j b}e^{-\kappa_{j+1} b}\mathbb{E}\left[e^{(-\frac{\kappa_{j+1}^2}{2}-\kappa_{j+1} c)\tau}\mathbb{1}_{\{\tau<\infty\}}\right]$$
$$= e^{-\kappa_j b}\left(e^{\kappa_{j+1} x_0} + e^{-\kappa_{j+1} x_0}\right)$$

Subtracting the two equations immediately, we have

$$e^{(\kappa_j+\kappa_{j+1})b}\mathbb{E}\left[e^{(-\frac{\kappa_j^2}{2}+\kappa_j c)\tau}\mathbb{1}_{\{\tau<\infty\}}\right] - e^{-(\kappa_j+\kappa_{j+1})b}\mathbb{E}\left[e^{(-\frac{\kappa_{j+1}^2}{2}-\kappa_{j+1} c)\tau}\mathbb{1}_{\{\tau<\infty\}}\right]$$
$$= e^{\kappa_{j+1} b}\left(e^{\kappa_j x_0} + e^{-\kappa_j x_0}\right) - e^{-\kappa_j b}\left(e^{\kappa_{j+1} x_0} + e^{-\kappa_{j+1} x_0}\right) \tag{4.21}$$

Now let $A_j = \mathbb{E}[e^{(-\frac{\kappa_j^2}{2}+\kappa_j c)\tau}\mathbb{1}_{\{\tau<\infty\}}]$. Since $\kappa_j = 2cj + \kappa_0$, then $\frac{\kappa_{j+1}^2}{2} + \kappa_{j+1}c =$

$\frac{\kappa_{j+2}^2}{2} - \kappa_{j+2}c$, hence $A_{j+2} = \mathbb{E}[e^{(-\frac{\kappa_{j+1}^2}{2} - \kappa_{j+1}c)\tau} \mathbb{1}_{\{\tau<\infty\}}]$. Therefore, with the assumption that the standard Brownian motion starts from 0, we can write equation (4.21) as

$$\begin{aligned} & A_j - e^{-2(\kappa_j+\kappa_{j+1})b} A_{j+2} = 2e^{-(\kappa_j+\kappa_{j+1})b} \left(e^{\kappa_{j+1}b} - e^{-\kappa_j b}\right) \\ \Rightarrow \quad & A_j = e^{-(\kappa_j+\kappa_{j+1})b} \left[2\left(e^{\kappa_{j+1}b} - e^{-\kappa_j b}\right) + e^{-(\kappa_j+\kappa_{j+1})b} A_{j+2}\right] \end{aligned}$$

In general, for $j = 0, 1, 2, \cdots$,

$$A_0 = 1 + 2\sum_{i=1}^{j} (-1)^j e^{-2b\sum_{l=0}^{2i-1}\kappa_l} - e^{-2b\sum_{k=0}^{2j+1}\kappa_k} \left[1 + A_{2(j+1)}\right] \tag{4.22}$$

where $A_0 = \mathbb{E}[e^{(-\frac{\kappa_0^2}{2} + \kappa_0 c)\tau} \mathbb{1}_{\{\tau<\infty\}}]$. In order to find $\mathbb{P}(\tau < \infty)$, let $\frac{\kappa_0^2}{2} - \kappa_0 c = 0$ in A_0, implies $\kappa_0 = 2c$, then $\kappa_j = 2c + 2cj = 2c(j+1)$, and

$$\begin{aligned} \sum_{l=0}^{2i-1} \kappa_l &= 2ci(2i+1) \\ \sum_{k=0}^{2j+1} \kappa_k &= 2c(2j+3)(j+1) \end{aligned}$$

Equation (4.22) becomes,

$$A_0 = 1 + 2\sum_{i=1}^{j} (-1)^i e^{-4bci(2i+1)} - e^{-4bc(2j+3)(j+1)} \left[1 + A_{2(j+1)}\right] \tag{4.23}$$

As $j \to \infty$ in equation (4.23), $e^{-4bc(2j+3)(j+1)} \left[1 + A_{2(j+1)}\right]$ vanishes, thus given that both b and c are nonnegative,

$$\mathbb{P}(\tau < \infty) = 1 + 2\sum_{i=1}^{\infty} (-1)^i e^{-4bci(2i+1)}$$

□

4.2.2 Asymmetric linear boundaries

In this section, we consider the same standard Brownian motion $\{X_t\}_{t\geq 0}$ which initially starts from 0, and the time-dependent linear boundaries are

$$c(t) = \begin{cases} b_1 + c_1 t & b_1, c_1 > 0 \\ -b_2 - c_2 t & b_2, c_2 > 0 \end{cases}$$

Recall the upper first-passage time τ_1 and lower first-passage time τ_2 defined as in equations (4.1) and (4.2) defined at the beginning of this chapter, now we are going to consider the probability that the standard Brownian motion hits the upper boundary before hitting the lower one without limit.

Theorem 4.16. *Let $\{X_t\}_{t\geq 0}$ be a standard Brownian motion with $X_0 = 0$, and two continuous functions $u(t) = b_1 + c_1 t$ and $l(t) = -b_2 - c_2 t$ for all t and $b_1, b_2, c_1, c_2 > 0$. The upper hitting time probability is given by*

$$P_u^{(2)} = e^{-2b_1 c_1}\left[1 - e^{-2b_2(2c_1+c_2)}\right] + e^{-(2c_1+c_2)}\sum_{l=0}^{\infty}\left(e^{-2B_l} - e^{-2C_l}\right) \tag{4.24}$$

where

$$\begin{aligned} B_l &= (b_1+b_2)(c_1+c_2)l^2 + [c_1(b_1+b_2) + 2b_2(c_1+c_2)]l \\ C_l &= (b_1+b_2)(c_1+c_2)l^2 + c_1(b_1+b_2)l - (4c_1+3c_2)b_2 \end{aligned}$$

Proof. Consider the well-known martingale $e^{-\frac{\beta^2}{2}t+\beta X_t}$, where β is a deterministic constant. Due to the martingale property and Doob's optional stopping theorem,

we get the following,

$$\begin{aligned}
&\mathbb{E}\left[e^{-\frac{\beta^2}{2}t+\beta X_t}\mathbb{1}_{\{(\tau_1\wedge\tau_2)\leq t\}}\right]+\mathbb{E}\left[e^{-\frac{\beta^2}{2}t+\beta X_t}\mathbb{1}_{\{(\tau_1\wedge\tau_2)\geq t\}}\right]=\mathbb{E}\left[e^{\beta X_0}\right]\\
&\mathbb{E}\left[e^{-\frac{\beta^2}{2}\tau_1+\beta X_{\tau_1}}\mathbb{1}_{\{\tau_1<t,\tau_1<\tau_2\}}\right]+\mathbb{E}\left[e^{-\frac{\beta^2}{2}\tau_2+\beta X_{\tau_2}}\mathbb{1}_{\{\tau_2<t,\tau_2<\tau_1\}}\right]\\
&+\mathbb{E}\left[e^{-\frac{\beta^2}{2}t+\beta X_t}\mathbb{1}_{\{(\tau_1\wedge\tau_2)\geq t\}}\right]=\mathbb{E}\left[e^{\beta X_0}\right] \qquad (4.25)
\end{aligned}$$

where $\mathbb{1}_{\{\tau_1<t,\tau_1<\tau_2\}}$, $\mathbb{1}_{\{\tau_2<t,\tau_2<\tau_1\}}$ and $\mathbb{1}_{\{(\tau_1\wedge\tau_2)\geq t\}}$ are indicator functions.

Applying the Dominated Convergence Theorem to the third term of equation (4.25),

$$\begin{aligned}
\lim_{t\to\infty}\mathbb{E}\left[e^{-\frac{\beta^2}{2}t+\beta X_t}\mathbb{1}_{\{(\tau_1\wedge\tau_2)\geq t\}}\right] &= \mathbb{E}\left[\lim_{t\to\infty}e^{-\frac{\beta^2}{2}t+\beta X_t}\mathbb{1}_{\{(\tau_1\wedge\tau_2)\geq t\}}\right]\\
&= \mathbb{E}\left[e^{-\lim_{t\to\infty}t(\frac{\beta^2}{2}-\beta\frac{X_t}{t})}\mathbb{1}_{\{(\tau_1\wedge\tau_2)=\infty\}}\right]\\
&= 0
\end{aligned}$$

where $\lim_{t\to\infty}\frac{X_t}{t}=0$ by the Strong Law of Large Number for Brownian motion.

Let $I_1=\{\tau_1<\infty,\tau_1<\tau_2\}$ and $I_2=\{\tau_2<\infty,\tau_2<\tau_1\}$, and the standard Brownian motion X_t starts from 0, hence

$$\begin{aligned}
\mathbb{E}\left[e^{-\frac{\beta^2}{2}\tau_1+\beta(b_1+c_1\tau_1)}\mathbb{1}_{I_1}\right]+\mathbb{E}\left[e^{-\frac{\beta^2}{2}\tau_2-\beta(b_2+c_2\tau_2)}\mathbb{1}_{I_2}\right] &= 1\\
e^{\beta b_1}\mathbb{E}\left[e^{-(\frac{\beta^2}{2}-\beta c_1)\tau_1}\mathbb{1}_{I_1}\right]+e^{-\beta b_2}\mathbb{E}\left[e^{-(\frac{\beta^2}{2}+\beta c_2)\tau_2}\mathbb{1}_{I_2}\right] &= 1 \qquad (4.26)
\end{aligned}$$

Two substitutions are required, when X_t touches the upper boundary, $u(t)$, first, let $\beta=k_j$ and $\frac{\beta^2}{2}=\frac{k_j^2}{2}$ into equation (4.26), for $j=0,1,2,\cdots$,

$$e^{k_jb_1}\mathbb{E}\left[e^{-(\frac{k_j^2}{2}-k_jc_1)\tau_1}\mathbb{1}_{I_1}\right]+e^{-k_jb_2}\mathbb{E}\left[e^{-(\frac{k_j^2}{2}+k_jc_2)\tau_2}\mathbb{1}_{I_2}\right]=1 \qquad (4.27)$$

On the other hand, when X_t reaches the lower boundary, $l(t)$, before reaching $u(t)$, let $\beta = -k_j^*$ and $\frac{\beta^2}{2} = \frac{k_j^{*2}}{2}$ in equation (4.26), for $j = 0, 1, 2, \cdots$,

$$e^{-k_j^* b_1}\mathbb{E}\left[e^{-(\frac{k_j^{*2}}{2}+k_j^* c_1)\tau_1}\mathbb{1}_{I_1}\right] + e^{k_j^* b_2}\mathbb{E}\left[e^{-(\frac{k_j^{*2}}{2}-k_j^* c_2)\tau_2}\mathbb{1}_{I_2}\right] = 1 \tag{4.28}$$

To find the probability $P_u^{(2)}$, we want $\frac{k_j^2}{2} + k_j c_2 = \frac{k_j^{*2}}{2} - k_j^* c_2$ in equations (4.27) and (4.28), so $k_j^* = k_j + 2c_2$. Multiplying the equations by $e^{k_j^* b_2}$ and $e^{-k_j b_2}$ respectively, we have

$$e^{k_j b_1}e^{k_j^* b_2}\mathbb{E}\left[e^{-(\frac{k_j^2}{2}-k_j c_1)\tau_1}\mathbb{1}_{I_1}\right] + e^{-k_j b_2}e^{k_j^* b_2}\mathbb{E}\left[e^{-(\frac{k_j^2}{2}+k_j c_2)\tau_2}\mathbb{1}_{I_2}\right] = e^{k_j^* b_2} \tag{4.29}$$

$$\begin{aligned} &e^{-k_j^* b_1}e^{-k_j b_2}\mathbb{E}\left[e^{-(\frac{k_j^{*2}}{2}+k_j^* c_1)\tau_1}\mathbb{1}_{I_1}\right] + e^{k_j^* b_2}e^{-k_j b_2}\mathbb{E}\left[e^{-(\frac{k_j^{*2}}{2}-k_j^* c_2)\tau_2}\mathbb{1}_{I_2}\right] \\ &= e^{-k_j b_2} \end{aligned} \tag{4.30}$$

Equation (4.29) subtracts equation (4.30), for $j = 0, 1, 2, \cdots$,

$$\begin{aligned} e^{k_j b_1 + k_j^* b_2}\mathbb{E}\left[e^{-(\frac{k_j^2}{2}-k_j c_1)\tau_1}\mathbb{1}_{I_1}\right] - e^{-(k_j^* b_1 + k_j b_2)}\mathbb{E}\left[e^{-(\frac{k_j^{*2}}{2}+k_j^* c_1)\tau_1}\mathbb{1}_{I_1}\right] \\ = e^{k_j^* b_2} - e^{-k_j b_2} \end{aligned} \tag{4.31}$$

Furthermore, now let us consider the $(j+1)$th equation of equation (4.27), which is

$$e^{k_{j+1} b_1}\mathbb{E}\left[e^{-(\frac{k_{j+1}^2}{2}-k_{j+1} c_1)\tau_1}\mathbb{1}_{I_1}\right] + e^{-k_{j+1} b_2}\mathbb{E}\left[e^{-(\frac{k_{j+1}^2}{2}+k_{j+1} c_2)\tau_1}\mathbb{1}_{I_2}\right] = 1 \tag{4.32}$$

Moreover, we also wish to have k_{j+1} such that $\frac{k_j^{*2}}{2} + k_j^* c_1 = \frac{k_{j+1}^2}{2} - k_{j+1} c_1$ in equations (4.31) and (4.32), so $k_{j+1} = k_j^* + 2c_1$. Denote $A_j = \mathbb{E}[e^{-(\frac{k_j^2}{2}-k_j c_1)\tau_1}\mathbb{1}_{I_1}]$, so

$$A_{j+1} = \mathbb{E}\left[e^{-(\frac{k_{j+1}^2}{2}-k_{j+1} c_1)\tau_1}\mathbb{1}_{I_1}\right] = \mathbb{E}\left[e^{-(\frac{k_j^{*2}}{2}+k_j^* c_1)\tau_1}\mathbb{1}_{I_1}\right]$$

. Therefore, equation (4.31) can be rewritten as

$$A_j = e^{-(b_1+b_2)(k_j+k_j^*)}A_{j+1} + e^{-k_j b_1}\left[1 - e^{-b_2(k_j+k_j^*)}\right] \tag{4.33}$$

Since $k_{j+1} = 2c_1 + k_j^*$ and $k_j^* = 2c_2 + k_j$, $k_j + k_j^* = 2(k_j + c_2)$, then equation (4.33) becomes

$$A_j = e^{-2(b_1+b_2)(k_j+c_2)}A_{j+1} + e^{-k_j b_1}\left[1 - e^{-2b_2(k_j+c_2)}\right] \tag{4.34}$$

Summing up the set of equations that in the form of equation (4.34), for $j = 0, 1, 2, \cdots$, in general,

$$\begin{aligned} A_0 &= e^{-2(b_1+b_2)\sum_{i=0}^{j}(k_i+c_2)}A_{j+1} \\ &\quad + \sum_{l=0}^{j} e^{-2(b_1+b_2)\sum_{n=0}^{l}(k_n+c_2)-k_{l+1}b_1}\left[1 - e^{-2b_2(k_{l+1}+c_2)}\right] \\ &\quad + e^{-k_0 b_1}\left[1 - e^{-2b_2(k_0+c_2)}\right] \end{aligned} \tag{4.35}$$

where $A_0 = \mathbb{E}[e^{-(\frac{k_0^2}{2} - k_0 c_1)\tau_1}\mathbb{1}_{I_1}]$.

To obtain $\mathbb{E}[\mathbb{1}_{I_1}] \equiv P_u^{(2)}$, let $\frac{k_0^2}{2} - k_0 c_1 = 0$ in A_0, i.e. $k_0 = 2c_1$, as $k_j > 0 \forall j$, and we have $k_j = k_0 + 2j(c_1 + c_2)$, then $k_j = 2j(c_1 + c_2) + 2c_1$. So,

$$\begin{aligned} \sum_{i=0}^{j} k_i + c_2 &= j(j+1)(c_1+c_2) + j(2c_1+c_2) \\ \sum_{n=0}^{l} k_n + c_2 &= l(l+1)(c_1+c_2) + l(2c_1+c_2) \\ k_{l+1} &= 2(l+1)(c_1+c_2) + 2c_1 \\ k_{l+1} + c_2 &= 2l(c_1+c_2) + (4c_1+3c_2) \\ k_0 + c_2 &= 2c_1 + c_2 \end{aligned}$$

Substituting these terms into equation (4.35), and as j tends to infinity, equation (4.24) in Theorem 4.16 follows immediately. □

As similar as $P_u^{(2)}$, the probability for the standard Brownian motion, X_t, reaches the lower limit before reaching the upper limit first, $P_l^{(2)}$, can be found analogously,

Corollary 4.3. *For a standard Brownian motion, $\{X_t\}_{t\geq 0}$, with two continuous functions $u(t)$ and $l(t)$ (as defined in Theorem 4.16), the lower hitting time probability is given by*

$$P_l^{(2)} = e^{-2b_2c_2}\left[1 - e^{-2b_1(c_1+2c_2)}\right] + e^{-(2c_2+c_1)b_2}\sum_{l=0}^{\infty}\left(e^{-2B_l^*} - e^{-2C_l^*}\right) \tag{4.36}$$

where

$$\begin{aligned} B_l^* &= (b_1+b_2)(c_1+c_2)l^2 + [(b_1+b_2)(2c_1+3c_2) - 2b_2(c_1+c_2)]l \\ C_l^* &= (b_1+b_2)(c_1+c_2)l^2 + (b_1+b_2)c_2 l - (4c_2+3c_1)b_1 \end{aligned}$$

Proof. Let us consider the two equations (4.27) and (4.28) again, and this time we need to choose k_j such that $\frac{k_j^2}{2} - k_j c_1 = \frac{k_j^{*2}}{2} + k_j^* c_1$, so $k_j = k_j^* + 2c_1$. Similarly, multiplying the two equations by $e^{-k_j^* b_1}$ and $e^{k_j b_1}$ respectively, and taking substraction to get the following equation,

$$e^{k_j b_1 + k_j^* b_2}\mathbb{E}\left[e^{-(\frac{k_j^{*2}}{2} - k_j^* c_2)\tau_2}\mathbb{1}_{I_2}\right] - e^{-(k_j^* b_1 + k_j b_2)}\mathbb{E}\left[e^{-(\frac{k_j^2}{2} + k_j c_2)\tau_2}\mathbb{1}_{I_2}\right] = e^{k_j b_1} - e^{-k_j^* b_1}$$

$$j = 0, 2, 4, \cdots$$

In addition, increase j to $j+1$ in equation (4.28) and let $\frac{k_j^2}{2} + k_j c_2 = \frac{{k_{j+1}^*}^2}{2} - k_{j+1}^* c_2$,

then $k^*_{j+1} = k_j + 2c_2$. We define that $A^*_j = \mathbb{E}[e^{-(\frac{k_j^{*2}}{2} - k^*_j c_2)\tau_2} \mathbb{1}_{I_2}]$, then

$$A^*_{j+1} = \mathbb{E}\left[e^{-(\frac{k^*_{j+1}{}^2}{2} - k^*_{j+1} c_2)\tau_2} \mathbb{1}_{I_2}\right] = \mathbb{E}\left[e^{-(\frac{k_j^2}{2} + k_j c_2)\tau_2} \mathbb{1}_{I_2}\right]$$

Therefore,

$$\begin{aligned} A^*_j &= e^{-(b_1+b_2)(k_j+k^*_j)} A^*_{j+1} + e^{-k^*_j b_2}\left[1 - e^{-b_1(k_j+k^*_j)}\right] \\ &= e^{-2(b_1+b_2)(k^*_j+c_1)} A^*_{j+1} + e^{-k^*_j b_2}\left[1 - e^{-2b_1(k^*_j+c_1)}\right] \end{aligned} \tag{4.37}$$

since $k_j + k^*_j = 2(k^*_j + c_1)$.

We noticed that equation (4.37) is same to equation (4.34) but b_1, c_1 and k_j are replaced by b_2, c_2 and k^*_j respectively. □

4.3 Stochastic boundaries

4.3.1 Compound Poisson process

General case

Consider the standard Brownian motion $\{X_t\}_{t\geq 0}$ again, with boundaries such that $Z_t = \sum_{i=1}^{N(t)} Y_i + b$, where $N(t)$ is a Poisson process with rate λ and the jump size $Y_i > 0$ has distribution function $H(y)$. Define the first-passage time as $\tau = \inf_{t>0}\{t : |X_t| \geq Z_t\}$, the first time that X_t exceeds one of the two boundaries, with the convention $\tau = \infty$ if $|X_t| < Z_t$ for all $t > 0$.

Theorem 4.17. *Let $\varphi(\gamma)$ be the Laplace transform of the distribution function of Y_i, then the probability for X_t exceeds any one of the two boundaries, Z_t and $-Z_t$*

can be obtained via

$$\mathbb{E}\left[e^{-\theta_0 Z_\tau}\mathbb{1}_{\{\tau<\infty\}}\right] = \mathbb{E}\left[e^{-(2\gamma_n-\theta_n)Z_\tau}\mathbb{1}_{\{\tau<\infty\}}\right] + \sum_{j=0}^{n}(-1)^j e^{-\gamma_j b}(e^{k_j x_0} + e^{-k_j x_0}) \quad (4.38)$$

by letting $\theta_0 = 0$ *and* $n \to \infty$*, where* γ_n *and* k_n *are the constants of the martingale,* $e^{-\gamma Z_t}\left(e^{kX_t} + e^{-kX_t}\right)$*, and,*

$$\theta_0 = \gamma_0 - \sqrt{2\lambda(1-\varphi(\gamma_0))}$$
$$\theta_n = \gamma_n - \sqrt{2\lambda(1-\varphi(\gamma_n))}$$

Proof. The martingale that we are interested in is $e^{-\gamma Z_t}(e^{kX_t} + e^{-kX_t})$, where γ and k are nonnegative constants. To determine them, let $\varphi(\gamma) = \int_0^\infty e^{-\gamma y}dH(y)$ be the Laplace transform of the distribution function of Y_i, $H(y)$. One can find that $\lambda(1-\varphi(\gamma)) = \frac{1}{2}k^2$ by equation (4.15), we notice that the two values of k will yield the identical martingales, so we will let $k = \sqrt{2\lambda(1-\varphi(\gamma))}$.

Due to the martingale property,

$$\begin{aligned}\mathbb{E}\left[e^{-\gamma Z_t}\left(e^{kX_t} + e^{-kX_t}\right)\mathbb{1}_{\{\tau<t\}}\right] &+ \mathbb{E}\left[e^{-\gamma Z_t}\left(e^{kX_t} + e^{-kX_t}\right)\mathbb{1}_{\{\tau\geq t\}}\right] \\ &= \mathbb{E}\left[e^{-\gamma Z_0}\left(e^{kX_0} + e^{-kX_0}\right)\right] \quad (4.39)\\ \mathbb{E}\left[e^{-\gamma Z_\tau}\left(e^{kX_\tau} + e^{-kX_\tau}\right)\mathbb{1}_{\{\tau<\infty\}}\right] &= e^{-\gamma b}\left(e^{kx_0} + e^{-kx_0}\right) \quad (4.40)\end{aligned}$$

When t tends infinity, $\frac{X_t}{t} \to 0$ and $\frac{Z_t}{t} \to \lambda\mathbb{E}(Y_i)$, then the second term on the left

hand side of equation (4.39) becomes,

$$\begin{aligned}
& \lim_{t\to\infty} \mathbb{E}\left[e^{-\gamma Z_t}\left(e^{kX_t}+e^{-kX_t}\right)\mathbb{1}_{\{\tau\geq t\}}\right] \\
= \;& \mathbb{E}\left[\lim_{t\to\infty} e^{-\gamma Z_t+kX_t}\mathbb{1}_{\{\tau\geq t\}} + \lim_{t\to\infty} e^{-\gamma Z_t-kX_t}\mathbb{1}_{\{\tau\geq t\}}\right] \\
= \;& \mathbb{E}\left[e^{\lim_{t\to\infty} -t(\gamma\frac{Z_t}{t}-k\frac{X_t}{t})}\mathbb{1}_{\{tau=\infty\}}\right] + \mathbb{E}\left[e^{\lim_{t\to\infty} -t(\gamma\frac{Z_t}{t}+k\frac{X_t}{t})}\mathbb{1}_{\{\tau=\infty\}}\right] \\
= \;& 0
\end{aligned}$$

Hence, equation (4.40) follows immediately.

Since we assume that the two stochastic boundaries are symmetric about the time horizon, consider the set of the following equations only, for $j = 0, 1, 2, \cdots$,

$$\mathbb{E}\left[e^{-\gamma_0 Z_\tau}\left(e^{k_0 X_\tau}+e^{-k_0 X_\tau}\right)\mathbb{1}_{\{\tau<\infty\}}\right] = e^{-\gamma_0 z_0}\left(e^{k_0 x_0}+e^{-k_0 x_0}\right);$$

$$\cdots$$

$$\mathbb{E}\left[e^{-\gamma_j Z_\tau}(e^{k_j X_\tau}+e^{-k_j X_\tau})\mathbb{1}_{\{\tau<\infty\}}\right] = e^{-\gamma_j z_0}\left(e^{k_j x_0}+e^{-k_j x_0}\right); \tag{4.41}$$

$$\mathbb{E}\left[e^{-\gamma_{j+1} Z_\tau}(e^{k_{j+1} X_\tau}+e^{-k_{j+1} X_\tau})\mathbb{1}_{\{\tau<\infty\}}\right] = e^{-\gamma_{j+1} z_0}\left(e^{k_{j+1} x_0}+e^{-k_{j+1} x_0}\right) \tag{4.42}$$

as $k_j = \sqrt{2\lambda(1-\varphi(\gamma_j))}$, equations (4.41) and (4.42) can be rewritten as,

$$\begin{aligned}
& \mathbb{E}\left[e^{-(\gamma_j-\sqrt{2\lambda(1-\varphi(\gamma_j))})Z_\tau}\mathbb{1}_{\{\tau<\infty\}}\right] + \mathbb{E}\left[e^{-(\gamma_j+\sqrt{2\lambda(1-\varphi(\gamma_j))})Z_\tau}\mathbb{1}_{\{\tau<\infty\}}\right] \\
& = e^{-\gamma_j b}\left(e^{k_j x_0}+e^{-k_j x_0}\right) \qquad (4.43) \\
& \mathbb{E}\left[e^{-(\gamma_{j+1}-\sqrt{2\lambda(1-\varphi(\gamma_{j+1}))})Z_\tau}\mathbb{1}_{\{\tau<\infty\}}\right] + \mathbb{E}\left[e^{-(\gamma_{j+1}+\sqrt{2\lambda(1-\varphi(\gamma_{j+1}))})Z_\tau}\mathbb{1}_{\{\tau<\infty\}}\right] \\
& = e^{-\gamma_{j+1} b}\left(e^{k_{j+1} x_0}+e^{-k_{j+1} x_0}\right) \qquad (4.44)
\end{aligned}$$

In equations (4.43) and (4.44), we choose γ_j such that,

$$\gamma_j + \sqrt{2\lambda(1-\varphi(\gamma_j))} = \gamma_{j+1} - \sqrt{2\lambda(1-\varphi(\gamma_{j+1}))} \tag{4.45}$$

so when subtracting equation (4.43) from equation (4.44) for $j = 0, 2, 4, \cdots$, we get the following equations,

$$\mathbb{E}\left[e^{-(\gamma_j - \sqrt{2\lambda(1-\varphi(\gamma_j))})Z_\tau}\mathbb{1}_{\{\tau<\infty\}}\right] - \mathbb{E}\left[e^{-(\gamma_{j+1} + \sqrt{2\lambda(1-\varphi(\gamma_{j+1}))})Z_\tau}\mathbb{1}_{\{\tau<\infty\}}\right]$$
$$= e^{-\gamma_j b}\left(e^{k_j x_0} + e^{-k_j x_0}\right) - e^{-\gamma_{j+1} b}\left(e^{k_{j+1} x_0} + e^{-k_{j+1} x_0}\right) \quad (4.46)$$

Using equation (4.45), when summing up equation (4.46) over j, we have,

$$\mathbb{E}\left[e^{-(\gamma_0 - \sqrt{2\lambda(1-\varphi(\gamma_0))})Z_\tau}\mathbb{1}_{\{\tau<\infty\}}\right] - \mathbb{E}\left[e^{-(\gamma_n + \sqrt{2\lambda(1-\varphi(\gamma_n))})Z_\tau}\mathbb{1}_{\{\tau<\infty\}}\right]$$
$$= \sum_{j=0}^{n}(-1)^j e^{-\gamma_j b}\left(e^{k_j x_0} + e^{-k_j x_0}\right) \quad (4.47)$$

Now let $\theta_0 = \gamma_0 - \sqrt{2\lambda(1-\varphi(\gamma_0))}$, then $\theta_n = \gamma_n - \sqrt{2\lambda(1-\varphi(\gamma_n))}$ and $\gamma_n + \sqrt{2\lambda(1-\varphi(\gamma_n))} = 2\gamma_n - \theta_n$. The equation (4.47) becomes to (4.38) in Theorem 4.17. □

In the rest of the section, we derive the first-passage time probability of boundaries with two specific jumps, exponential and constant.

Compound Poisson process with Exponential jumps

Theorem 4.18. *Suppose that the standard Brownian motion $\{X_t\}_{t\geq 0}$ with boundaries which are compound Poisson processes, such as $Z_t = \sum_{i=1}^{N(t)} Y_i + b$, and exponential jump sizes $Y_i's$, initially starts from 0. The first-passage time probability is*

$$\mathbb{P}(\tau < \infty) = 2\sum_{j=0}^{\infty}(-1)^j e^{-\gamma_j b} \quad (4.48)$$

where $\gamma_j = \frac{\alpha k_j^2}{2\lambda - k_j^2}$ *and* $k_j's$ *are satisfied the equation (4.49) with* $k_0 = \frac{\sqrt{\alpha^2+8\lambda}-\alpha}{2}$,

$$(2\lambda - k_j^2)k_{j+1}^2 + 2\lambda\alpha k_{j+1} - 2\lambda\alpha k_j + 2\lambda k_j^2 - 4\lambda^2 = 0 \tag{4.49}$$

λ *and* $\frac{1}{\alpha}$ *are rate of Poisson process and mean of exponential jumps respectively.*

Proof. The the proof is modification of the proof for Theorem 4.17. When the jump size, Y_i, is exponentially distributed with parameter α, $\varphi(\gamma_j) = \int_0^\infty e^{-\gamma_j y}\alpha e^{-\alpha y}dy = \frac{\alpha}{\alpha+\gamma_j}$. Hence the constants of the martingale in Theorem 4.17 are $k_j = \sqrt{\frac{2\lambda\gamma_j}{\alpha+\gamma_j}}$ and $\gamma_j = \frac{\alpha k_j^2}{2\lambda - k_j^2}$. Similarly, we want k_j satisfies equation (4.45), which means,

$$\frac{\alpha k_j^2}{2\lambda - k_j^2} + k_j = \frac{\alpha k_{j+1}^2}{2\lambda - k_{j+1}^2} - k_{j+1}$$

which yields equation (4.49) in Theorem 4.18, hence $k_j's$ satisfy the recurrence relation, such that,

$$k_{j+1} = \frac{\sqrt{\lambda^2\alpha^2 + 2\lambda(2\lambda - k_j^2)(\alpha k_j - k_j^2 + 2\lambda)} - \alpha\lambda}{2\lambda - k_j^2}$$

Moreover, $\theta_j = \frac{\alpha k_j^2}{2\lambda - k_j^2} - k_j = \frac{k_j(k_j^2 + \alpha k_j - 2\lambda)}{2\lambda - k_j^2}$ in equation (4.38), Theorem 4.17. Letting $\theta_0 = 0$, the initial value, k_0, can be found by λ and α only, which is $k_0 = \frac{\sqrt{\alpha^2+8\lambda}-\alpha}{2}$. Since both the parameters α and λ are nonnegative. Equation (4.38) becomes to,

$$\mathbb{P}(\tau < \infty) = \mathbb{E}\left[e^{-(2\gamma_n - \theta_n)Z_\tau}\mathbb{1}_{\{\tau<\infty\}}\right] + \sum_{j=0}^{n}(-1)^j e^{-\gamma_j b}\left(e^{k_j x_0} + e^{-k_0 x_0}\right) \tag{4.50}$$

Because that we are concerned about the boundary crossing probability over an infinity time interval, to the extent of Theorem 4.17, equation (4.49) can be rewritten

as

$$(2\lambda - k_j^2)(k_{j+1}^2 - k_j^2) + 2\lambda\alpha(k_{j+1} - k_j) - (2\lambda - k_j^2)^2 = 0$$
$$(2\lambda - k_j^2)(k_{j+1}^2 - 2\lambda) + 2\lambda\alpha(k_{j+1} - k_j) = 0 \tag{4.51}$$

Denote $\lim_{j\to\infty} k_j = k$ and because of equation (4.51), we get that $\lim_{j\to\infty} k_j = \sqrt{2\lambda}$, both γ_j and θ_j are monotonic functions, then equation (4.50) becomes,

$$\mathbb{P}(\tau < \infty) = \sum_{j=0}^{\infty} 2(-1)^j e^{-\gamma_j b}$$

with the assumption that the process starts from 0, i.e. $x_0 = 0$. □

Numerical solutions To illustrate the use of Theorem 4.18, we set the following example values of the first-passage time probabilities for different combinations of the variables (λ, α, b) and the outcomes are present by Table 4.1. In Table 4.1, there are the boundary crossing probabilities, according to equation (4.48), for $\lambda = 0.05, 0.1, 1$ and $\alpha = \frac{1}{50}, \frac{1}{20}, \frac{1}{10}$, with 8 different starting positions of the boundaries, b = 1,2,3,4,5,10,15,20. We have that the first-passage time probabilities reach the tabulated values very quickly (smaller value of b, more iterations required, but at most 16 iterations are sufficient), i.e. in equation (4.48),

$$\mathbb{P}(\tau < \infty) = 2\sum_{j=0}^{\infty}(-1)^j e^{-\gamma_j b} \approx 2\sum_{j=0}^{16}(-1)^j e^{-\gamma_j b}$$

Meanwhile, the values of k_j (Table C.1-C.9), which are varied by λ, the rate of Poisson process, particularly, convergence fast.

On the other hand, the values of both θ_j and γ_j (Table C.1-C.9) are strictly increasing. Although, it has not been shown on the tables, if we use more iterations

Table 4.1: first-passage time probabilities for various values of λ, α, b

	b	$\lambda = 0.05$	$\lambda = 0.1$	$\lambda = 1$
$\alpha = \frac{1}{50}$	1	0.9557	0.9124	0.4633
	2	0.8394	0.7116	0.1202
	3	0.6897	0.5028	0.0296
	4	0.5416	0.3378	0.0073
	5	0.4135	0.2219	0.0018
	10	0.0932	0.0252	1.59×10^{-6}
	15	0.0202	0.0028	1.42×10^{-9}
	20	0.0044	0.0003	1.27×10^{-12}
$\alpha = \frac{1}{20}$	1	0.9609	0.9191	0.4697
	2	0.8547	0.7277	0.1238
	3	0.7134	0.5228	0.0309
	4	0.5694	0.3570	0.0077
	5	0.4419	0.2382	0.0019
	10	0.1074	0.0291	1.85×10^{-6}
	15	0.0250	0.0035	1.78×10^{-9}
	20	0.0058	0.0004	1.71×10^{-12}
$\alpha = \frac{1}{10}$	1	0.9685	0.9295	0.4803
	2	0.8779	0.7535	0.1299
	3	0.7500	0.5559	0.0333
	4	0.6148	0.3896	0.0085
	5	0.4894	0.2665	0.0022
	10	0.1338	0.0366	2.36×10^{-6}
	15	0.0348	0.0050	2.56×10^{-9}
	20	0.0090	0.0006	2.78×10^{-12}

$(j > 16, j \to \infty)$, both θ_j and γ_j are intending to infinity numerically, so does $2\gamma_j - \theta_j$. Hence, the term $\mathbb{E}[e^{-(2\gamma_n - \theta_n)Z_\tau} \mathbb{1}_{\{\tau<\infty\}}]$ in equation (4.50) will equal to 0 for large n.

Figure 4.1: First-passage probabilities of Theorem 4.18 for various values of b

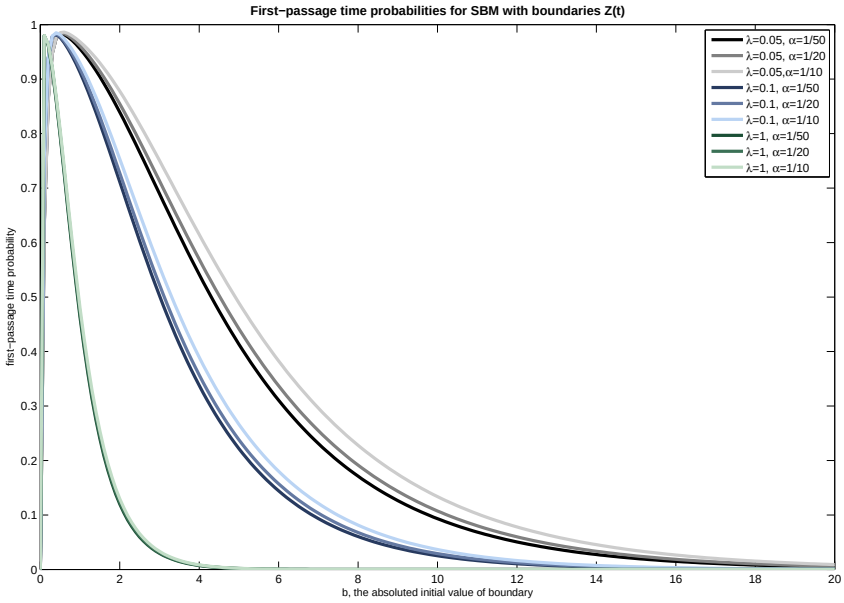

Figure 4.1 illustrates the results in Table 4.1 across for various values of b, where horizontal axis is the value of b and vertical axis represents the probabilities. In the figure, the plots are separated into different groups. In each group, the three plots have equal λ in common but α, the lighter the color of the curve, the larger the value of α. Within groups, from $b = 0$ till the point where the curves reach the maximum, they do not apart away from others; after the peak, the probabilities with the same λ tend to be separated; nevertheless, a confluence is achieved at the end (i.e $b = 20$). Among groups of curves, although the maximums occurre over a short interval of b, the order still can be observed. The green curves, which indicate $\lambda = 1$, show the peak at the first while b is changing, followed by curves with λ

decreasing. Moreover, when the frequency of changes for boundaries becomes higher and higher, the difference between first-passage time probabilities are becoming less and less visible. Figures 4.2-4.5 give extra illustrations over a wilder range of λ and α. To conclude, it indicates that, in comparison with the effect of the value of λ, the rate of Poisson process, the values of the mean size of exponential jumps, $\frac{1}{\alpha}$, vary the probabilities over a more narrower interval. Last but not least, the initial value of boundaries is the most deterministic factor to the boundary crossing probabilities, when a boundary starts from $b \geq 20$ initially, it is less likely to cross it ultimately.

Monte Carlo simulation results The corresponding simulated results are provided in this section. A discrete time standard Brownian motion is generated by Monte Carlo Markov Chain, and the two symmetric compound Poisson processes with exponential changes are simulated in the same time horizon. In the simulation, we investigate the number of times when the standard Brownian motion meets up with one of the boundaries over 1000 simulations. 100 repeats are carried out, the results are averaged.

Table 4.2 are the simulated corresponding probabilities and the associated variances are in parentheses. For different values of b, the interval needs to be fined at different levels for the simulated discrete time standard Brownian motion. However, generally speaking, the simulated averaged probabilities closely agree with the ones in Table 4.1.

Compound Poisson process with constant jumps

When the jump sizes are identical and equal to a constant, say $c > 0$, the boundaries become to $|Z_t| = b + cN_t$, where N_t is a Poisson process with parameter λ. To find the probabilities $\mathbb{P}(\tau > \infty)$, by the definition of function $\varphi(\gamma_j)$ in Theorem 4.17, we

Figure 4.2: $\frac{1}{\alpha} = 1, \frac{1}{20}, \frac{1}{50}, \frac{1}{100}, \frac{1}{500}, \frac{1}{1000}$, $\lambda \in [0, 1000]$

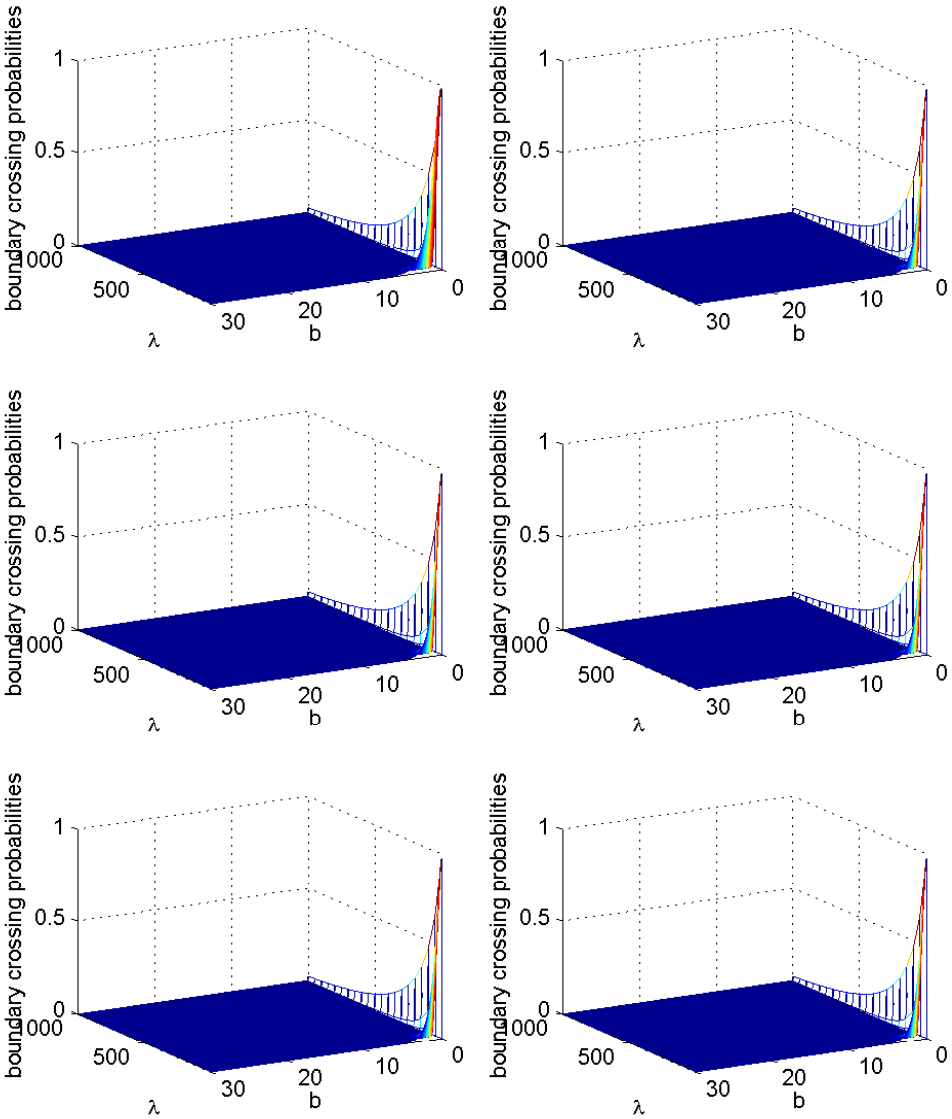

Figure 4.3: $\frac{1}{\alpha} = 1, \frac{1}{20}, \frac{1}{50}, \frac{1}{100}, \frac{1}{500}, \frac{1}{1000}$, $\lambda \in [0.05, 1]$

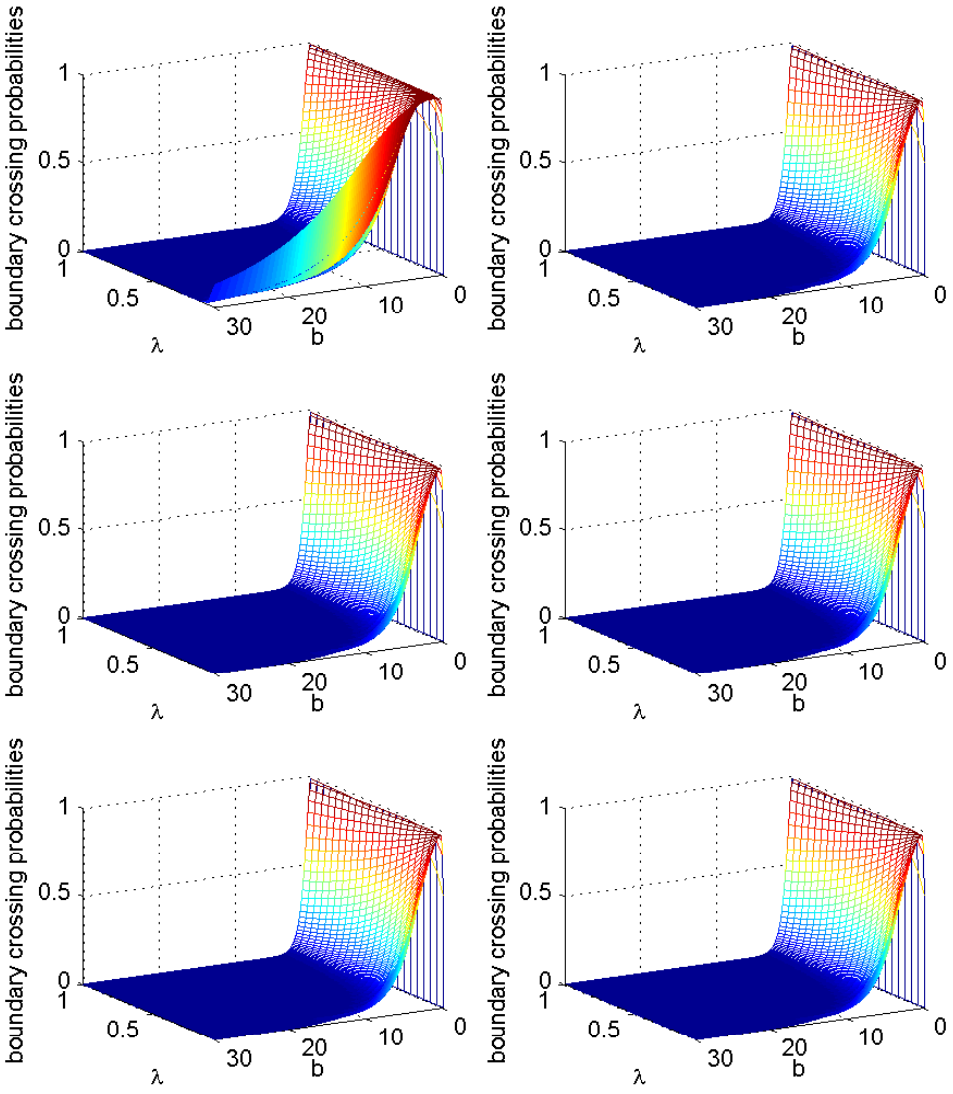

Figure 4.4: $\lambda = \frac{1}{20}, \frac{1}{10}, 1, 10, 100, 1000$, $\alpha \in [\frac{1}{1000}, 1]$

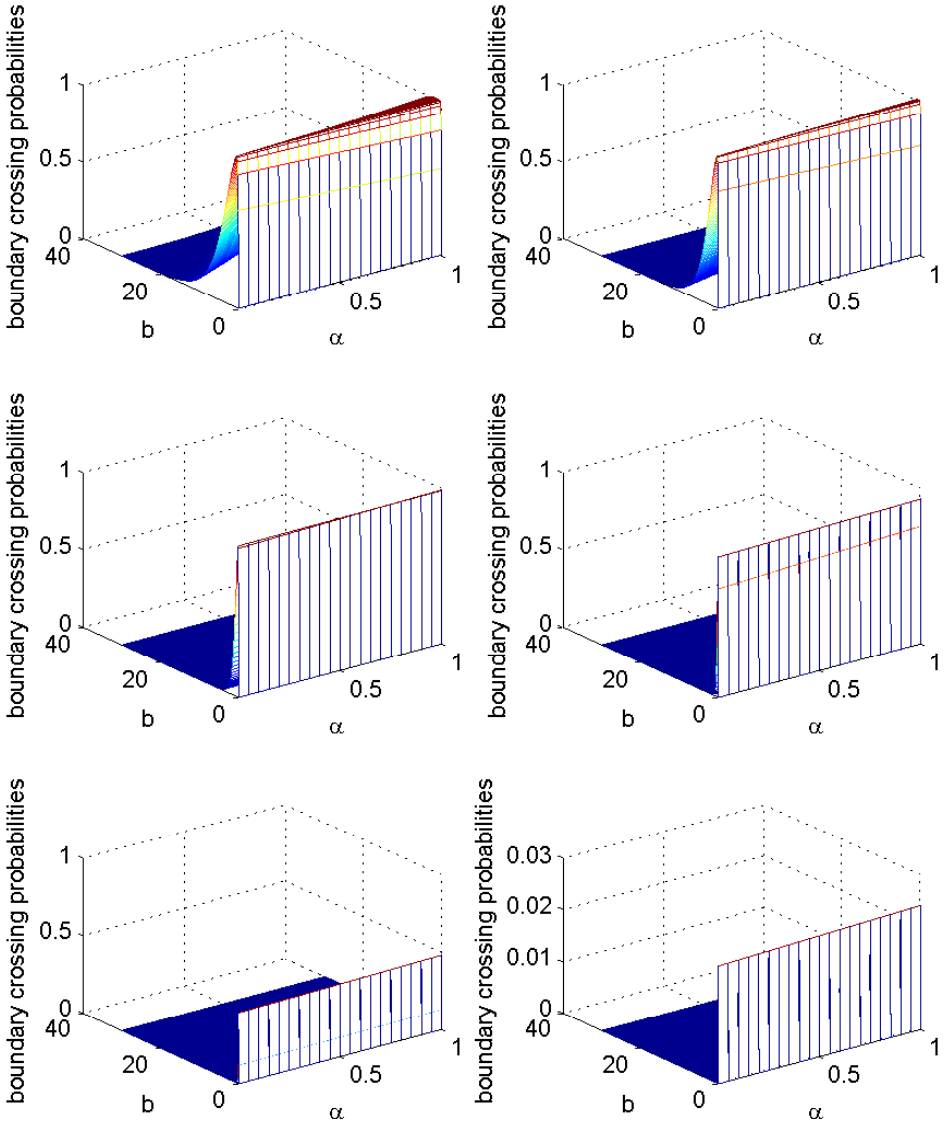

Figure 4.5: $\lambda = \frac{1}{20}, \frac{1}{10}, 1, 10, 100, 1000$, $\alpha \in [\frac{1}{5000}, \frac{1}{1000}]$

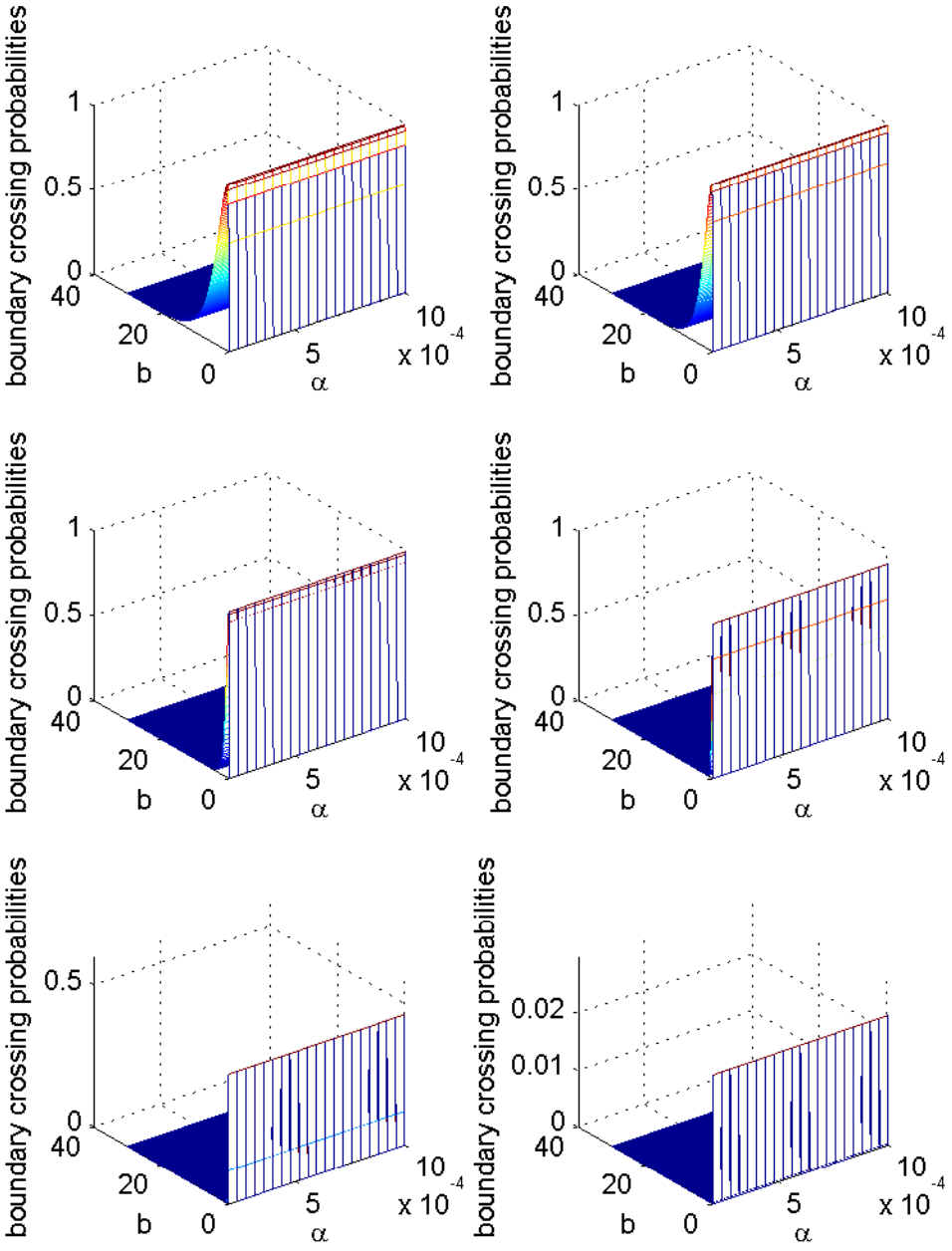

Table 4.2: Simulated mean probabilities and its variance

	b	$\lambda = 0.05$		$\lambda = 0.1$		$\lambda = 1$	
$\alpha = \frac{1}{50}$	1	0.9554	(0.000046)	0.9141	(0.000088)	0.4633	(0.000224)
	2	0.8309	(0.000149)	0.6995	(0.000254)	0.1273	(0.000125)
	3	0.6895	(0.000231)	0.5046	(0.000293)	0.0258	(0.000024)
	4	0.5412	(0.000238)	0.3311	(0.000195)	0.0071	(0.000007)
	5	0.4123	(0.000256)	0.2269	(0.000166)	0.0020	(0.000002)
	10	0.0968	(0.000083)	0.0264	(0.000032)	0.0000	(0.000000)
	15	0.0274	(0.000026)	0.0029	(0.000003)	0	(0)
	20	0.0041	(0.000004)	0.0003	(0.000000)	0	(0)
$\alpha = \frac{1}{20}$	1	0.9637	(0.000038)	0.9172	(0.000068)	0.4645	(0.000269)
	2	0.8743	(0.000118)	0.7147	(0.000173)	0.1212	(0.000107)
	3	0.6880	(0.000206)	0.5229	(0.000198)	0.0307	(0.000029)
	4	0.5676	(0.000266)	0.3491	(0.000307)	0.0074	(0.000007)
	5	0.4572	(0.000234)	0.2381	(0.000148)	0.0013	(0.000001)
	10	0.1037	(0.000116)	0.0310	(0.000027)	0.0000	(0.000000)
	15	0.0267	(0.000026)	0.0036	(0.000004)	0	(0)
	20	0.0067	(0.000007)	0.0009	(0.000001)	0	(0)
$\alpha = \frac{1}{10}$	1	0.9665	(0.000031)	0.9272	(0.000056)	0.4868	(0.000237)
	2	0.8767	(0.000105)	0.7553	(0.000176)	0.1317	(0.000117)
	3	0.7495	(0.000165)	0.5466	(0.000211)	0.0334	(0.000030)
	4	0.6230	(0.000244)	0.3886	(0.000234)	0.0088	(0.000009)
	5	0.4904	(0.000187)	0.2610	(0.000227)	0.0028	(0.000003)
	10	0.1328	(0.000132)	0.0347	(0.000039)	0.0000	(0.000000)
	15	0.0364	(0.000037)	0.0057	(0.000007)	0	(0)
	20	0.0090	(0.000008)	0.0009	(0.000001)	0	(0)

find that, as similar as the proof of Theorem 4.17, $\varphi(\gamma_j) = \mathbb{E}[e^{-\gamma_j c}] = e^{-\gamma_j c}$, and

$$\gamma_j = -\frac{1}{c} \ln \left(1 - \frac{k_j^2}{2\lambda}\right)$$

By choosing γ_j and k_j to satisfying equation (4.45), we have,

$$\begin{aligned} \gamma_j + k_j &= \gamma_{j+1} - k_{j+1} \\ \frac{2c - k_j^2}{2c - k_{j+1}^2} &= e^{c(k_j + k_{j+1})} \end{aligned}$$

The initial k_0 can be found by letting $\gamma_0 - k_0 = 0$, in other words,

$$e^{-ck_0} + \frac{k_0^2}{2\lambda} - 1 = 0$$

which could not be solved explicitly.

4.3.2 Telegraph process

A telegraph process is the path of a particle starts from the origin with constant velocity c_1 or $-c_2$ with equal probability $\frac{1}{2}$. The switch between positive and negative velocities is determined by a non-homogeneous Poisson process $N(t)$. The current velocity $V = V(t)$, $t > 0$ switches from c_1 to $-c_2$ after an exponentially distributed time with parameter λ_1, and from $-c_2$ to c_1 after a random time with exponential distribution with parameter λ_2. The time intervals separated by velocity changes are independent random variables.

The displacement $X(t)$ is defined by $X(t) = v(0)\int_0^t (-1)^{N(s)} ds$, where

$$V(0) = \begin{cases} c_1 & \text{with probability} \frac{1}{2} \\ -c_2 & \text{with probability} \frac{1}{2} \end{cases}$$

Figure 4.6 is an example of a Telegraph process with $c_1 = c_2$ and $\lambda_1 = \lambda_2$ [19].

Figure 4.6: An example sampling of a Telegraph process with $c_1 = c_2$, $\lambda_1 = \lambda_2$

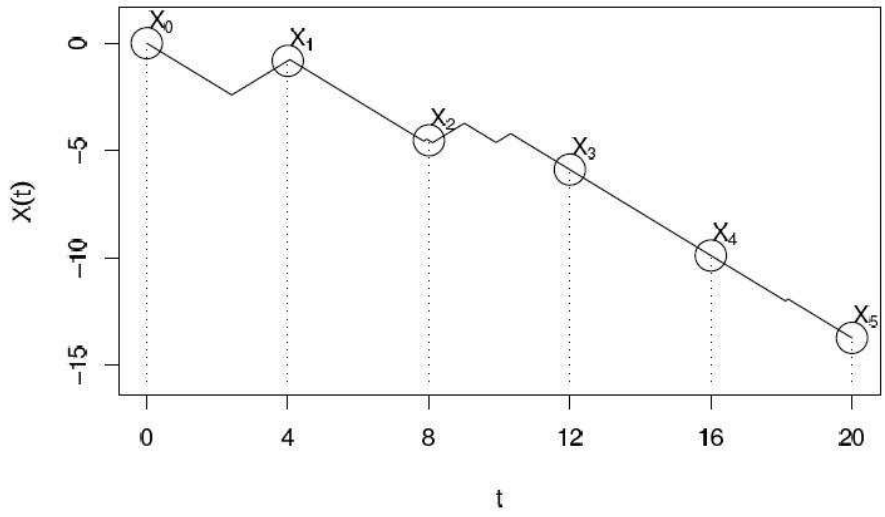

Define the following two functions

$$\begin{aligned} f_1(x,t)dx &= \mathbb{P}(X(t) \in dx, V(t) = c_1) \\ f_2(x,t)dx &= \mathbb{P}(X(t) \in dx, V(t) = -c_2) \end{aligned}$$

They are the well-known solutions of the following partial differential equations [34]

$$\frac{\partial f_1}{\partial t} = -c_1 \frac{\partial f_1}{\partial x} + \lambda_2 f_2 - \lambda_1 f_1 \tag{4.52}$$

$$\frac{\partial f_2}{\partial t} = c_2 \frac{\partial f_2}{\partial x} + \lambda_1 f_1 - \lambda_2 f_2 \tag{4.53}$$

Moreover, define that $p = f_1 + f_2$ and $w = f_1 - f_2$, it follows that, (4.52)+(4.53):

$$\begin{aligned}
\frac{\partial f_1}{\partial t} + \frac{\partial f_2}{\partial t} &= -c_1\frac{\partial f_1}{\partial t} + \lambda_2 f_2 - \lambda_1 f_1 + c_2\frac{\partial f_2}{\partial t} + \lambda_1 f_1 - \lambda_2 f_2 \\
\frac{\partial p}{\partial t} &= -\frac{c_1}{2}\frac{\partial p}{\partial x} - \frac{c_1}{2}\frac{\partial w}{\partial x} + \frac{c_2}{2}\frac{\partial p}{\partial x} - \frac{c_2}{2}\frac{\partial w}{\partial x} \\
\frac{\partial p}{\partial t} &= -\frac{c_1 - c_2}{2}\frac{\partial p}{\partial x} - \frac{c_1 + c_2}{2}\frac{\partial w}{\partial x}
\end{aligned} \tag{4.54}$$

(4.52)-(4.53):

$$\begin{aligned}
\frac{\partial f_1}{\partial t} - \frac{\partial f_2}{\partial t} &= -c_1\frac{\partial f_1}{\partial x} + \lambda_2 f_2 - \lambda_1 f_1 - c_2\frac{\partial f_2}{\partial x} - \lambda_1 f_1 + \lambda_2 f_2 \\
\frac{\partial w}{\partial t} &= -\frac{c_1 + c_2}{2}\frac{\partial p}{\partial x} - \frac{c_1 - c_2}{2}\frac{\partial w}{\partial x} - 2\lambda_1 f_1 + 2\lambda_2 f_2 \\
\frac{\partial w}{\partial t} &= -\frac{c_1 + c_2}{2}\frac{\partial p}{\partial x} - \frac{c_1 - c_2}{2}\frac{\partial w}{\partial x} - (\lambda_1 - \lambda_2)p - (\lambda_1 + \lambda_2)w
\end{aligned} \tag{4.55}$$

with subsequent differentiations and substitutions, we could get a second-order hyperbolic equation. Firstly, differentiate equation (4.54) with respect to t and x respectively to get,

$$\frac{\partial^2 p}{\partial t^2} = -\frac{c_1 - c_2}{2}\frac{\partial^2 p}{\partial x \partial t} - \frac{c_1 + c_2}{2}\frac{\partial^2 w}{\partial x \partial t} \tag{4.56}$$

$$\frac{\partial^2 p}{\partial x \partial t} = -\frac{c_1 - c_2}{2}\frac{\partial^2 p}{\partial x^2} - \frac{c_1 + c_2}{2}\frac{\partial^2 w}{\partial x^2} \tag{4.57}$$

and then differentiate equation (4.55) with respect to x,

$$\frac{\partial^2 w}{\partial x \partial t} = -\frac{c_1 + c_2}{2}\frac{\partial^2 p}{\partial x^2} - \frac{c_1 - c_2}{2}\frac{\partial^2 w}{\partial x^2} - (\lambda_1 - \lambda_2)\frac{\partial p}{\partial x} - (\lambda_1 + \lambda_2)\frac{\partial w}{\partial x} \tag{4.58}$$

Finally, with appropriate substitutions, equation (4.56) becomes

$$\begin{aligned}
\frac{\partial^2 p}{\partial t^2} &= -\frac{c_1-c_2}{2}\frac{\partial^2 p}{\partial x \partial t} + \left(\frac{c_1+c_2}{2}\right)^2 \frac{\partial^2 p}{\partial x^2} + \frac{c_1-c_2}{2}\frac{c_1+c_2}{2}\frac{\partial^2 w}{\partial x^2} \\
&\quad +(\lambda_1-\lambda_2)\frac{c_1+c_2}{2}\frac{\partial p}{\partial x} - (\lambda_1+\lambda_2)\frac{c_1-c_2}{2}\frac{\partial p}{\partial x} - (\lambda_1+\lambda_2)\frac{\partial p}{\partial t} \\
&= -\frac{c_1-c_2}{2}\frac{\partial^2 p}{\partial x \partial t} + \left(\frac{c_1+c_2}{2}\right)^2 \frac{\partial^2 p}{\partial x^2} - \left(\frac{c_1-c_2}{2}\right)^2 \frac{\partial^2 p}{\partial x^2} - \frac{c_1-c_2}{2}\frac{\partial^2 p}{\partial x \partial t} \\
&\quad + \left[(\lambda_1-\lambda_2)\frac{c_1+c_2}{2} - (\lambda_1+\lambda_2)\frac{c_1-c_2}{2}\right]\frac{\partial p}{\partial x} - (\lambda_1+\lambda_2)\frac{\partial p}{\partial t} \\
&= (c_2-c_1)\frac{\partial^2 p}{\partial x \partial t} + c_1 c_2 \frac{\partial^2 p}{\partial x^2} + \frac{1}{2}[(\lambda_1-\lambda_2)(c_1+c_2) - (\lambda_1+\lambda_2)(c_1-c_2)]\frac{\partial p}{\partial x} \\
&\quad -(\lambda_1+\lambda_2)\frac{\partial p}{\partial t} \qquad (4.59)
\end{aligned}$$

where $\frac{\partial p}{\partial x}$ and $\frac{\partial^2 p}{\partial x \partial p}$ are related to the drift of the motion.

In particular, if $c_1 = c_2 = c$ and $\lambda_1 = \lambda_2 = \lambda$, equation (4.59) becomes

$$\frac{1}{c}\frac{\partial^2 p}{\partial t^2} = c\frac{\partial^2 p}{\partial x^2} - \frac{2\lambda}{c}\frac{\partial p}{\partial t} \qquad (4.60)$$

The initial conditions of the telegraph equation are;

$$\begin{aligned}
p(x,0) &= \mathbb{P}(X(t) \in dx) \\
\left.\frac{\partial p}{\partial t}\right|_{t=0} &= 0
\end{aligned}$$

Equation (4.60) is the so called classical telegraph equation, and it has been studied in many papers by various authors (e.g. [11] [19] [24] [33] [45]). Most of the important probabilistic distributions and representations have been obtained by a number of different methods, in the rest of this section we are particularly going to state the result by Orsingher [45] [2].

[2] the reason of picking up this set of result particularly is they are closely related to any further result in this session

Theorem 4.19 (Orsingher 1990)**.** *The explicit form of $p(x,t)$ of a classical telegraph equation is*

$$p(x,t;\lambda,c) = \frac{e^{-\lambda t}}{2c}\left[\lambda I_0\left(\frac{\lambda}{c}\sqrt{c^2t^2-x^2}\right) + \frac{\partial}{\partial t} I_0\left(\frac{\lambda}{c}\sqrt{c^2t^2-x^2}\right)\right] \tag{4.61}$$

for $|x| < ct$, and

$$I_0(x) = \sum_{k=0}^{\infty} \frac{1}{(k!)^2}\left(\frac{x}{2}\right)^{2k}$$

is the Bessel function with imaginary argument of order zero.

Orsingher [45] also derived an alternative form of $p(x,t;\lambda,c)$

$$p(x,t;\lambda,c) = \frac{\lambda}{c} e^{-\lambda t} I_0\left(\frac{\lambda}{c}\sqrt{c^2t^2-x^2}\right) + \frac{1}{2c}\frac{\partial}{\partial t}\left[e^{-\lambda t} I_0\left(\frac{\lambda}{c}\sqrt{c^2t^2-x^2}\right)\right] \tag{4.62}$$

In equation (4.62), the first term can be viewed as an overestimation of the density which is corrected by its derivative.

There are two special cases of the classical telegraph equation. First of all, when $\lambda = 0$, which means the probability of reversing direction is zero. So if an article starts moving in one direction, it would never stop. This is a well-known classical case of vibrating string. The other case is where both λ and c tend to infinity such that $\frac{2\lambda}{c^2} = \frac{1}{D}$, D is a constant. When $\lambda \to \infty$, it means the velocity changes occur continuously and $\frac{2\lambda}{c^2} \to \frac{1}{D}$ means the speed of the moving particle must become infinite. Then the classical telegraph equation (4.60) becomes,

$$\frac{1}{D}\frac{\partial p}{\partial t} = \frac{\partial^2 p}{\partial x^2}$$

Hence, the limiting behavior of the telegraph becomes similar to that of Brownian motion.

Theorem 4.20 (Orsingher, 1990)**.** *If the distribution function of a classical telegraph equation is given by equation (4.61), then we have*

$$\lim_{\lambda\to\infty,\frac{2\lambda}{c^2}\to\frac{2}{\sigma^2}} p(x,t;\lambda,c) = \frac{1}{\sqrt{2\pi\sigma^2 t}} e^{-\frac{x}{2\sigma^2 t}}$$

by letting $\frac{1}{D} = \frac{2}{\sigma^2}$*, which is indeed the transition density of a Brownian motion.*

When $c_1 \neq c_2$ and $\lambda_1 \neq \lambda_2$, the motion differs from the classical case in the way that it displays a drift, where one component depends on the different velocities and the other on the different rates. The elimination of the drift requires the Lorentz transformation of Special Relativity Theory [11], and it allows us to derive the distribution of $p(x,t;\lambda_1,\lambda_2,c_1,c_2)$.

Theorem 4.21 (Beghin, Nieddu and Orsingher, 2001)**.** *The distribution of the position of the particle has been derived as*

$$\begin{aligned} p(x,t;\lambda_1,\lambda_2,c_1,c_2) = & \frac{\exp\left(\frac{-(\lambda_2 c_1+\lambda_1 c_2)}{c_1+c_2}t + \frac{\lambda_2-\lambda_1}{c_2+c_1}x\right)}{c_1+c_2} \\ \times & \left[\frac{\lambda_1+\lambda_2}{2} I_0\left(\frac{2\sqrt{\lambda_1\lambda_2}}{c_1+c_2}\sqrt{(x+c_2t)(c_1t-x)}\right)\right. \\ + & \frac{\partial}{\partial t} I_0\left(\frac{2\sqrt{\lambda_1\lambda_2}}{c_1+c_2}\sqrt{(x+c_2t)(c_1t-x)}\right) \\ + & \left.\frac{c_1-c_2}{2}\frac{\partial}{\partial x} I_0\left(\frac{2\sqrt{\lambda_1\lambda_2}}{c_1+c_2}\sqrt{(x+c_2t)(c_1t-x)}\right)\right] \\ + & \frac{1}{2}e^{-\lambda_1 t}\delta(x-c_1t) + \frac{1}{2}e^{-\lambda_2 t}\delta(x+c_2t) \end{aligned} \tag{4.63}$$

for $-c_2t \leq x \leq c_1t$*, where*

$$I_0(x) = \sum_{k=0}^{\infty}\left(\frac{x}{2}\right)^{2k}\frac{1}{(k!)^2}$$

is the zero-order Bessel function with imaginary argument, and Dirac's Delta func-

tion δ.

The classical approach based on Fourier transforms permits us to obtain the characteristic function

$$F(\beta, t) = \int_{-\infty}^{+\infty} e^{i\beta x} dp(x, t)$$

Theorem 4.22 (Beghin, Nieddu and Orsingher, 2001)**.** *The characteristic function is*

$$\begin{aligned} F(\beta, t) &= \frac{1}{2} e^{-\frac{1}{2}[i\beta(c_2 - c_1) + (\lambda_1 + \lambda_2)]t} \times \\ &\quad \left[\left(1 + \frac{\lambda_1 + \lambda_2}{B} \right) e^{\frac{t}{2}B} + \left(1 - \frac{\lambda_1 + \lambda_2}{B} \right) e^{-\frac{t}{2}B} \right] \end{aligned} \tag{4.64}$$

where

$$B = \sqrt{(\lambda_1 + \lambda_2)^2 - \beta^2 (c_1 + c_2)^2 + 2i\beta(c_1 + c_2)(\lambda_2 - \lambda_1)}$$

for $\beta \in \mathbb{R}$ and $t \geq 0$.

$c_2 = 0, \lambda_1 \leq \lambda_2$

Assuming that the negative velocity of the telegraph process is zero, $c_2 = 0$, we could represent the non-decreasing telegraph process as,

$$Z_t = \sum_{i=1}^{N_1(t)} \int_0^{s_i} c_1 dt \sum_{i=1}^{N_1(t)} c_1 s_i \tag{4.65}$$

where $N(t)$ is a Poisson process with parameter λ_1 and s_i's are exponentially distributed with parameter λ_2 according to earlier notations. We notice that expression (4.65) is very similar to a compound Poisson process but the jumps are time-dependent. Thus, the boundary crossing probabilities for a standard Brownian motion with boundaries such as the non-decreasing telegraph processes could be solved

similarly as problem of the compound Poisson process with exponential jumps.

Corollary 4.4. *For a standard Brownian motion $\{X_t\}_{t\geq 0}$ with boundaries which are symmetric non-decreasing telegraph processes, $|Z_t|$, such that the negative velocity is zero, and the process switches from increasing to constant over an exponential distributed time with parameter λ_1, and from constant to increasing after a random time with exponential distribution with parameter $\lambda_2 \geq \lambda_1$. The boundary crossing probability, therefore, is*

$$P_u^{(2)} = P_l^{(2)} = 2\sum_{j=0}^{\infty}(-1)^j e^{-\gamma_j b}$$

where $\gamma_j = \frac{k_j^2\lambda_2}{2\lambda_1 c_1 - k_j^2 c_1}$ and k_{j+1}'s are the solutions of

$$(2\lambda_1 c_1 - k_j^2 c_1)k_{j+1}^2 + 2\lambda_1\lambda_2 k_{j+1} - 2\lambda_1\lambda_2 k_j + 2\lambda_1 c_1 k_j^2 - 4\lambda_1^2 c_1 = 0$$

with initial value $k_0 = \frac{\sqrt{\lambda_2^2 + 8\lambda_1 c_1^2} - \lambda_2}{2c_1}$.

Proof. Recalling the proof of Theorem 4.18, the Laplace transform $\varphi(\gamma)$ of the jumps is $\varphi(\gamma) = \frac{\lambda_2}{\lambda_2 + c_1\gamma}$. When considering the martingale $e^{-\gamma Z_t}(e^{kX_t} + e^{-kX_t})$, coefficients γ and k have to satisfy,

$$\lambda_1\left(1 - \frac{\lambda_2}{\lambda_2 + c_1\gamma}\right) = \frac{1}{2}k^2$$

i.e., $\gamma = \frac{k^2\lambda_2}{2\lambda_1 c_1 - k^2 c_1}$, we choose k_j as equation (4.45) so that,

$$\frac{k_j^2\lambda_2}{2\lambda_1 c_1 - k_j^2 c_1} + k_j = \frac{k_{j+1}^2\lambda_2}{2\lambda_1 c_1 - k_{j+1}^2 c_1} - k_{j+1}$$

Thus, k_{j+1}'s are the solutions of

$$(2\lambda_1 c_1 - k_j^2 c_1)k_{j+1}^2 + 2\lambda_1\lambda_2 k_{j+1} - 2\lambda_1\lambda_2 k_j + 2\lambda_1 c_1 k_j^2 - 4\lambda_1^2 c_1 = 0$$

which is

$$k_{j+1} = \frac{\sqrt{\lambda_1^2\lambda_2^2 + 2\lambda_1 c_1(2\lambda_1 - k_j^2)(\lambda_2 k_j - c_1 k_j^2 + 2\lambda_1)} - \lambda_1\lambda_2}{2\lambda_1 c_1 - k_j^2 c_1}$$

and k_0 is found by solving $c_1 k_0^2 + \lambda_2 k_0 - 2\lambda_1 c_1 = 0$, so we have

$$k_0 = \frac{\sqrt{\lambda_2^2 + 8\lambda_1 c_1^2} - \lambda_2}{2c_1}$$

□

A number of probabilities has been calculated for various values of the parameters $\lambda_1, \lambda_2, c_1$ and b as examples in Table 4.3 - 4.4. Not surprisingly, it is straightforward to conclude that when the time space between positive velocity c_1 and zero velocity is equal (i.e. $\lambda_1 = \lambda_2$), higher the positive velocity c_1 is, lower the boundary crossing probabilities are, and no large velocity is required to achieve a pair of "untouchable" boundaries in terms of probabilities. Moreover, the equal-valued exponential time parameter is also important, a small increase of $\lambda_1 = \lambda_2$ will result a significant change in the probabilities given all other parameters remain the same. The initial position of the boundaries b is still crucial as emphasized in the compound Poisson processes cases.

When the two exponential distribution parameters λ_1 and λ_2 are not equalled, we notice that from Table 4.4 as long as $\lambda_1 \propto \lambda_2$ at the same rate, for instance, $\lambda_1 = 0.5, \lambda_2 = 5$ and $\lambda_1 = 1, \lambda_2 = 10$, given the same positive velocity, the probabilities are barely changed. Additionally, as expected the positive velocity c_1 is negatively related to the probabilities.

Table 4.3: Boundary crossing probabilities when $\lambda_1 = \lambda_2$

$\lambda_1 = \lambda_2 = 5$			
b	$c_1 = 5$	$c_1 = 1$	$c_1 = 0.1$
1	0.1337	0.4230	0.9999
2	0.0090	0.0935	0.9877
3	0.0006	0.0202	0.9249
4	0.0000	0.0044	0.8196
5	0.0000	0.0009	0.7012
10	0.0000	0.0000	0.2721
15	0.0000	0.0000	0.1008
20	0.0000	0.0000	0.0372
$\lambda_1 = \lambda_2 = 1$			
b	$c_1 = 5$	$c_1 = 1$	$c_1 = 0.1$
1	0.5015	0.6629	0.9997
2	0.1427	0.2676	0.9856
3	0.0384	0.0995	0.9246
4	0.0103	0.0366	0.8232
5	0.0028	0.0135	0.7080
10	0.0000	0.0001	0.2804
15	0.0000	0.0000	0.1055
20	0.0000	0.0000	0.0396

Table 4.4: Some example values of first-passage time probabilities of $\lambda_1, \lambda_2, c_1$ and b

	b	c=0.05			c=0.02		
		λ_1=0.5	λ_1=1	λ_1=3	λ_1=0.5	λ_1=1	λ_1=3
$\lambda_2 = 5$	1	0.4014	0.6665	0.9335	0.6948	0.8514	0.9734
	2	0.1597	0.4405	0.8671	0.4848	0.7241	0.9468
	3	0.0629	0.2886	0.8006	0.3369	0.6150	0.9202
	4	0.0246	0.1874	0.7332	0.2337	0.5215	0.8937
	5	0.0095	0.1207	0.6648	0.1619	0.4417	0.8672
	10	0.0001	0.0119	0.3504	0.0253	0.1884	0.7334
	15	0.0000	0.0010	0.1610	0.0038	0.0776	0.5962
	20	0.0000	0.0001	0.0710	0.0006	0.0310	0.4644
$\lambda_2 = 10$	1	0.1462	0.4031	0.7888	0.4593	0.6950	0.9104
	2	0.0212	0.1610	0.6175	0.2175	0.4851	0.8278
	3	0.0030	0.0637	0.4795	0.1012	0.3371	0.7518
	4	0.0004	0.0250	0.3690	0.0470	0.2339	0.6820
	5	0.0001	0.0097	0.2815	0.0218	0.1621	0.6178
	10	0.0000	0.0001	0.0644	0.0005	0.0253	0.3694
	15	0.0000	0.0000	0.0130	0.0000	0.0038	0.2131
	20	0.0000	0.0000	0.0025	0.0000	0.0006	0.1189

4.4 Applications and conclusions

By deriving the unconditional boundary crossing probabilities for a standard Brownian motion with symmetric and asymmetric linear boundaries, we demonstrate an alternative method by applying the powerful tools as martingales and infinitesimal generator of Brownian motion that allows to obtain a simple expression. Given the raise of liquidity risk in large-valued interbank payment systems due to the reform, we are concentrated on the problem of bilateral/multi-lateral limits exists in the current UK payment system. The boundary crossing probabilities for a standard Brownian motion with symmetric stochastic process boundaries are studied.

In the area of large-valued interbank payment systems, one of the potential applications of the results will be credit control of bilateral/multi-lateral limits, i.e. Real Time Gross Settlement payment system in most of cases around the world. Due to the feature of RTGS payment system, participating banks are required to make payments immediately upon an order from "customer(s)", and the fact that intra-day loan from central bank is costly, the incoming payments by others in the system are important resources. They wish to use the liquidity in the most effective way, in the sense of minimizing unnecessary costs. The participating banks inform central bank that they would generally set up a limit for the net position with any other banks in the system, which is so called bilateral/multi-lateral limit, and the limit made at the beginning of a business day are based on pervious business day performances [9] [10]. In the course of the day, they would be adjusted often under some circumstances. To the extent of policy maker on bilateral limits in payment system, with the consideration of the results, participating banks are suggested to make decisive regulations. Boundaries with lower boundary crossing probabilities means that banks are in a strong position to control their exposures to

other participants.

Compound Poisson process boundaries Banks may think about changing the frequency for adjusting the limits rather than making effort to change the size of every single adjustment. Moreover, the initial position of the limit should be taken into account. If a bank wishes to be generous and set up a bilateral/multi-lateral limit where the other(s) are less likely to excess, it can simply consider putting a relatively high starting value for the boundaries.

Non-decreasing telegraph process boundaries If banks are considering changing limit over an exponential distributed time with the same parameter, lower the intensity of changing, it is more likely the limits are surpassed by others; and the intensity has a high sensitivity to the functionality of the bilateral/

multi-lateral limits. Banks are also advised to look at their strategy to manage the frequencies for adjustment. Nevertheless, banks should be aware that even if the two time intervals are not identically distributed, as long as they are proportional at the same rate, the efficacy of the limits will be affected unnoticeably.

Chapter 5

Other non-decreasing Lévy boundaries

In this chapter, we attempt to apply the methods we proposed in Chapter 4 to broader and more complex non-decreasing Lévy processes as boundaries. Before having look of individual subordinators, we will give a brief introduction to Lévy process.

5.1 Introduction to Lévy process

First of all, we are going to present some of the most important definitions and theories about Lévy process. Lévy process has right continuous path with left limit, are initiated from the origin and has stationary and independent increments. The formal definition is given below,

Definition 5.1. *A process* $\{X_t\}_{t\geq 0}$ *defined on a probability space* $(\Omega, \mathcal{F}, \mathbb{P})$ *is said to be a Lévy process if it has the following properties:*

1. *The paths of* X *are* $\mathbb{P}$*-almost surely right continuous with left limits.*

2. $\mathbb{P}(X_0 = 0) = 1$.

3. For $0 \leq s \leq t$, $X_t - X_s$ *is equal in distribution to* X_{t-s}.

4. For $0 \leq s \leq t$, $X_t - X_s$ *is independent of* $\{X_u : u \leq s\}$.

Let $\{X_t\}_{t\geq 0}$ denote a Lévy process with triple $(a, \sigma^2, \nu(dx))$, where $a \in \mathbb{R}$, $\sigma^2 > 0$ and $\nu(dx)$ is the Lévy measure on $\mathbb{R} \setminus \{0\}$ and satisfying

$$\int (1 \wedge x^2)\nu(dx) < \infty$$

Now we define for all $\theta \in \mathbb{R}$, $t \geq 0$,

$$\Psi_t(\theta) = -\log \mathbb{E}\left(e^{i\theta X_t}\right)$$

and for any Lévy process, we have that for all $t \geq 0$,

$$\mathbb{E}\left(e^{i\theta X_t}\right) = e^{-t\Psi(\theta)}$$

where $\Psi(\theta) := \Psi_1(\theta)$ is the *characteristic exponent* of X_t. The Lévy-Khintchine formula provides an expression of the characteristic exponent for X_t on a probability space $(\Omega, \mathcal{F}, \mathbb{P})$,

$$\Psi(\theta) = ia\theta + \frac{1}{2}\sigma^2\theta^2 + \int_{\mathbb{R}} \left(1 - e^{i\theta x} + i\theta x \mathbb{1}_{\{|x|\leq 1\}}\right) \nu(dx)$$

Among all Lévy processes, there are ones whose paths are almost surely non-decreasing, and they are called *subordinators*. The examples are including compound Poisson process, Gamma process and Inverse-Gaussian process. The boundary crossing probabilities for compound Poisson processes were discussed in Chapter 4, in rest

of this chapter, Gamma process and Inverse-Gaussian process will be studied in details for the specific problem. Finally, we are studying the methods to approximate a subordinator and extend our approach to a general case.

5.2 Gamma process

Gamma process is an example of subordinator, in which the increments are independent and non-negative random variables that have a Gamma distribution with a constant rate parameter, namely α, and time-dependent shape function, $\beta(t)$. The rate parameter α controls the size of increments, while shape parameter β controls the rate of increments. However, a Gamma process is different from a compound Poisson process in two ways: firstly, Gamma process's Lévy measure has infinite total mass unlike the Lévy measure of a compound Poisson process, which is necessarily finite and equal to the arrival rate of jumps. Secondly, whilst a compound Poisson process with positive jumps does have paths, that are almost surely non-decreasing, it does not have paths that are almost surely strictly increasing [36].

For a Gamma process with parameters (α, β), the Lévy-Khintchine formula takes the form

$$\Psi(\theta) = \beta \int_0^\infty (1 - e^{i\theta x}) \frac{1}{x} e^{-\alpha x} dx = \beta \log(1 - \frac{i\theta}{\alpha})$$

To derive the boundary crossing probabilities for the standard Brownian motion $\{X_t\}_{t\geq 0}$ with symmetric Gamma process boundaries, the martingale should be considered is again of the form, $e^{-\gamma Z_t}(e^{kX_t} + e^{-kX_t})$, thus, the equation about γ and k, $\beta \log\left(1 + \frac{\gamma}{\alpha}\right) = \frac{1}{2}k^2$, therefore,

$$\gamma = \alpha \left(e^{\frac{k^2}{2\beta}} - 1 \right) \tag{5.1}$$

We want that k_j is chosen to satisfy,

$$\begin{aligned} \alpha\left(e^{\frac{k_j^2}{2\beta}}-1\right)+k_j &= \alpha\left(e^{\frac{k_{j+1}^2}{2\beta}}-1\right)-k_{j+1} \\ k_{j+1}+k_j &= \alpha\left(e^{\frac{k_{j+1}^2}{2\beta}}-e^{\frac{k_j^2}{2\beta}}\right) \end{aligned} \tag{5.2}$$

with initial k_0 is the root of $\gamma_0 - k_0 = 0$, i.e.,

$$\alpha\left(e^{\frac{k_0^2}{2\beta}}-1\right)-k_0=0 \tag{5.3}$$

and it can be solved numerically. Given that $k_0 \neq 0$, some numerical examples are tabulated in Table 5.1.

Table 5.1: example k_0's for different α and β of equation (5.3)

β	α	k_0
1	1	1.2859
	5	0.3853
	10	0.1980
10	1	6.3068
	5	3.1103
	10	1.8362
20	1	9.7458
	10	3.4381
	20	1.9102
30	5	7.3734
	20	2.8073
	30	1.9381
50	10	7.4688
	20	4.5089
	50	1.9618
100	20	8.3558
	50	3.8534
	100	1.9805
1000	200	9.7636
	500	3.9841
	1000	1.9980

Further calculations show that with these initial k_0's, the recurrence relation (5.2) produces two values of k_j; one is the opposite value of k_{j-1}, denoted as $k_j^{(1)}$, and keeps alternating for $j = 1, 2, \cdots$, hence, $\gamma_j^{(1)}$ given by equation (5.1) will remain unchange. The other one, $k_j^{(2)}$, could yield a negative infinite k_n for large n, thus, $\gamma_j^{(2)}$ tends to positive infinite at a higher speed.

From the proof of Theorem 4.17, when equation (5.3) holds, we have

$$\mathbb{P}(\tau < \infty) = \mathbb{E}\left[e^{-(\gamma_n^{(2)}+k_n^{(2)})z_\tau}\mathbb{1}_{\{\tau<\infty\}}\right] + 2\sum_{j=0}^{n}(-1)^j e^{-\gamma_j^{(2)}b} \tag{5.4}$$

and in the first term of the right-hand side of the equation, as $n \to +\infty$,

$$\gamma_n^{(2)} + k_n^{(2)} = \alpha\left(e^{\frac{(k_n^{(2)})^2}{2\beta}} - 1\right) + k_n^{(2)} \to +\infty$$

and the expectation term vanished, therefore, we could only obtain the numerical values by

$$\mathbb{P}(\tau < \infty) = 2\sum_{j=0}^{+\infty}(-1)^j e^{-\gamma_j^{(2)}b}$$

5.3 Inverse-Gaussian process

Another well-known example of subordinator is Inverse-Gaussian process, which describes the time a Brownian motion with positive linear drift takes to hit a positive level. Assuming that the Brownian motion is in the form of $\sigma B_t + \nu t$, where B_t denotes a standard Brownian motion, then the stopping time τ_a has an Inverse Gaussian distribution with mean $\mu = \frac{a}{\nu}$ and shape parameter $\lambda = \frac{a^2}{\sigma^2}$. Its characteristic exponent takes the form of

$$\Psi(\theta) = \frac{a}{\sigma^2}\left(\nu - \sqrt{\nu^2 - 2i\theta}\right)$$

Thus, an equation about γ and k is, when considering the martingale $e^{-\gamma Z_t}(e^{kX_t} + e^{-kX_t})$,

$$\frac{\lambda}{\mu}\left(\sqrt{1+\frac{2\mu^2\gamma}{\lambda}}-1\right)=\frac{1}{2}k^2$$

Then, $\gamma = \frac{(\mu k^2+2\lambda)^2}{8\lambda\mu^2-4\lambda^2}$. According to equation (4.45), k_j's have to satisfy the following equation,

$$\mu k_{j+1}^3 - \mu k_j k_{j+1}^2 + (\mu k_j^2 + 4\lambda)k_{j+1} - \mu k_j^3 - 4\lambda k_j - 8\mu\lambda = 0 \tag{5.5}$$

where the solutions are

$$k_{j+1}^{(1)} = \frac{1}{3}\frac{D_j}{\mu} - \frac{2}{3}\frac{\mu k_j^2+6\lambda}{D_j} + \frac{1}{3}k_j \tag{5.6}$$

$$k_{j+1}^{(2)} = -\frac{1}{6}\frac{D_j}{\mu} + \frac{1}{3}\frac{\mu k_j^2+6\lambda}{D_j} + \frac{1}{3}k_j + \frac{\sqrt{3}}{2}i\left(\frac{1}{3}\frac{D_j}{\mu} + \frac{2}{3}\frac{\mu k_j^2+6\lambda}{D_j}\right) \tag{5.7}$$

$$k_{j+1}^{(3)} = -\frac{1}{6}\frac{D_j}{\mu} + \frac{1}{3}\frac{\mu k_j^2+6\lambda}{D_j} + \frac{1}{3}k_j - \frac{\sqrt{3}}{2}i\left(\frac{1}{3}\frac{D_j}{\mu} + \frac{2}{3}\frac{\mu k_j^2+6\lambda}{D_j}\right) \tag{5.8}$$

where

$$D_j = \left[\left(10\mu k_j^3 + 36\lambda k_j + 108\lambda\mu + 6\sqrt{3}C_j\right)\mu^2\right]^{\frac{1}{3}}$$

$$C_j = \sqrt{\frac{\mu^3 k_j^6 + 8\mu^2 k_j^4\lambda + 20\mu k_j^2\lambda^2 + 16\lambda^3 + 20\mu^3 k_j^3\lambda + 72\lambda^2 k_j\mu^2 + 108\lambda^2\mu^3}{\mu}}$$

Because that equation (5.5) would have a real root and two conjugate complex roots for sure, instead of using the martingale in the form of $e^{-\gamma Z_t}(e^{kX_t}+e^{-kX_t})$, given the formulae of k_{j+1}, let us consider a new martingale, $e^{-\gamma Z_t}e^{\phi X_t}(e^{i\psi X_t} + e^{-i\psi X_t})$. With

such substitutions, we have,

$$\begin{aligned}\phi_{j+1} &= -\frac{1}{6}\frac{D_j}{\mu} + \frac{1}{3}\frac{\mu k_j^2 + 6\lambda}{D_j} + \frac{1}{3}k_j \\ \psi_{j+1} &= \frac{\sqrt{3}}{2}\left(\frac{1}{3}\frac{D_j}{\mu} + \frac{2}{3}\frac{\mu k_j^2 + 6\lambda}{D_j}\right)\end{aligned}$$

k_0 can be found by setting $\gamma_0 - k_0 = 0$, which is the solution of the equation (5.9) below,

$$\mu k_0^3 + 4\lambda k_0 - 8\mu\lambda = 0 \tag{5.9}$$

It is clear that equation (5.9) has three roots; one real root and two conjugate complex roots. The real root $k_0^{(+)}$ will be considered only.

5.4 Approximations of Lévy processes

Let $\{X_t\}_{t\geq 0}$ denote a Lévy process with triple $(a, \sigma^2, \nu(dx))$ as defined early in this chapter. The Lévy-Itô representation reveals the structure of a Lévy process as

$$X_t = at + \sigma B_t + \lim_{\epsilon\to 0}\left\{\sum_{s\leq t} J(s)\mathbb{1}_{\{|J(s)|>1\}} - t\int_{\epsilon<|x|<1} x\nu(dx)\right\} \tag{5.10}$$

where B_t denotes a standard Brownian motion that is independent of the jump process $J(s)$. The Lévy measure, $\nu(dx)$, thus is the intensity of jumps of size x. There exists a probability space on which independent Lévy processes exist, and a Lévy process can be represented by three components such as

$$X_t = X^{(1)} + X^{(2)} + X^{(3)}$$

where

- $X^{(1)}$ is a linear Brownian motion with drift
- $X^{(2)}$ is a compound Poisson process
- $X^{(3)}$ is a square integrable martingale with an almost surely countable number of jumps on each finite time interval which are of martingales less than unity. The Lévy measure $\nu(dx)$ indicates how the jumps occur. Jumps of sizes in the set A occur according to a Poisson process with intensity parameter $\lambda_A = \int_A \nu(dx)$.

When $\nu(\mathbb{R}) < \infty$ and $\int(|x| \wedge 1)\nu(dx) < \infty$, then $\sum_{s \leq t} |J(s)| < \infty$ almost surely, equation (5.10) can be reduced to

$$X_t = \mu t + \sigma B_t + \sum_{s \leq t} J(s) \tag{5.11}$$

with $\mu = a - \int_{|x|<1} x\nu(dx)$.

Note that since Brownian motion has infinite variation, a Lévy process has bounded variation on each time interval if and only if it does not have Brownian component (i.e. $\sigma^2 = 0$).

Approximated Lévy processes have been applied to option pricing in recent years, for instance, pricing 50% recovery rate equity default swaps (EDS) contracts [5], pricing American options in models where a multi-normal model was used to approximate the general exponential Lévy process that the stock prices followed [39] and approximation of the prices and sensitivities of barrier options in generalised exponential Lévy processes [32].

5.4.1 Methods of approximations

So far, the method we proposed to derive the boundary crossing probabilities when the boundaries are non-decreasing Lévy processes (subordinators), by using martingales and the properties of individual subordinators, produced a desirable result when the boundaries are compound Poisson processes. We are aim to represent most of the non-decreasing Lévy processes by the compound Poisson processes, thereby, the method is becoming applicable to more situations. In this section, the three most well-known techniques will be exploited.

Random walk approximation

Let $\{X_{jh}\}_{j=0,1,2,\cdots}$ be a discrete random walk, if a simulation method (at least an approximation) of X_h is available, then we could approximate $\{X_t\}_{t\geq 0}$.

In details, let X_t be a Lévy process determined by the Lévy-Khintchine formula,

$$\Psi(u) = iau - \frac{\sigma^2 u^2}{2} + \int_{-\infty}^{+\infty} \left(e^{iux} - 1 - iux\mathbb{1}_{\{|x|\leq 1\}}\right) \nu(dx)$$

with $\sigma = 0$ (no Brownian motion component) and an infinite Lévy measure $\nu(dx)$. The time domain $[0, T)$ is made into partitions by letting $h = \frac{T}{n}$, $n \geq 1$, as $[jh, (j+1)h)$, for $j = 0, 1, \cdots$. The original Lévy process has finite variance over each interval. Then generate the increments $\Delta_j^h X = X_{jh} - X_{(j-1)h}$ as independent and identically distributed random variables from the distribution $P_h(\cdot) = \mathbb{P}(X_h \in \cdot)$, which is subject to the original Lévy process and can be very complicated with special functions. For $k = 1, \cdots, n-1$, let

$$X_t^h = \begin{cases} 0 & \text{if } t \in [0, h) \\ \sum_{j=1}^{k} \Delta_j^h X & \text{if } t \in [jh, (j+1)h) \end{cases}$$

Hence, $\{X_t^h\}_{0\leq t<T}$ is a random walk, by the theorems of Khinthine and Skorohod, it was proved that a random walk can use to approximate a Lévy process [18].

Theorem 5.1 (Khintchine)**.** *As $\Delta_j^k X, j = 1, \cdots, n$ be independently identically distributed with distribution changing with $n \geq 1$, and such that $\Delta_j^h X \to 0$ in probability as n tends to infinity. If $X_t^h \to Z$ in distribution, then Z has a so-called infinity divisible distribution.*

Theorem 5.2 (Skorohod)**.** *In Theorem 5.1, $j \geq 1, n \geq 1$, $X_t^h = \sum_{j=1}^k \Delta_j^h X \to X_t$ in distribution as $n \to \infty$. Furthermore, $X^{(n)} \to X$ where X is a Lévy process.*

The biggest drawback of the random walk approximation is that the location and size of large jumps could not be precisely identified, which causes uncertainties especially in the heavy tail cases. Moreover, because of the complication of the density function of X_h, the simulation could be numerically tedious.

Series representations of Lévy processes

Rosiński presented a comprehensive list of generating series representations of Lévy process [53]. We extend his work to Lévy processes over any arbitrary finite interval $[0, T]$.

Consider a Lévy process $\{X_t\}_{0\leq t\leq T}$, by the Lévy-Itô integral representation (5.10), for every $t \geq 0$,

$$X_t = at + \int_{|x|\leq 1} x\left[N([0,t],dx) - t\nu(dx)\right] + \int_{|x|>1} xN([0,t],dx) \tag{5.12}$$

where N is the jump process of X_t, and itself is a Poisson point process.

Suppose that the jumps of X_t are $J_1, J_2, \cdots$, which are specified by a particular

distribution, say f_j, then N has representation

$$N = \sum_{i=1}^{\infty} \delta(U_i, J_i)$$

where $\delta(\cdot)$ denotes the dirac measure, and U_i's are independent and identically distributed random variables on $[0, T]$, which are independent of J_i's.

Assume that there exists a small number, named ϵ, then if we define

$$X_t(\epsilon) = at + \int_{\frac{1}{\epsilon} \leq |x| \leq 1} x \left[N([0,t], dx) - t\nu(dx) \right] + \int_{|x|>1} xN([0,t], dx) \tag{5.13}$$

then

$$X_t(\epsilon) = \sum_{i \in \Lambda_n} J_i \mathbb{1}_{\{U_i \leq t\}} - tb_n \tag{5.14}$$

where

$$b_n = \int_{\frac{1}{\epsilon} \leq |x| \leq 1} t\nu(dx) - a \quad \Lambda_n = \{i \geq 1 : |J_i| \geq \frac{1}{\epsilon}\}$$

Thus, $\sum_{i \in \Lambda_n} J_i \mathbb{1}_{\{U_i \leq t\}} - tb_n \to X(t)$ almost surely, as $n \to \infty$.

Generally, a series representation of X_t is obtained by placing the random set Λ_n in expression (5.14) by a non-random set $\{1, 2, \cdots, n\}$, which yields

$$X_t = \sum_{i=1}^{\infty} \left(J_i \mathbb{1}_{\{U_i \leq t\}} - tc_i \right) \tag{5.15}$$

almost surely, for a suitable c_i.

Rosiński has investigated various properties of $\{X_t\}_{0 \leq t \leq T}$ [53]. Most importantly, in terms of speed of convergence of a series representation, the method of enumerating J_i's is a priority that needs to be considered. Beside, other properties such the

need to center with certain c_i's also depend on the specific representation of J_i's.

Bondesson proposed a method to obtain a nonnegative infinitely divisible random variable as a shot noise [13]. In details, defining a probability kernel from $(0, \infty)$ to $\mathbb{R}^d$, namely γ, and let J_i be a set of $\mathbb{R}^d$-valued conditionally independent random variables given Γ_k such that

$$\mathbb{P}(J_i \in A | \{\Gamma_k\}_{k\geq 1}, \{J_k\}_{k\neq i}) = \gamma(\Gamma_i, A), \quad A \in \mathcal{B}(\mathbb{R}^d)$$

where Γ_i's are arrival times in a Poisson process with rate one. The probabilistic structure of J_i's can be better understood if we notice that J_i can be expressed as

$$J_i = H(\Gamma_i, V_i)$$

for some independent and identically distributed random variables V_i's that are independent of U_i's (uniform on $[0, T]$) and Γ_i's, and a joint measurable $\mathbb{R}^d$-valued function H, such that

$$\mathbb{P}(H(r, V_i) \in A) = \gamma(r, A), \quad A \in \mathcal{B}(\mathbb{R}^d), \quad r > 0$$

Therefore, a series representation of the Lévy process X_t, can be written from equation (5.15) as

$$X_t = \sum_{i=1}^{\infty} [H(\Gamma_i, V_i)\mathbb{1}_{\{U_i \leq t\}} - tc_i] \tag{5.16}$$

The choice of H and V_i's is not unique, but they have to satisfy the condition

$$\int_{-\infty}^{+\infty} f(x)\nu(dx) = \frac{1}{T}\int_{0}^{+\infty} \mathbb{E}[f(H(r, V))]dr$$

for a nonnegative Borel function $f(\cdot)$ with $f(0) = 0$.

The convergence of generalised shot noise series was investigated in the existing literature [53].

Theorem 5.3 (Rosiński 2001). • $\sum_{i=1}^{\infty} H(\Gamma_i, V_i)$ *converges almost surely if and only if*

1. $\mathbb{Q}$ *is a Lévy measure on* $\mathbb{R}_0^d$, *i.e.*

$$\int_{\mathbb{R}^d} (|x|^2 \wedge 1)\mathbb{Q}(dx) < \infty$$

2. $a \equiv \lim_{s\to\infty} A(s)$ *exists in* $\mathbb{R}^d$, *where*

$$A(s) = \int_0^s \int_{|x|<1} x\mathbb{P}(H(r, V_i) \in dx)dr, \quad s \geq 0$$

If (1) and (2) are satisfied, then $\mathcal{L}(\sum_{i=1}^{\infty} H(\Gamma_i, V_i))$ *is infinitely divisible with characteristic function* $\phi(u)$ *given by*

$$\phi(u) = \exp\left[iua + \int_{\mathbb{R}_0^d} \left(e^{iux} - 1 - iux\mathbb{1}_{\{|x|\leq 1\}}\right) \mathbb{Q}(dx)\right] \tag{5.17}$$

- *If only (1) holds, then* $\sum_{i=1}^{\infty}[H(\Gamma_i, V_i) - c_i]$ *converges almost surely for* $c_i = A(i) - A(i-1)$. *The characteristic function is given by equation (5.17) with* $a = 0$.

The series representations approximations of Lévy process are easy to simulate in most of the cases. Quite commonly, the largest jumps of a Lévy process would appear at the early stage of the series. The disadvantage about this method is that the speed of converge maybe slow for some reasons, consequently, a huge number of

iterations are needed to be generated to reach a satisfactory approximation, however, a slow convergence may be not an important issue for some applications.

Poisson and Gaussian approximations

The problem is closely related to the simulation of a Lévy process based on series representations. When the series converge slowly, the normal/Gaussian approximation of the small jumps is advisable.

Let us consider the Lévy process $\{X_t\}_{t\geq 0}$ with triple $(a, \sigma^2, \nu(dx))$ again, it can be decomposed into a sum of two independent Lévy processes,

$$X_t = X_t^\epsilon + X_t(\epsilon) \tag{5.18}$$

where $\{X_t^\epsilon\}_{t\geq 0}$ is a compound Poisson process with a drift, the distribution of jumps is proportional to $\nu^\epsilon = \nu(|x| > \epsilon)$. $\{X_t(\epsilon)\}_{t\geq 0}$ has mean μ and Lévy measure $\nu(|x| \leq \epsilon)$. Then $X_t(\epsilon)$ can be viewed as the small jumps part of the original Lévy process, hence we could simulate the right-hand side of equation (5.18) as an approximation to $\{X_t\}_{t\geq 0}$.

First of all, we discretize the Lévy measure $\nu(dx)$ by choosing some small $\epsilon \in (0, 1)$, then make a partition of $\mathbb{R}\backslash[-\epsilon, \epsilon]$ of the following form, for any $a_i \in \mathbb{R}$,

$$a_0 < a_1 < \cdots < a_k = -\epsilon, \quad \epsilon = a_{k+1} < a_{k+2} < \cdots < a_{d+1}$$

Jumps that are greater than ϵ, which are parts of X_t^ϵ, are approximated by a sum of independent Poisson processes as described below;

1. Set an independent Poisson process $N^{(i)}(t)$ for each interval $[a_{i-1}, a_i)$, $1 \leq i \leq k$ and $[a_i, a_{i+1})$, $k+1 \leq i \leq d$, with intensity λ_i, given by the Lévy measure of

the interval.

2. Choose a point J_i (the jump size) in each interval such that the variance of the Poisson process matches the part of the variance of the Lévy process corresponding to this interval.

In the finite variation case, small jumps do not need to be compensated and we can use zero truncation function in the Lévy-Khintchine representation (5.10), therefore,

$$X_t \approx X_t^\epsilon$$

On the other hand, in the infinite variation case, the approximation of the small jumps, $X_t(\epsilon)$, can simply be their mean value. However, when the intensity of small jumps is high, this method may require simulating of an enormous number of jumps to obtain a reasonable accuracy of the approximation. In that case, a possible improvement is to consider the contribution from the variation of small jumps. The small jumps are going to be replaced by a Brownian motion with variance $\sigma_\epsilon^2 = \int_{|x|\leq\epsilon} x^2\nu(dx)$ [55].

The error process of approximating X_t using expression (5.18) is given by

$$R_t^\epsilon = -N_t^\epsilon + \lim_{\delta\to 0} N_t^\delta \tag{5.19}$$

where

$$N_t^\epsilon = \sum_{s\leq t} J_s \mathbb{1}_{\{\epsilon\leq|x|\leq 1\}} - t\int_{\epsilon\leq|x|\leq 1} x\nu(dx)$$

and it is an infinity activity Lévy process with bounded jumps and, therefore, finite variation,

$$Var(R_t^\epsilon) = t\int_{|x|\leq\epsilon} x^2\nu(dx) = t\sigma_\epsilon^2$$

Hence, the quality of the approximation depends on the speed at which σ_ϵ^2 converges to zero as $\epsilon \to 0$.

It can be shown that in many cases, the normalised error process, $\sigma_\epsilon^{-1} R^\epsilon$ converges to a Brownian motion in distribution.

Theorem 5.4 (Asmussen, Rosiński 2001)**.** *$\sigma_\epsilon^{-1} R_t^\epsilon \xrightarrow{d} W$ as $\epsilon \to \infty$ if the condition holds,*

$$\lim_{\epsilon \to \infty} \frac{\sigma_\epsilon}{\epsilon} = \infty \tag{5.20}$$

Let $Y_t^\epsilon = \sigma_\epsilon^{-1} R_t^\epsilon$, the normalised error process, since the jumps of R^ϵ are bounded by ϵ, condition (5.20) means that the jumps of Y^ϵ are bounded by some numbers that converge to zero. In other words, the limiting process has no jumps. Also, because Y^ϵ, for every ϵ, is a Lévy process with zero mean and the variance of Y_1^ϵ is one, the limiting process will be a continuous Lévy process with mean zero and variance at time 1 equals to one, thus, a standard Brownian motion. Therefore, a better approximation will be of the form, when W_t denotes a Brownian motion,

$$\tilde{X}_t = X_t^\epsilon + \sigma_\epsilon W_t$$

Asmussen and Rosiński also showed that the Brownian motion approximation of small jumps is valid if and only if for each $\kappa > 0$,

$$\sigma_{\kappa\sigma_\epsilon \wedge \epsilon} \sim \sigma_\epsilon \quad \text{as} \quad \epsilon \to 0 \tag{5.21}$$

Also, if the Lévy measure, $\nu(dx)$, does not have atoms in some neighborhood of the

origin, then the two conditions (5.20) and (5.21) above are equivalent [4].

Therefore, using the Gaussian approximation, when a series representation is available, X_t can be approximated by

$$at + \sum_{i=1}^{d} J_i \left(N_t^{(i)} - \lambda_i t \mathbb{1}_{\{|J_i|<1\}} \right) + \tilde{\sigma} W_t \tag{5.22}$$

with d independent Poisson processes $N_t^{(i)}$ with intensity parameter λ_i, such that,

$$\lambda_i = \begin{cases} \nu([a_{i-1}, a_i)) & \text{for } i \in [1, k] \\ \nu([a_i, a_{i+1})) & \text{for } i \in [k+1, d] \end{cases}$$

$$J_i^2 \lambda_i = \begin{cases} \int_{a_{i-1}}^{a_i^-} x^2 \nu(dx) & \text{for } i \in [1, k] \\ \int_{a_i}^{a_{i+1}^-} x^2 \nu(dx) & \text{for } i \in [k+1, d] \end{cases}$$

and $\tilde{\sigma} = \sigma$ when using mean to replace small jumps and $\tilde{\sigma}^2 = \sigma^2 + \sigma_\epsilon^2$ when using Gaussian approximation.

Note that in the case where small jumps are approximated simply by their expected value, if the original Lévy process has no Brownian component (i.e. $\sigma = 0$), then neither does the approximating process. In the Gaussian approximation, a Brownian term appears even when the original process does not have one.

The choice of the intervals $[a_{i-1}, a_i)$ for $1 \leq i \leq k$, and $[a_i, a_{i+1})$, $k+1 \leq k \leq d$ is crucial. For Lévy measure on $\mathbb{R}$, we typically set $d = 2k$, so that the number of Poisson processes that reflecting a positive jump is same as the one reflecting a negative jump. There are three different ways of choosing the intervals [55];

Equally spaced intervals We choose intervals that have equal length, i.e. $|a_{i-1} - a_i|$ is kept fixed for all i, $i \neq k+1$.

Equally weighted intervals We choose to keep the intensities for the up-jumps

and down-jumps corresponding to be constant. Thereby, the Lévy measures of intervals on the negative part of the real line $\nu([a_{i-1} - a_i))$ are kept fixed for all $i \in [1, k]$, for equally weighted intervals. Similarly, the measure of intervals corresponding to positive jumps $\nu([a_i - a_{i+1}))$ is also kept fixed for all $i \in [k + 1, d)$. However, for equally weighted intervals, the outer intervals can become very large.

Interval with inverse linear boundaries Suppose that the boundaries are given by $a_{i-1} = -\frac{\alpha}{i}$ and $a_{2k+2-i} = \frac{\alpha}{i}$, $1 \leq i \leq k + 1$ and $\alpha > 0$. This leads to much more gradually decaying intensity parameters, λ_i, and no explosion to infinity near zero.

To conclude the Poisson and Gaussian approximation, if the small jumps part of a Lévy process has zero mean, or if the intensity of small jumps is relatively low, it is, therefore, reasonable to discard them, and approximate the Lévy process by a compound Poisson process (with a drift). This is so called Poisson approximation. It converges uniformly in t on every finite interval, the series representations provide a consistent way to construct such approximation. On the other hand, when neither the small jumps tend to zero nor the intensity of small jumps is low, dropping them from an approximation may lead to substantial error. In this case, we can simply replace them with their mean value, or more precisely, use a Brownian motion with small variance to approximate the small jumps, and it is called Gaussian approximation. The Gaussian approximation complements the series representations since it is applicable particularly when the series converges slowly.

5.4.2 Boundary crossing probability with approximated Lévy processes

Given the downside of random walk approximation and the convergence issue of series representations approximation, we construct an approximation for a Lévy process by equation (5.18), which composing of d independent compound Poisson processes with intensity λ_i, $N_t^{(i)}$, and a Brownian motion, W_t, with small variance σ^2 and a linear drift. The jump size of the compound Poisson process, $N_t^{(i)}$, is given by a nonnegative constant c_i, $i = 1, \cdots, d$. Therefore, the approximation takes the form of

$$|Z_t^{(1)}| = b + \sum_{i=1}^{d} c_i N_t^{(i)} + \sigma W_t + at \tag{5.23}$$

In this section, we investigate the probability for a standard Brownian motion, $\{X_t\}_{t\geq 0}$, that touches one of the boundaries $|Z_t^{(1)}|$ the first time without time limit by modifying the method in Chapter 4.

Recall the proof of Theorem 4.17 in Chapter 4, the method of using martingales and characteristic exponent of Lévy processes works well on non-decreasing Lévy processes, thus, the result of a finite variation Lévy process can be obtained immediately. As stated earlier in this section, a Lévy process has bounded variance if and only it does not have any Brownian component. In other words, an approximation by Poisson approximation of a Lévy process will be,

$$|Z_t^{(1)}| = b + \sum_{i=1}^{d} c_i N_t^{(i)} \tag{5.24}$$

The martingale that we are going to consider is $e^{-\gamma Z_t}(e^{kX_t} + e^{-kX_t})$, the equation

that is needed to be solved for γ and k is

$$\sum_{i=1}^{d} \lambda_1 - \frac{1}{\gamma} \sum_{i=1}^{d} \lambda_i c_i = \frac{1}{2} k^2$$

Then, in terms of k,

$$\gamma = \frac{2 \sum_{i=1}^{d} \lambda_i c_i}{2 \sum_{i=1}^{d} \lambda_i - k^2} \tag{5.25}$$

with $\varphi(\gamma)$ as defined in Theorem 4.17, is the Laplace transform of the distribution function of jump size, c_i, which is equal to $\frac{c_i}{\gamma}$, as the size of jumps in a single compound Poisson process is constant.

As similarly as in Theorem 4.17, we choose k_j such that,

$$\frac{2 \sum_{i=1}^{d} \lambda_i c_i}{2 \sum_{i=1}^{d} \lambda_i - k_j^2} + k_j = \frac{2 \sum_{i=1}^{d} \lambda_i c_i}{2 \sum_{i=1}^{d} \lambda_i - k_{j+1}^2} - k_{j+1} \tag{5.26}$$

The recurrent relation of k_{j+1}'s is obtained as

$$\begin{aligned} k_{j+1} \quad = \quad & \frac{\sqrt{(\sum_{i=1}^{d} \lambda_i c_i)^2 - 4(\sum_{i=1}^{d} \lambda_i - k_j^2)[\sum_{i=1}^{d} \lambda_i k_j^2 - \sum_{i=1}^{d} \lambda_i c_i k_j - 2(\sum_{i=1}^{d} \lambda_i)^2]}}{2 \sum_{i=1}^{d} \lambda_i - k_j^2} \\ & - \frac{\sum_{i=1}^{d} \lambda_i c_i}{2 \sum_{i=1}^{d} \lambda_i - k_j^2} \end{aligned}$$

by solving the quadratic equation from equation (5.26)

$$\begin{aligned} \left(2 \sum_{i=1}^{d} \lambda_i - k_j^2 \right) k_{j+1}^2 + 2 \sum_{i=1}^{d} \lambda_i c_i k_{j+1} + 2 \sum_{i=1}^{d} \lambda_i k_j^2 \\ -2 \sum_{i=1}^{d} \lambda_i c_i k_j - 4 \left(\sum_{i=1}^{d} \lambda_i \right)^2 = 0 \end{aligned} \tag{5.27}$$

We have notice that equation (5.27) is similar as equation (**??**) that the rate param-

eter of the single compound Poisson process and constant jump size are substituted by the terms above. Hence, the corollary follows,

Corollary 5.1. *The boundary crossing probability for a pair of symmetric Lévy boundaries approximated by the Poisson approximations could be obtained vi*

$$\mathbb{P} = 2\sum_{j=0}^{\infty}(-1)^j e^{-\gamma_j b}$$

with initial $k_0^+ = \frac{1}{3}A_0 + \frac{2\sum_{i=1}^{d}}{A_0}$, *where*

$$A_0 = \left[-27\sum_{i=1}^{d}\lambda_i c_i + 3\sqrt{-24\left(\sum_{i=1}^{d}\lambda_i\right)^3 + 81\left(\sum_{i=1}^{d}\lambda_i c_i\right)^2}\right]^{\frac{1}{3}}$$

and γ_j *is given by equation (5.25).*

Note that when $d = 1$ and $c_i = c_j$ for $i \neq j$, Corollary 5.1 is reduced to Corollary **??**.

Figure 5.1 illustrates the corollary in an example that $d = 5$ when $c_i = c_j$ and $\lambda_i = \lambda_j$. It shows the first-passage time probabilities of the boundaries which are approximated bounded variation Lévy processes are related to all the parameters (b, λ_i, c_i) with λ_i's being the most sensitive ones.

Extra examples are shown in Figures 5.2 - 5.3. In Figure 5.2, we assume that the approximation consists of 5 independent compound Poisson processes and each of them has different rate parameter given by $\lambda_i, i = 1, \cdots, 5$ respectively, but the positive jumps have the same size for all compound Poisson processes. Figure 5.3 gives some instances when the 5 independent compound Poisson processes have different jump rates but same exponential distributed length of time between jumps, i.e. $\lambda_i = \lambda_j$ when $i \neq j$. In summary, these illustrations, not surprisingly, reveal

that the first-passage time probabilities are highly correlated to the rate parameters of the compound Poisson processes, moreover, the correlation is negative.

Despite the enormous number of jumps needed to be simulated to obtain a reasonable approximation of an infinite variation Lévy process, the approximation of small jumps can simply be their mean value, say $\mu > 0$. In this case, it is equivalent to change the starting position of the boundaries from $|b|$ to $|b + \mu|$ and the Poisson components remains the same, the approximation is

$$|Z_t^{(2)}| = b + \mu + \sum_{i=1}^{d} c_i N_t^{(i)}$$

The boundary crossing probabilities for boundaries as $|Z_t^{(2)}|$ are able to be gained by Corollary 5.1 with $b + \mu$ instead of b.

5.5 Conclusions

In this chapter, we modified our method in Chapter 4 to be applicable to more complex forms of boundaries. Some non-decreasing Lévy processes, such as Gamma process, Inverse Gaussian process have been discussed individually;

Gamma process Due to the form of the characteristic exponent of a Gamma process, our method only allows to find some numerical values of the boundary crossing probabilities for a standard Brownian motion.

Inverse Gaussian process Also as the expression of the characteristic exponent of an Inverse Gaussian process, the martingale has to be adjusted from $e^{-\gamma Z_t}\left(e^{kX_t} + e^{-kX_t}\right)$ to $e^{-\gamma Z_t}e^{\phi X_t}\left(e^{i\psi X_t} + e^{-i\psi X_t}\right)$, whereafter with which a desirable result is drawn.

Figure 5.1: First-passage time probabilities of Corollary 5.1
when $c_i = c_j, \lambda_i = \lambda_j$ and $d = 5$

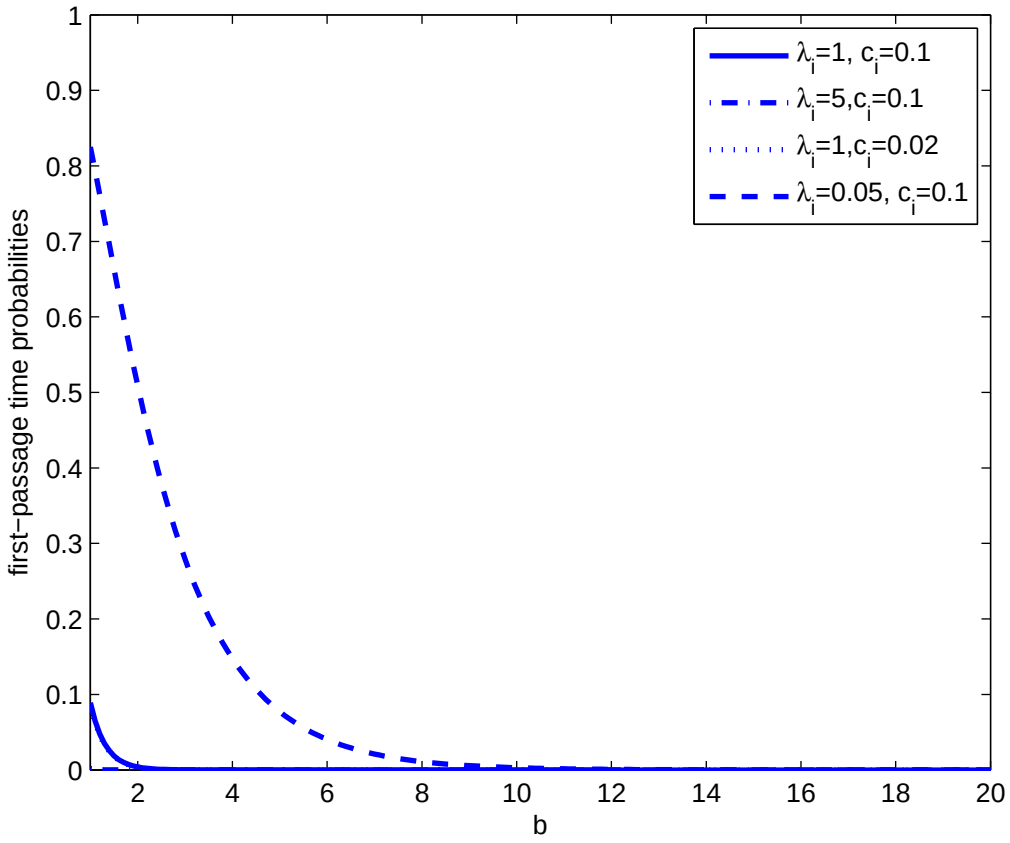

Figure 5.2: First-passage time probabilities of Corollary 5.1
when $d = 5$ and $\lambda_i = 0.01, 0.05, 0.1, 1, 10$ for $i = 1, \cdots, 5$

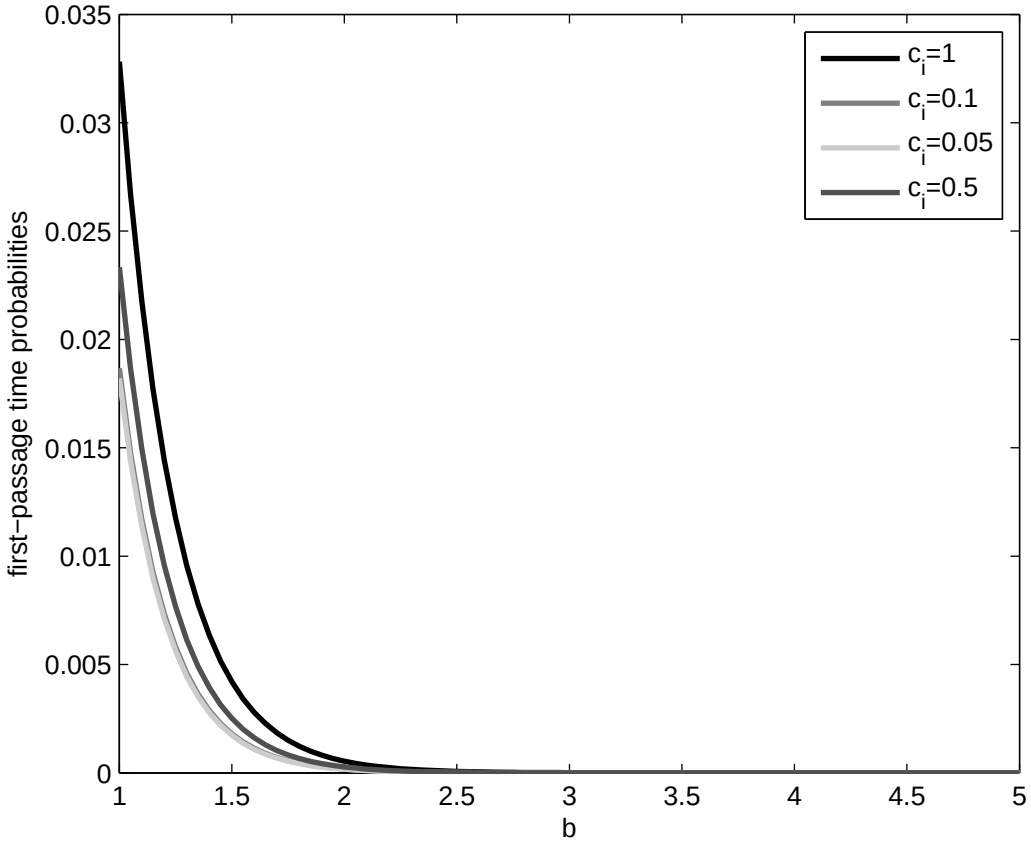

Figure 5.3: First-passage time probabilities of Corollary 5.1
when $d = 5$ and $c_i = 0.01, 0.05, 0.1, 0.5, 1$ for $i = 1, \cdots, 5$

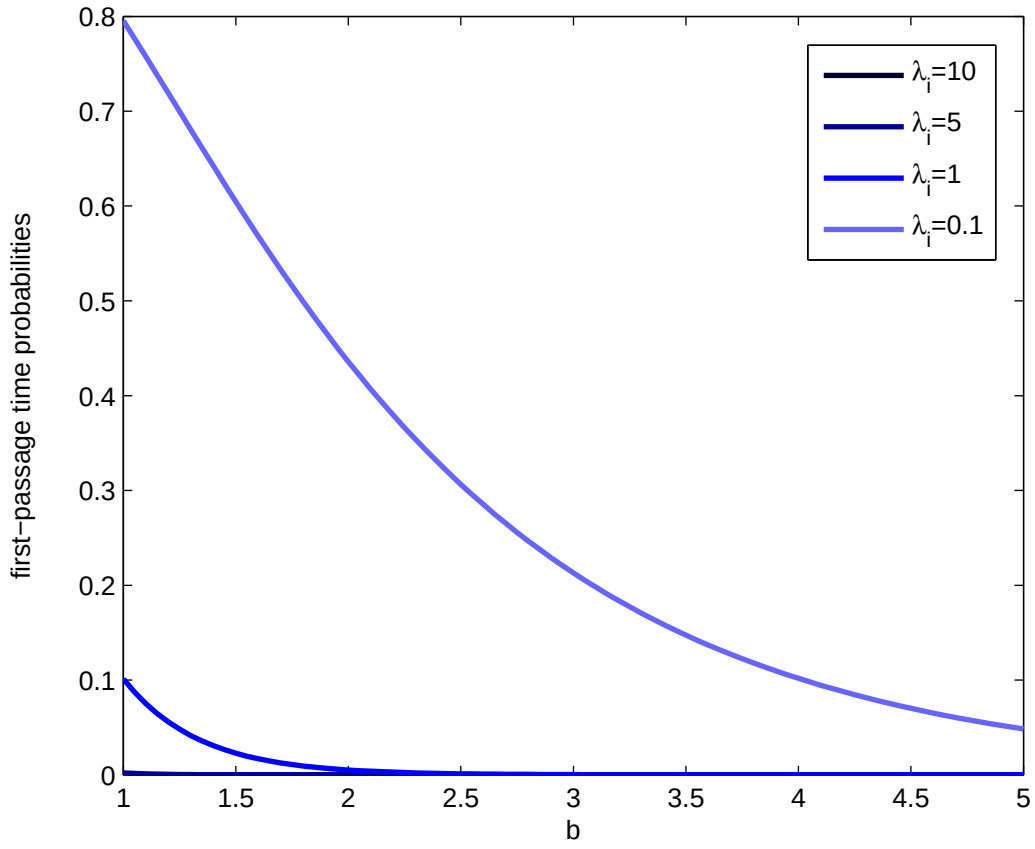

In additional to some of the well-known Lévy processes, we attempted to extend our approach to boundary crossing probabilities to more general non-decreasing Lévy processes. Hence, after studying the existing method of approximating a Lévy process, we applied the method of Poisson approximation to form a non-decreasing Lévy process with bounded variation. The impact of every parameters of the compound Poisson processes that proxies a non-decreasing Lévy process are investigated; λ_i for $i = 1, \cdots, d$ is again the most dominated parameters among d, the number of compound Poisson processes, c_i jump size of the ith compound Poisson process.

Chapter 6

Conclusions

In this thesis, firstly, we have proposed a discrete time Markov-type model to a Real Time Gross Settlement payment system with queueing facilities, which is driven by the strong interest in analyzing the large-valued interbank payment systems. A simple homogeneous model was presented, in addition to which a modified "cluster" model has been developed, where the participating banks are not identical, they have been classified into different groups according to the corresponding business management, therefore, the payment flow was not distributed evenly in the system. The model took the management of central bank for each group into account.

Especially, we are interested in the relation between the values of the parameters and the performance of the proposed "cluster" model. The parameters are

- n, the number of participating banks in a payment system;
- p, the probability that an individual bank has one unit of cash at the beginning of a business day;
- q, the probability that a payment order is delayed and submit to central queue;

- P_{ij}, the probability that a payment order requires a bank in group i to make a payment to a bank in group j.

It has been found that debts are settled at the end of the simulation after 480 iterations, the average number of debts per bank at the end of a business day depends on the parameters. The model has shown an significant linear relationship phenomenon for the position of end-of-the-day debts after the Monte Carlo iterations in the critical case corresponding to $P_{ii} = \frac{n}{N}$, moreover, the linear function was independent of the other parameters (n, p and q). In the sub-critical cases ($P_{ii} \neq \frac{n}{N}$), the linear relationship did not appear. We also notice that the simulation results suggested that the proposed model was stable, since the distribution reached an equilibrium (getting to zero) regardless the values of the parameters.

With both the simple homogeneous model and the modified "cluster" model are developed under the consideration of some existing empirical research of the UK and US Real Time Gross Settlement payment systems data, the assumption of the simulations has been kept at the simplest level. In Chapter 3, we investigated the potential impact of offering a particular liquidity saving solution to the UK large-valued interbank payment system, CHAPS, by applying our proposed model. It has been continuously controversial about should simulations of all kinds use artificial or historical data. Therefore, we thought it was worth to check our results with others where actual data has been used. Considering the similarity of the mechanisms, RRGS by Ercevik and Jackson [21], and ours, and the fact that they have used both real payment data and synthetic data, we had put their work in the comparison.

Instead of using actual historical payment dataset, we simulated a system that captured one of the most important structure features of CHAPS dataset. Nonetheless, same as where actual historical payment dataset was used, we found that

liquidity saving was achieved by implementing this particular mechanism. Nevertheless, the efficiencies were not equal for banks with different sizes; big banks[1] had a poor performance throughout the process presumable due to shortage of incoming funds. For individual banks, the total amount of intra-day liquidity was similar from time to time, and the proportions of liquidity between Real Time Gross Settlement payment system and Liquidity Saving Mechanism were needed to be defined by the value of q and bank's size. Banks were encouraging to make individual strategies to post collateral most efficiently, some of which was heavily relying on the transparency of information: if bank is not being aware of other members' plan[2], it would require collateral proactively to avoid any possibility of unsettled payments. From a central bank's point of view, the system-wide payments information is always available, central bank could guide banks on collateral borrowing, so as to reduce delayed payments significantly. Particularly in the UK, when considering recruiting second-tier banks to CHAPS, central bank can use these experiences to train the banks and coach them through the liquidity management process.

Significantly, despite only the most simplest possible system was studied, the main result was consistent with the research where real historical data was used. In addition to which, the simulation also allowed us to investigate the distribution of particular length cycles, it is potentially interested by central banks and policy makers. With a stable distribution of cycles, central bank can estimate the approximate number of particular cycles, therefore calculate the cost of queue management.

Till the time any liquidity saving solution was enforced in the UK large-valued interbank payment system, CHAPS, there is anecdotical evidence that participating banks would set up bilateral or multi-lateral limits between it and other members

[1] banks dominate approx. 80% payments

[2] schedule of incoming/outgoing payments

of the system to protect itself from unexpected credit exposures. The interest in the efficiency of these limits leads to the calculation of boundary crossing probabilities for a Brownian motion with stochastic boundaries.

After studying the existing literatures about boundary crossing probabilities, by deriving the unconditional boundary crossing probabilities for a standard Brownian motion with symmetric and asymmetric linear boundaries, we have
demonstrated an alternative method by applying powerful tools as martingales and infinitesimal generator of Brownian motions, that allows us to obtain a simple expression. Furthermore, with the help of characteristic exponent of Lévy processes, a basic theorem (Theorem 4.17) has been derived when the boundary is a general compound Poisson process and various corollaries (Corollary 4.18-**??**) follows when the jumps have an explicit form.

In the area of large-valued interbank payment systems, one of the potential applications of the results will be credit control of bilateral/multi-lateral limits. Due to the feature of Real Time Gross Settlement payment system, participating banks wish to use the liquidity in the most effective way, in the sense of minimizing unnecessary costs. The participating banks inform central bank that they would generally set up a limit for the net position with any other banks in the system, which is so called bilateral/multi-lateral limit, and the limit made at the beginning of a business day are based on pervious business day performances. In the course of the day, they would be adjusted often under some circumstances. To the extent of policy makers on bilateral limits in payment system, with the consideration of the results, participating banks are suggested to make decisive regulations. Boundaries with lower boundary crossing probabilities means that banks are in a strong position to control their exposures to other participants.

Compound Poisson process boundaries Banks may think about changing the frequency for adjusting the limits rather than making effort to change the size of every single adjustment. Moreover, the initial position of the limit should be taken into account. If a bank wishes to be generous and set up a bilateral/multi-lateral limit where the other(s) are less likely to excess, it can simply consider putting a relatively high starting value for the boundaries.

Non-decreasing telegraph process boundaries If banks are considering changing limit over an exponential distributed time with the same parameter, lower the intensity of changing, more likely the limits are surpassed by others; and the intensity has a high sensitivity to the functionality of the bilateral/multi-lateral limits. Banks are also advised to look at their strategy to manage the frequencies of adjustment. Nevertheless, banks should be aware that even if the two time intervals are not identically distributed, as long as they are proportional and in the same rate, the efficacy of the limits will be affect unnoticeably.

An immediate extension of the method we derived to find the boundary crossing probabilities for a standard Brownian motion with stochastic boundaries is general Lévy process boundaries. With doing a survey of the existing literatures on the approximation methods of Lévy processes, we has tried to extend the theorems to an approximated Lévy process; finite variation one as independent sum of compound Poisson processes and infinite variation one as combination of compound Poisson processes and linear Brownian motion.

To our knowledge, it is a relatively new task to model the large-valued interbank payment systems and is eager to be expand, one potential further development would be assigned values to individual payment orders in both the simple homo-

geneous and "cluster" models, therefore we could acquire more practicable results of implementing a liquidity saving mechanisms accordingly. Moreover, we sincerely hope that our models could have been brought to a broader context of investigating payment systems and the methods we presented to derive the boundary crossing probabilities would be applicable to other areas of Statistics, such as risk analysis in Finance.

Bibliography

[1] Abundo, M. (2002). Some conditional crossing results of Brownian motion over a piecewise-linear boundary. *Statistics & Probability Letters* **58**, 131–145.

[2] Anderson, T. W. (1960). A modification of the sequential probability ratio test to reduce the sample size. *Annals of Mathematiccal Statistics* **31**, 165–197.

[3] Angelini, P. (1998). An analysis of competitive externalities in Gross Settlement system. *Journal of Banking and Finance* **22**, 1–18.

[4] Asmussen, S. and Rosiński, J. (2001). Approximations of small jumps of Lévy processes with a view towards simulation. *Journal of Applied Probability* **38**, 482–493.

[5] Asmussen, S., Madan, D. and Pistorius, M. (2007). Pricing equity default swaps under an approximation to the CGMY Lévy model. *Journal of Computational Finance* **11**, 79–93.

[6] Atalay, E., Martin, A. and McAndrews, J. (2010). The welfare effects of a Liquidity-Saving Mechanism. Federal Reserve Bank of New York Staff Report, no. 331.

[7] Bech, M. and Garratt, R. (2003). The intraday liquidity manangement game. *Journal of Economic Theory* **109**, 198–219.

[8] Bech, M. L., Preisig, C. and Soramäki, K. (2008). Global trends in large-value payments. *Federal Reserve Bank of New York Economic Policy Review* **14**.

[9] Becher, C., Millard, S. and Soramäki, K. (2008). The network topology of CHAPS Sterling. Bank of England working paper No. 355.

[10] Becher, C., Galbiati, M. and Tudela, M. (2008). The timing and funding of CHAPS Sterling payments. *Economic Policy Review* **14**, 113–133.

[11] Beghin, L., Nieddu, L. and Orsingher, E. (2001). Probabilitic analysis of the telegrapher's process with drift by means of relativistic transformations. *Journal of Applied Mathematics and Stochastic Analysis* **41**, 11–25.

[12] Bollobás, B. (2001). *Random Graphs*, second edition, Cambridge University Press, Cambridge GB.

[13] Bondesson, L. (1982). On simulation from infinitely devisible distributions. *Advances in Applied Probability* **14**, 855–869.

[14] Bank of International Settlements (1997). Real-Time Gross Settlement Systems. *Committee on Payment and Settlement Systems Pubilication* No. 22.

[15] Brwon, R. L., Durbin, J. and Evans, J. M. (1975). Techniques for testing the constancy of regression relationships over time. *Journal of the Royal Statistical Society* **37**, 149–193.

[16] Buckle, S. and Campbell, E. (2003). Settlement bank behaviour nd throughput rules in an RTGS payment system with collateralised intraday credit. Bank of England working paper No. 209.

[17] Carrington, P. J., Scott, J. and Wasserman, S. (2005). *Models and Methods in Social Network Analysis*, Cambridge University Press, Cambridge GB.

[18] Cont, R. and Tankov, P. (2004). *Financial modelling with jump processes*, Chapter 6: Simulating Lévy processes, Chapman & Hall/CRC Financial mathematics series, Florida USA, 171–199.

[19] De Greogrio and Iacus, S. M. (2008). Parametric estimation for the standard and geometric telegraph process observed at discrete times. *Statistical Inference for Stochastic Process* **11**, 249–263.

[20] Durbin, J. (1985). The first-passage density of a continuous Gaussian process to a general boundary. *Journal of Applied Probability* **22**, 99–122.

[21] Ercevik, A. K. and Jackson, J. P. (2010). Simulating the impact of a hybrid design on the efficiency of large-value payment systems. Bank of England working paper.

[22] Erdös, P. and Rényi, A. (1961). On the evolution of random graphs. *Bulletin of the Institute of International Statistics* **38**, 343–347.

[23] Folkerts-Landau, D., Garber,P. and Schoenmaker, D. (1997). The reform of wholesale payment systems. *IMF, Finance and Development*, **34**.

[24] Foong, S. K. and Kanno, S. (1994). Properties of the telegrapher's random process with or without a trap. *Stochastic Processes and their Applications* **53**, 147–173.

[25] Foss, S., and Konstantopoulos, T. (2004). An overview of some stochastic stability method. *Journal of the Operations Research, Society of Japan* **47**, 275–303.

[26] Frank, O. and Strauss, D. (1986). Markov graphs. *Journal of the American Statistical Association* **81**, 832–842.

[27] Frishling, V., Antic, A., Kuchera, A. and Rider, P. (1997). Pricing barrier options with time-dependent drift, volatility and barriers. Commonwealth Bank of Australia working paper.

[28] Furfine, C. H.and Stehm, J. (1998). Analyzing alternative intraday credit policies in the Real-Time Gross Settlement systems. *Journal of Money, Credit and Banking* **30**, 832–848.

[29] Gillespie, D. T. (1977). Exact Stochastic Simulation of Coupled Chemical Reactions. *The Journal of Physical Chemistry* **81**, 2340–2361.

[30] Hall, W. J. (1997). The distribution of Brownian motion on linear stopping boundaries. *Sequential Analysis* **16**, 345–352.

[31] Holland, P. W., Laskey, K. B. and Leinhardt, S. (1983). Stochastic blockmodels: First steps. *Social Networks* **5**, 109–137.

[32] Jeannin, M. and Pisorius, M. (2010). A transform approach to calculate prices and greeks of barrier options deriven by a class of Lévy processes. *Quantitative Finance* **10**, 629–644.

[33] Kac, M. (1974). A stochastic model related to the telegrapher's equation. *Rocky Mountain Journal of Mathematics* **4**, 497–510.

[34] Kolesnik, A. D. (1998). The equations of Markovian random evolution on the line. *Journal of Applied Probability* **35**, 27–35.

[35] Krämer, W., Ploberger, W. and Alt, R. (1988). Testing for structural change in dynamic models. *Econometrica* **56**, 1355–1369.

[36] Kyprianou, A. E. (2006). *Introductory lectures on fluctuations of Lévy processes with applications*, Springer, Berlin Germany.

[37] Leinonen, H. and Soramäki, K. (2003). Simulating interbank payment securities settlement mechanisms with the BoF-PSS2. Bank of Finland discussion papers No. 23.

[38] Lerche, H. R. (1986). *Boundary crossing of Brownian motion*, Springer-Verlag, Berlin Germany.

[39] Maller, R., Solomon, D. and Szimayer, A. (2006). A multinomial approximation for American option prices in Lévy process models. *Mathematical Finance* **16**, 613–633.

[40] Manning, M., Nier, E. and Schanz, J. (2009). *The economics of large-valued payments and settlements, theory and policy issues for Central Banks*, Chapter 4: Liquidity risk in large value payment systems, Oxford University Press, Oxford UK.

[41] Martin, A. and McAndrews, J. (2008). Liquidity-saving mechanisms. *Journal of Monetary Economics* **55**, 554–567.

[42] Newman, M., Watts, D. and Strogatz, S. (2002). Random graph models of social networks. *PNAS* **99**, 2566–2572.

[43] Novikov, A., Frishling, V. and Kordzakhia, N. (1999). Approximations of boundary crossing probabilities for a Brwonian motion. *Journal of Applied Probability* **36**, 1019–1030.

[44] Novikov, A., Frishling, V. and Kordzakhia, N. (2003). Time-dependent barrier options and boundary crossing probabilities. *Georgian Mathematical Journal* **2**, 325–334.

[45] Orsingher, E. (1990). Probability law, flow function, maximum distribution of wave-governed random motions and their connections with Kirchoff's Laws. *Stochastic Processes and their Applications* **34**, 49–66.

[46] Ricciardi, L. M. (1977). *Diffusion processes and related topics in Biology (Lecture notes in Biomathematics)*, Springer, Berlin Germany.

[47] Robbins, H. (1970). Statistical method related to the law of the iterated logarithm. *Annals of Mathematical Statistics* **41**, 1379–1409.

[48] Robbins, H. and Siegmund, D. (1970). Boundary crossing probabilities for the Wiener process and smaple sums. *Annals of Mathematical Statistics* **41**, 1410–1429.

[49] Robbins, H. and Siegmund, D. (1973). Statistical tests of power one and the integrl representation of solutions of certain partial differential equations. *Bulletin of the Institute of Mathematics* **1**, 93–120.

[50] Roberts, G. O. and Shortland, C. F. (1997). Pricing barriers options with time-dependent coefficients. *Mathematical Finance* **7**, 83–93.

[51] Robins, G. and Pattison, P. (2001). Random graph models for temporal processes in social network. *Journal of Mathematical Sociology* **25**, 5–41.

[52] Robins, G., Pattison, P., Kalish,Y. and Lusher, D. (2007). An introduction to exponential random graph (p^*) models for social networks. *Social Newtorks* **29**, 173–191.

[53] Rosiński, J. (2001). *Lévy process: theory and applications*, O.E. Barndorff-Nielsen, T. Miksch, S.I. Resnick, Birkhäuser, 401–415.

[54] Scheike, T. H. (1992). A boundary-crossing result for Brownian motion. *Journal of Applied Probability* **29**, 448–453.

[55] Schoutens, W. (2003). *Lévy processes in Finance: pricing financial derivatives*, Chapter 8: Simulation techniques, John Wiley & Sons, Ltd., 101–118.

[56] Sen, P. K. (1981). *Sequential nonparametrics: invariance principles and statistical inference*, Wiley, New York USA.

[57] Siegmund, D. (1985). *Sequential analysis: tests and confidence intervals*, Springer, New York USA.

[58] Siegmund, D. (1986). Boundary crossing probilities and statistical applications. *Annals of Statistics* **14**, 361–404.

[59] Soramäki, K., Bech, M. L., Arnold, J., Glass, R. J. and Beyeler, W. E. (2007). The topology of interbank payment flows. *Physica A: Statistical Mechanics and its Applications* **379**, 317–333.

[60] Wang, Y. J. and Wong, G. Y. (1987). Stochastic blockmodels for directed graphs. *Journal of the American Statistical Association* **82**, 8–19.

[61] Wang, L. and Pötzelberger, K. (1997). Boundary crossing probability for Brownian motion and genarl boundaries. *Journal of Applied Probability* **34**, 54–65.

[62] Wasserman, S. (1980). Analyzing social networks as stochastic processes. *Journal of the American Statistical Association* **75**, 280–294.

[63] Wiktorsson, M. (2002). Simulation of stochastic integrals with repect to Lévy processes of typy G. *Stochastic Processes and their Applications* **101**, 113–125.

[64] Willison, M. (2005). Real-Time Gross Settlement and hybrid payments system: a comparison. Bank of England working paper No. 252.

Appendix A

Chapter 2

A.1 Dynamical Monte Carlo method

Due to the complexity of the dynamics of the payment systems, we use Monte Carlo methods to obtain an equilibrium properties for the system in the question. However, Monte Carlo methods can be also used to investigate dynamical phenomena according to adequate dynamical interpretation of the method.

For an dynamical phenomena, the Monte Carlo method provides a numerical solution to the Kolmogorov equation,

$$\frac{\partial P(i,t)}{\partial t} = \sum_j r(j \to i)P(j,t) - \sum_j r(i \to j)P(i,t) \tag{A.1}$$

where i and j are the successive states of the system, $P(i,t)$ is the probability that the system is in state i at time t, and $r(i \to j)$ is the probability that the system will undergo a transition from state i to state j per unit time. The solution to the Kolmogorov equation (A.1) can be found computationally by randomly picking up a possible transition and accepting particular transitions with appropriate probabil-

ities. After each transition, time is increased by one unit time τ_j, which is a function of transition rates.

At the equilibrium state, the right hand side of equation (A.1) equals to zero, in other words, the sum of all transitions into a particular state i is equal to the sum of all transitions out of the state. Moreover, the so-called detailed-balance equation should hold:

$$r(j \to i)P(j, eq) = r(i \to j)P(i, eq)$$

with

$$P(i, eq) = \frac{-\exp(-H(i)/\varphi)}{Z}$$

where $H(i)$ is the Hamiltonian and Z is the partition function of the system. The detailed-balance equation ensures that the Monte Carlo transition probabilities can be constructed in order to guarantee that the system will reach a statistical equilibrium. However, it does not specify the unique probabilities.

In dynamical interpretation of Monte Carlo methods, it can be assumed that the time resolution is so fine that no two events occur at the same time [29]. Hence, we could just simulate a sequence of distinct events that are separated by certain different time intervals. Then we have a list of distinct events, say $E = \{e_1, e_2, \cdots, e_n\}$, which are characterised by average transition rates $R = \{r_1, r_2, \cdots, r_n\}$. In theory, any particular transition that becomes possible at time t can occur at any time $t + \Delta t$ with a uniform probability based on its rate and is independent of the events occurred before time t. Thus, the average rate of forward/backward transition can be expressed as a time density of events. Let Δt's be small and identical time intervals of a larger time interval t, say, and $t = n\Delta t$. Then the average rate is the limit of the ratio of the number of intervals that contain events $n_{\Delta t}$ to the total number of intervals sampled n per unit time Δt as Δt goes to zero and n goes to infinity.

i.e.

$$r = \lim_{\Delta t \to 0, n \to \infty} \frac{n_{\Delta t}}{t}$$

In this limit, each interval could contain one event at most, and each time interval has the same probability $r\Delta t$ of containing an event, which implies that, in the time interval t, there are at most n events in total.

Let N_t be a random number that counts the number of events which have occurred within the time t, then the probability that n_t events may occur at time t is

$$\mathbb{P}(N_t = n_t) = \frac{n_t}{n}(r\Delta t)^{n_t}(1 - r\Delta t)^{n-n_t}$$

As we decrease the length of the interval, the stationary series of random, independent events with average rate r is of the Poisson process, i.e. as $\Delta t \to 0$, we have

$$\mathbb{P}(N_t = n_t) = \frac{(rt)^{n_t}}{n_t!}e^{-rt}$$

and another useful property of the Poisson process is that the probability density of time t_e between successive events is

$$f_{t_e}(t) = re^{-rt}$$

From the above two equations, we could get that the mean number of events occurring within a time t is rt, and the mean time period between successive events is $\frac{1}{r}$.

Furthermore, a group of independent Poisson processes performs as an entire large Poisson process, therefore, the statistical properties of the entire process could be formulated in terms of the dynamics of individual processes. Consider L independent forward-reverse Poisson processes and each with some finite rate $r_{i \to j}$. Let

N_L be a random number that counts the overall number of events among the L processes which have occurred within a time interval t, and

$$N_L = \sum_{i=1}^{L} N_t$$

which means that N_L is the sum of number of events occurred during the interval t in each individual process. The overall probability that n_t events occurred in time t is

$$\mathbb{P}(N_L = n_t) = \frac{(\upsilon t)^{n_t}}{n_t!} e^{-\upsilon t}$$

where $\upsilon = \sum_{i=1}^{L} r_{i \to j}$. The logic described is also applicable to systems which are not stationary or toward equilibrium.

To conclude, we could generalised a system from the above. Consider L types of agents, which are capable of undergoing I transition events that are classified by rates $R = \{r_1, r_2, \cdots, r_I\}$. Hence, the L agents could be divided according to the various transition events as $L = \{e_1, e_2, \cdots, e_I\}$, where e_i is the number of types of agents that capable of undergoing a transition with a rate $r_{i \to j}$ and $L = \sum_{i=1}^{I} e_i$. This means that a particular configuration of the system at a particular time can be characterised by the distribution of L over R, and the distribution is constructed by a Monte Carlo algorithm which selects randomly among various possible events at each step and which effects the events with appropriate transition probabilities. When an event is realised, time should be updated by an increment τ_i selected from an exponential distribution

$$\tau_i = \frac{1}{\sum_i n_i r_i} \ln(\mu)$$

where μ is a uniform random number between 0 and 1.

Then generate another random number C, we simulate the events from given

distribution as

$$\sum_{i=1}^{k-1} n_i r_i < C \sum_{i} n_i r_i \leq \sum_{i=1}^{k} n_i r_i$$

A.2 MatLab codes for simulations

Cluster model

```
clear all

dn=1000;

so=480; s=so; %=====Iteration Number=====

i=40;j=i;


Res=zeros(dn,i); Nr=zeros(dn,1); Nri=zeros(dn,1);

SIn=zeros(1,so);Sn=zeros(1,s);

STa=zeros(1,i); ST=zeros(1,i);

T=0; z2=1;

Cred=0.3; %=====Start Credit Value p=====

Bv=0.2; %=====Queueing Prob q======

B3=zeros(dn,1);


group_No=5; %=====n=====

in_group_prob=1/(i-1); %=====P_{ii}=====

if in_group_prob > group_No/i || in_group_prob < 1/i,

    error('in group probability no in range');

end

between_group_prob=((1-i*in_group_prob/group_No)*group_No)...

/((group_No-1)*i);
```

```
temp1=in_group_prob*(ones(i/group_No)-eye(i/group_No));
temp2=between_group_prob+zeros(i/group_No);
payment_transition=kron(eye(group_No),temp1)+kron(ones(group_No)...
-eye(group_No),temp2);
clear temp*

for d=1:dn
    Ab=zeros(i,j);Ar=zeros(i,j);
%   A=zeros(i,j+1);
    H=zeros(s,5);
    Black=zeros(s,i);
    Index=zeros(s,i+1);Ind=zeros(s,i);
    Black2=zeros(s,i);Black3=zeros(s,i);
    Red=zeros(s,i);
%   Redi=sum(Red);
    B=zeros(i,j);

    N=i^2-i; %=====number of nonzero elements=====
    Rd=1-Bv;
    Pb=Bv/N; Pr=Rd/N;

    Ab(:,:)=Pb; %=====Black Probability Matrix=====
    Ar(:,:)=Pr; %=====Red Probability Matrix=====
    for k=1:j+1:i^2
        Ab(k)=0;
```

```
end
A=[Ab Ar]; %=====United Probability Matrix=====

for o=1:i %=====Start Cash Table Filling=====
    P=rand;
    if P < Cred
        Red(1,o)=1;
    end
end
Redi=sum(Red);

for z=1:s
    X=zeros(i,2*j); X2=zeros(i,j);
    Z2=rand; t=-log(Z2); T=T+t;
    Index(z,1)=z;
    %=====Start of Trading Procedure=====
    %=====Monte I procedure=====
    y1=randperm(i); y1=y1(1);
    x1=Monte_new(payment_transition(y1,:));

    H(z,1)=z; H(z,2)=T; H(z,3)=y1; H(z,4)=x1;
    if B(y1,x1)>0 %=====if 2/2=====
        for k2=1:z  %=====for5=====
            if Black2(k2,x1)==-1  %=====if5=====
                if Black2(k2,y1)==1 %=====if6=====
                    Black2(k2,x1)=0; Black2(k2,y1)=0;
```

```
                    Black3(k2,x1)=0;
                    Ind(k2,x1)=z-Index(k2,x1+1);
                    Index(k2,x1+1)=-1;
                end  %=====end if6======
                break  %=====break for5=====
            end  %=====end if5=====
        end  %=====end for5=====
        B(y1,x1)=B(y1,x1)-1; B(x1,y1)=B(x1,y1)+1;
    elseif Redi(y1)==0

        v=Monte_new(A);%=====Monte II procedure=====
        X(v)=1;
        [y,x]=find(X);%=====Index Table=====
        if rand>Bv %=====Red Arrow - cash paying=====
            H(z,5)=x1; Black(z,y1)=0;
            Redi(x1)=Redi(x1)+1; Red(z,x1)=1;
            r1=x1; r2=y1;
            while sum(Black3(1:z,r1))<0
                for f2=1:z+i %=====for5=====
                    if Black3(f2,r1)==-1 %=====if5=====
                        for f3=1:i
                            if Black2(f2,f3)==1 %=====if6=====
                                Black2(f2,r1)=0;
                                Black2(f2,f3)=0;
                                Black3(f2,r1)=0;
                                B(r1,f3)=B(r1,f3)+1;
```

```
                                B(f3,r1)=B(f3,r1)-1;
                                Redi(r1)=Redi(r1)-1;
                                Redi(f3)=Redi(f3)+1;
                                Ind(f2,r1)=z-Index(f2,r1+1);
                                Index(f2,r1+1)=-1; r1=f3;
                                break
                            end %=====end if6=====
                        end
                        break %=====break for5=====
                    end %=====end if5=====
                end %=====end for5=====
            end %=====end while=====

            %=====Tables Filling=====
            %=====MARKET I=====
        else %x<=i
            Black(z,y1)=-1; Black2(z,y1)=-1;
            Index(z,y1+1)=z;
            Black2(z,x1)=1; Black3(z,y1)=-1;
            B(y1,x1)=B(y1,x1)-1; B(x1,y1)=B(x1,y1)+1;
        end
    elseif Redi(y1)>0
        Redi(x1)=Redi(x1)+1; Redi(y1)=Redi(y1)-1;
        r1=x1; r2=y1;
        while sum(Black3(1:z,r1))<0
            for f2=1:z+i %=====for5=====
```

```
                    if Black3(f2,r1)==-1 %=====if5=====
                        for f3=1:i
                            if Black2(f2,f3)==1 %=====if6=====
                                Black2(f2,r1)=0;
                                Black2(f2,f3)=0;
                                Black3(f2,r1)=0;
                                Redi(r1)=Redi(r1)-1;
                                Redi(f3)=Redi(f3)+1;
                                B(r1,f3)=B(r1,f3)-1;
                                B(f3,r1)=B(f3,r1)+1;
                                Ind(f2,r1)=z-Index(f2,r1+1);
                                Index(f2,r1+1)=-1;
                                r1=f3;
                                break
                            end %=====end if6=====
                        end
                        break %=====break for5=====
                    end %=====end if5=====
                end %=====end for5=====
            end %=====end while=====
        end %=====end if2=====
            %=====End of Black Arrow=====
        De=sum(Black2);
        Deb(z,1:i)=De;
    end %=====GLOBAL END=====
```

```
    ST=sum(Black3);
    if ST==0
       B3(d,1)=1;
    end

    STa=STa+ST; In=Ind'; Sn=sum(In);

    debit_time_distribution=zeros(s,i);
     for name1=1:s,
         for name2=1:i,
             debit_time_distribution(name1:min(s,name1+...
             Ind(name1,name2)-1),name2)=...
             debit_time_distribution(name1:min(s,name1+...
             Ind(name1,name2)-1),name2)+1;
         end
     end

     debit_time_distribution=debit_time_distribution(1:so,:);
     debit_time_distribution=sum(debit_time_distribution,2);

    SIn=SIn+debit_time_distribution'; SIn=SIn+Sn;
end

S3=sum(B3); AvB3=-STa/d; AvDeb=SIn/d;
AvB4=sort(AvB3);
subplot(1,2,1); bar(AvB4);
```

```
title('Ave. End Market Debts');
xlabel('Settlement Banks'); xlim([1,40]);
ylabel('Ave. End Market Debts')

subplot(1,2,2); bar(AvDeb);
title('Av. Debt Life Time Distribution');
xlabel('Iterations');xlim([0,480])
ylabel('Aggregated Debts')

Bin=1:480; n=sum(AvDeb); n1=round(n);
Bin=Bin'; Bin2=Bin.^2;
Data1=AvDeb*Bin; Data2=AvDeb*Bin2;
mu=Data1/n1; %=====sample mean=====
sigma=(1/(n1-1))*(Data2-Data1^2/n1); %=====sample variance=====
theta=sigma/mu; %=====scale parameter======
k=mu/theta; %=====shape parameter======
display(theta);display(k)
```

Function Monte_new

```
function u=Monte_new(A)
R=sum(A); Z1=rand; Sum=A(1);
for k=1:length(A) %=====for3-n=====
    Sum=Sum+A(k);
    if Sum>=Z1*R %=====if1=====
        break
    end %=====end if1=====
```

```
end  %=====endfor3-n=====

u=k;
```

Appendix B

Chapter 3

B.1 Outcomes of simulation

The outcomes of the experiment are the matrices list below

- **H**, contains the information of every payment row by row, including the order of the payments, the time if occurred, its payer, payee and the type, which depends on payments' statue.
- **Red1**, the records of RTGS payments column by column. For instance, on the kth column, the only two nonzero entries are 1 and -1, which are payee and payer of the payment occurred on the kth iteration respectively.
- **Red2**, a i-by-i matrix (i is the number of settlement banks, $i = 14$), the (m, n)th element indicates the cumulative number of RTGS payments in that direction ($m \to n$).
- **Green1** and **Green2** keep the record of LSM payments in the same manner as Red1 and Red2 for RTGS payments.

- **Black2**, the cumulative amount of delayed payments in the internal queue up to the latest iteration.

- **Black3**, the cumulative amount of payments made due to offset with other payments in the internal queue, up to the latest iteration.

At every iteration, a payment is picked up according to the dynamic Monte Carlo, in the mean time, the decision on if this payment is submitted into LSM is made. There exist two subsystems, for example, on the jth iteration, the payment is from bank m to bank n.

If the payment is time-critical and needs to be made via RTGS payment system, the following steps would execute.

1. Payment which is made in RTGS is denoted as type I payment, H.

2. The record of the payment is kept in the Red1 matrix on the jth column, where its mth row is rewritten as -1 and nth row is 1.

3. Also, in Red2 matrix the (m, n)th element is increased by 1.

4. The liquidity positions of both banks are updated.

5. Queue in RTGS is not considered here.

6. The jth entries in both Black2 (number of type 0 payments) and Black3 (number of type II payments) will be calculated according to matrix H.

7. End of the jth iteration.

If the payment is submit into LSM

1. The programme performs the search of the shortest "cycle" of payments which is completed by the newly arrived payment.

2. In the case where the shortest "cycle" exists, every payment in that "cycle" is cleared, so their records in Green1 and Green2 are updated and they become type II payments.

3. Otherwise, everything remains unchanged, and this is a type 0 payment.

4. The jth entries in both Black2 (number of type 0 payments) and Black3 (number of type II payments) will be calculated according to matrix H.

5. End of the jth iteration.

B.2 MatLab code of the simulation

LSM simulation

```
clear all
dn=200; s=8400; i=14; j=i; T=0;
q=1; %=====probability of queueing=====
payment_transition=zeros(i,j); %=====the probability matrix=====
payment_transition(:,:)=1/45; %=====filling the matrix=====
payment_transition(1:4,1:4)=0.267;
payment_transition(5:14,1:4)=0.2;
payment_transition(1:4,5:14)=0.02;

for h=1:j+1:i^2
    payment_transition(h)=0; %===the diagonal elements are zero===
end

Green=zeros(i,j); Black=zeros(1,s+1);
```

```
HC=zeros(i,1); Hm=zeros(i,dn); Hr=zeros(i,dn);
queued=zeros(1,s+1); Red=zeros(i,j);

for d=1:dn; %=====repeat the experiment dn times=====
    Green1=zeros(i,s); Green2=zeros(i,j);
    Red1=zeros(i,s); Red2=zeros(i,j);
    Black2=zeros(1,s+1);
    Black3=zeros(1,s+1);
    Cash=zeros(i,s+1); %===the cash position change over payments===
    H=zeros(s,5);
    %===H matrix keeps record of all payments happens on that day===
    Hc=zeros(i,1);
    for k=1:s %=====for every payment=====
        X=zeros(i,j);
        Z2=rand; %=====generate a uniform random variable=====
        t=-log(Z2); %===generate the exponential random variable===
        T=T+t; %=====time adds up for every payment=====

        n=Monte(i,payment_transition);
        X(n)=1; %=====locate the payment in the matrix X=====
        [x,y]=find(X); %===find the coordinate of the payment===
                       %=====x, the sender=====
                       %=====y, the receiver=====

        H(k,1)=k; %=====the order of payment=====
        H(k,2)=T; %=====the time when the payment occurred=====
```

```
H(k,3)=x; %=====the payer of the payment=====
H(k,4)=y; %=====the payee of the payment=====
Cash(:,k+1)=Cash(:,k);
%=====cash position change over payments=====
%=====decide if the payment is queued=====
a=rand;
if a>q %===payment submit to RTGS===
    H(k,5)=1; %===indicate the RTGS payment===
    Red1(x,k)=-1; Red1(y,k)=1;
    Red2(x,y)=Red2(x,y)+1;
    Cash(x,k+1)=Cash(x,k)-1;
    %=====update the cash position of x and y=====
    Cash(y,k+1)=Cash(y,k)+1;
else %===payment submit to LSM===
    Green1(x,k)=-1; Green1(y,k)=1;
    Green2(x,y)=Green2(x,y)+1;
    Hk=H(1:k,:); A=Black1(Hk);
    [dis path]=graphshortestpath(A,y,x);
    if dis<=13
        for f=1:length(path)-1
            v=path(f); w=path(f+1);
            col=find_column(v,w,Green1);
            Green1(v,col)=0; Green1(w,col)=0;
            Green2(v,w)=Green2(v,w)-1;
            H(col,5)=k;
        end
```

```
                H(k,5)=k;
                Green1(x,k)=0; Green1(y,k)=0;
                Green2(x,y)=Green2(x,y)-1;
                Black2(1,k+1)=Black2(1,k)-dis;
                Hc(length(path))=Hc(length(path))+1;
            end
            Cash(:,k+1)=Cash(:,k);
        end
        H0=H(1:k,:); H0(H0(:,5)~=0,:)=[];
        Black2(1,k+1)=size(H0,1);

        H1=H(1:k,:); H1(H1(:,5)<=1,:)=[];
        Black3(1,k+1)=size(H1,1);
    end
    Green=Green+Green2; Black=Black+Black2;
    queued=queued+Black3;
    Hm(:,d)=sum(Green2,2); Hr(:,d)=sum(Red2,2);
    HC=HC+Hc;
    Red=Red+Red2; Hg(:,d)=min(Cash,[],2);
    CASH=CASH+min(Cash,[],2);
end

figure(1)
queued_payments=sum(Green,2)/d;
cash_payments=sum(CASH,2)/d*(-1);
rtgs_payments=sum(Red,2)/d;
```

```
liquidity=[queued_payments cash_payments];
HM=max(Hm,[],2); HR=max(Hr,[],2); HG=min(Hg,[],2);

subplot(1,2,1)
bar(liquidity,'stack')
colormap summer
title('{\bf Ave. Delayed Payments & Ave. RTGS Payments by banks}')
xlabel('{Settlement Banks}'); ylabel('{No. payments}')

subplot(1,2,2)
Max=[HM HG];
bar(Max,'stack');
colormap summer
title('{\bf Max.in LSM & RTGS}')
xlabel('{Settlement Banks}'); ylabel('{No. payments}')
legend('location','southoutside', 'Delayed Payments in LSM',
'Net RTGS Payments')

ave_life=Black/d; ave_queued=queued/d;

figure(2)
imagesc(Green2)
colorbar('location','eastoutside')
title('{\bf Distribution of Delayed Payments}')
ylabel('Sending banks'); xlabel('Receiving banks')
set(gca,'YDir','normal')
```

```
disp(ave_queued(s+1)); disp(ave_life(s+1)); disp(HC/d);
disp(ave_queued(s+1)/(ave_queued(s+1)+ave_life(s+1)));
```

Function `Monte`

```
function u=Monte(i,A)
A1=sum(A); R=sum(A1); Z1=rand; Sum=A(1);

for k=1:2*i^2 %=====for1=====
    Sum=Sum+A(k);
    if Sum>=Z1*R %=====if1=====
        break
    end %=====end if1=====
end %=====end for1=====
u=k;
```

Function `Black1`

```
function A=Black1(H)
sender=H(:,3); receiver=H(:,4); type=H(:,5);
Queue=[sender receiver type];
condition=Queue(:,3)~=0;
Queue(condition,:)=[];
A=zeros(14,14);

for j=1:length(Queue(:,1))
    A(Queue(j,1),Queue(j,2))=A(Queue(j,1),Queue(j,2))+1;
end
```

```
for i=1:14
    for j=1:14
        if A(i,j)>=1;
            A(i,j)=1;
        end
    end
end

A=sparse(A);
```

Function `find_column`

```
function col=find_column(v,w,Green1)
b=find(Green1(v,:)==-1); c=find(Green1(w,:)==1);
for c1=1:length(b)
    for c2=1:length(c)
         if b(c1)==c(c2)
             col=b(c1);
         end
         if b(c1)==c(c2)
             break
         end
    end
    if b(c1)==c(c2)
        break
    end
```

```
end
```

Appendix C

Chapter 4

C.1 MatLab codes for simulation results in Table 4.2

```
clear all
T=240; %=====the time interval=====
lambda=5; %=====rate of poisson process=====
alpha=3; %=====parameter of exponential distribution=====
c=0.05; a=1000;
protau=zeros(1,a);
d=0.2; m=100;
Taupro=zeros(1,m);

for m1=1:m;
    for l=1:a;
        N_t=poissrnd(lambda*T);
```

```
%=====simulate the total number of jumps on [0,T]=====
U=unifrnd(0,T,N_t,1); %=====N iid uniform r.v.'s=====
Y=exprnd(alpha,N_t,1);
%=====N iid jump size exponential variables=====
ind=zeros(N_t,1); %=====indicator function=====
X=zeros(T,1); %=====the compound poisson process=====
for t=1:T;
    for j=1:N_t;
        if U(j)<t;
            ind(j)=1;
        else ind(j)=0;
        end
    end
    X(t)=sum(ind.*Y);
end
X1=[0; X]; ti=0:d:T; T1=0:T;
Xi=interp1(T1',X1,ti);
N=size(0:d:T,2);
W=[0 cumsum(randn(1,N-1))]/sqrt(N);
%=====S is running sum of N(0,1/N) variables=====
W=W*sqrt(N); %=====generate Brownian motion=====
b=20; Xi=Xi+b;
p=find(sign(abs(W)-Xi)>=0,1);
    if isempty(p)==1;
        protau(l)=0;
    elseif isempty(p)==0;
```

```
                protau(l)=1;
            end
    end
    taupro=sum(protau)/a; Taupro(m1)=taupro;
end

Pro=mean(Taupro); Variance=var(Taupro);

display(Pro); display(Variance);
display(b);display(d);

plot(0:d:T-d, W');
hold on
plot(0:d:T-d, Xi,'r'); plot(0:d:T-d,-Xi,'r');
hold off
```

C.2 Values of k_j, θ_j and γ_j for Theorem 4.18

Table C.1: values of k_j, θ_j and γ_j when $\lambda = 0.05, \alpha = \frac{1}{50}$

j	k_j	θ_j	γ_j
0	0.3064	0	0.3064
1	0.3129	0.6128	0.9256
2	0.3142	1.2385	1.5527
3	0.3148	1.8669	2.1817
4	0.3151	2.4965	2.8116
5	0.3153	3.1267	3.4420
6	0.3155	3.7573	4.0728
7	0.3156	4.3883	4.7038
8	0.3156	5.0194	5.3350
9	0.3157	5.6506	5.9663
10	0.3157	6.2820	6.5978
11	0.3158	6.9135	7.2293
12	0.3158	7.5451	7.8609
13	0.3159	8.1768	0.4926
14	0.3159	8.8085	9.1244
15	0.3159	9.4402	9.7562

Table C.2: values of k_j, θ_j and γ_j when $\lambda = 0.05, \alpha = \frac{1}{20}$

j	k_j	θ_j	γ_j
0	0.2922	0	0.2922
1	0.3077	0.5844	0.8922
2	0.3111	1.1999	1.5110
3	0.3126	1.8221	2.1347
4	0.3134	2.4473	2.7607
5	0.3139	3.0741	3.3880
6	0.3143	3.7019	4.0162
7	0.3145	4.3305	4.6450
8	0.3147	4.9596	5.2743
9	0.3149	5.5891	5.9039
10	0.3150	6.2188	6.5339
11	0.3151	6.8489	7.1640
12	0.3152	7.4792	7.7944
13	0.3153	8.1096	8.4249
14	0.3154	8.7402	9.0555
15	0.3154	9.3709	9.6863

Table C.3: values of k_j, θ_j and γ_j when $\lambda = 0.05$, $\alpha = \frac{1}{10}$

j	k_j	θ_j	γ_j
0	0.2702	0	0.2702
1	0.2990	0.5403	0.8392
2	0.3058	1.1382	1.4440
3	0.3088	1.7498	2.0586
4	0.3105	2.3674	2.6779
5	0.3115	2.9884	3.2999
6	0.3123	3.6115	3.9237
7	0.3128	4.2360	4.5488
8	0.3132	4.8616	5.1748
9	0.3135	5.4881	5.8016
10	0.3138	6.1151	6.4289
11	0.3140	6.7427	7.0567
12	0.3142	7.3708	7.6849
13	0.3143	7.9991	8.3135
14	0.3145	8.6278	8.9423
15	0.3146	9.2568	9.5714

Table C.4: values of k_j, θ_j and γ_j when $\lambda = 0.1, \alpha = \frac{1}{50}$

j	k_j	θ_j	γ_j
0	0.4373	0	0.4373
1	0.4439	0.8747	1.3185
2	0.4452	1.7624	2.2076
3	0.4458	2.6528	3.0986
4	0.4461	3.5443	3.9904
5	0.4463	4.4365	4.8828
6	0.4464	5.3291	5.7756
7	0.4465	6.2220	6.6686
8	0.4466	7.1151	7.5617
9	0.4467	8.0083	8.4550
10	0.4467	8.9017	9.3484
11	0.4468	9.7952	10.2420
12	0.4468	10.6890	11.1360
13	0.4468	11.5820	12.0290
14	0.4469	12.4760	12.9230
15	0.4469	13.3700	13.8170

Table C.5: values of k_j, θ_j and γ_j when $\lambda = 0.1$, $\alpha = \frac{1}{20}$

j	k_j	θ_j	γ_j
0	0.4229	0	0.4229
1	0.4388	0.8458	1.2846
2	0.4421	1.7233	2.1655
3	0.4436	2.6076	3.0512
4	0.4444	3.4948	3.9392
5	0.4449	4.3836	4.8285
6	0.4453	5.2734	5.7187
7	0.4455	6.1640	6.6095
8	0.4457	7.0550	7.5008
9	0.4459	7.9465	8.3924
10	0.4460	8.8383	9.2843
11	0.4461	9.7303	10.1760
12	0.4462	10.6230	11.0690
13	0.4463	11.5150	11.9610
14	0.4463	12.4080	12.8540
15	0.4464	13.3000	13.7470

Table C.6: values of k_j, θ_j and γ_j when $\lambda = 0.1$, $\alpha = \frac{1}{10}$

j	k_j	θ_j	γ_j
0	0.4000	0	0.4000
1	0.4301	0.8000	1.2301
2	0.4369	1.6601	2.0971
3	0.4399	2.5340	2.9739
4	0.4415	3.4137	3.8553
5	0.4426	4.2968	4.7394
6	0.4433	5.1819	5.6252
7	0.4438	6.0685	6.5123
8	0.4442	6.9561	7.4004
9	0.4445	7.8446	8.2891
10	0.4448	8.7337	8.1785
11	0.4450	9.6233	10.0680
12	0.4452	10.5130	10.9580
13	0.4453	11.4040	11.8490
14	0.4455	12.2940	12.7400
15	0.4456	13.1850	13.6310

Table C.7: values of k_j, θ_j and γ_j when $\lambda = 1, \alpha = \frac{1}{50}$

j	k_j	θ_j	γ_j
0	1.3976	0	1.3976
1	1.4086	2.7953	4.2039
2	1.4109	5.6126	4.2039
3	1.4118	8.4343	9.8461
4	1.4124	11.2580	12.6700
5	1.4127	14.0830	15.4950
6	1.4129	16.9080	18.3210
7	1.4131	19.7340	21.1470
8	1.4132	22.5600	23.9730
9	1.4133	25.3870	26.8000
10	1.4134	28.2130	29.6270
11	1.4135	31.0400	32.4540
12	1.4135	33.8670	35.2810
13	1.4136	36.6740	38.1080
14	1.4136	39.5210	40.9350
15	1.4137	42.3490	43.7620

Table C.8: values of k_j, θ_j and γ_j when $\lambda = 1, \alpha = \frac{1}{20}$

j	k_j	θ_j	γ_j
0	1.3894	0	1.3894
1	1.4058	2.7789	4.1847
2	1.4092	5.5905	6.9997
3	1.4106	8.4089	9.8196
4	1.4114	11.2300	13.6420
5	1.4119	14.0530	15.4650
6	1.4123	16.8770	18.2890
7	1.4125	19.7010	21.1140
8	1.4127	22.5270	23.9390
9	1.4129	25.3520	26.7650
10	1.4130	28.1780	29.5910
11	1.4131	31.0040	32.4170
12	1.4132	33.8300	35.2430
13	1.4133	36.6570	38.0700
14	1.4133	39.4830	40.8960
15	1.4134	42.3100	43.7230

Table C.9: values of k_j, θ_j and γ_j when $\lambda = 1, \alpha = \frac{1}{10}$

j	k_j	θ_j	γ_j
0	1.3651	0	1.3651
1	1.3974	2.7302	4.1276
2	1.4041	5.5250	6.9291
3	1.4070	8.3332	9.7402
4	1.4086	11.1470	12.5560
5	1.4096	13.9640	15.3740
6	1.4103	16.7840	18.1940
7	1.4109	19.6040	21.0150
8	1.4113	22.4260	23.8370
9	1.4116	25.2490	26.6600
10	1.4118	28.0720	29.4840
11	1.4120	30.8950	32.3070
12	1.4122	33.7190	35.1320
13	1.4124	36.5440	37.9560
14	1.4125	39.3690	40.7810
15	1.4126	42.1940	43.6060